RADIAL VELOCITY MEASUREMENTS OF μ^1 BOOTIS

by

RUSSELL JOSEPH NIEHAUS

B.Sc., University of Victoria, 1966

A THESIS SUBMITTED IN PARTIAL FULFILLMENT

OF THE REQUIREMENTS FOR THE DEGREE OF

MASTER OF SCIENCE

in the Department

of

Physics

[redacted]

We accept this thesis as conforming
to the required standard

[redacted]

UNIVERSITY OF VICTORIA

April, 1970

ABSTRACT

Supervisor: Dr. C. D. Scarfe

Radial velocity measurements of spectrograms of μ^1 Bootis taken at the Dominion Astrophysical Observatory in Victoria show no evidence for variability in the radial velocity of the star, with either a short or a long period. This conclusion was reached after statistical tests for variability were performed on the data.

A comparison of radial velocity measurements from normal contrast, Kodak IIaO, plates and high contrast, Kodak IIIO, plates reveals no detectable gain in accuracy from the use of high contrast.

Measurements of radial velocities of μ^1 Bootis made with the oscilloscope machine are internally more consistent than those made with visual measuring machines.

The mean radial velocity of μ^1 Bootis, taken over 83 measurements each of unit weight, is -13.0 km/sec, with a standard error of about 2 km/sec. This large standard error is chiefly the result of errors in the effective wavelengths adopted for the star.

ACKNOWLEDGEMENTS

I would like to thank my supervisor, Dr. C. D. Scarfe, for the help and guidance given to me throughout this work, and also Dr. A. H. Batten, for many valuable discussions. I would like to express my gratitude to the many observers of the D.A.O. staff who obtained spectra of μ^1 Bootis, without whose efforts, much of this investigation could not have been undertaken, and especially Mr. J. M. Fletcher for his help with the measuring of several spectrograms. For his allotment of observing time and permission to use the equipment, I thank Dr. K. O. Wright, Director of the D.A.O. Also, I would like to thank Mr. R. V. Bennett for his helpful drafting advice and my wife, Vera, for her careful typing of this thesis.

Much of this work was carried out during the tenure of a National Research Council of Canada scholarship.

TABLE OF CONTENTS

LIST OF TABLES

LIST OF FIGURES

CHAPTER 1

GENERAL INTRODUCTION

1.1 Proper motion and radial velocity

A star's motion in space may be considered to be made up of two velocities, one parallel to the line joining the star and the observer (the line-of-sight), and the other perpendicular to this line. This latter velocity is called the "tangential velocity" of the star and its angular measurement (typically seconds of arc per year) is called the star's "proper motion", μ . It is the magnitude of the tangential velocity and the star's distance which determine the star's proper motion. Unless the distance to the star is known, it is not possible to convert the proper motion into a tangential velocity. The radial component, however, can be measured directly in velocity units and the star's distance need not be known. This component, known as the "radial velocity" of the star, combines with the tangential velocity to yield its space velocity, as shown in Figure 1.

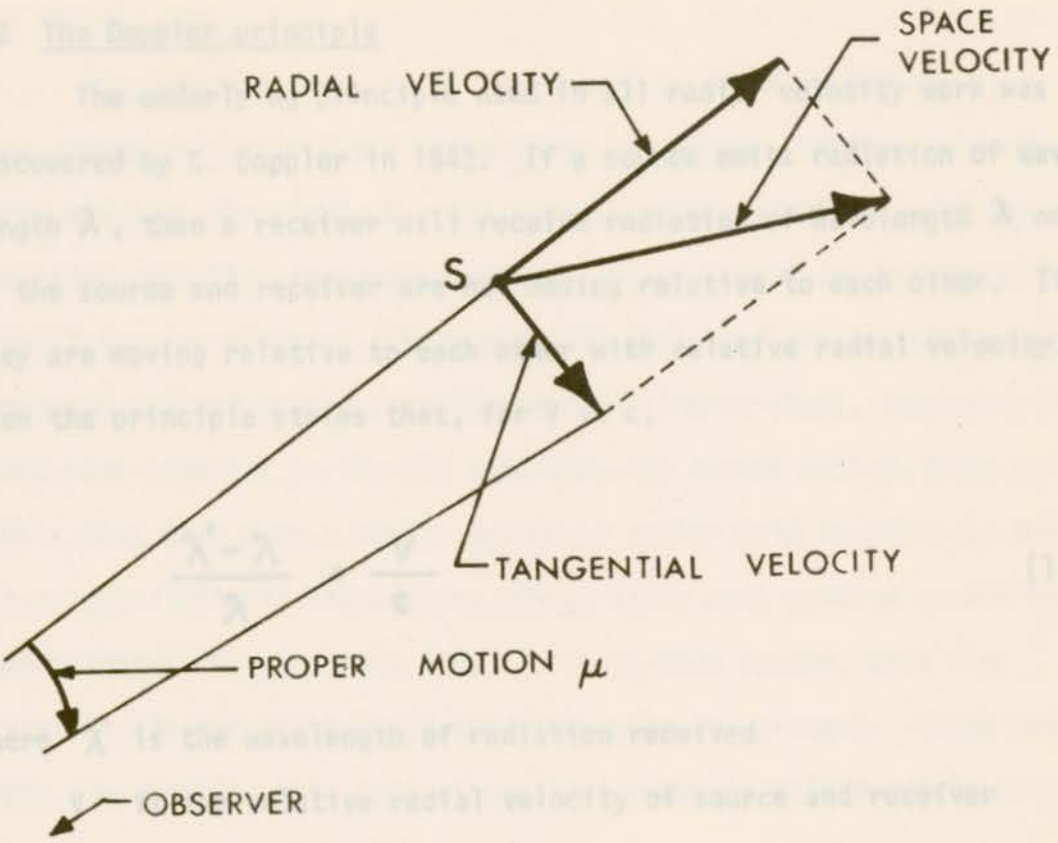

Figure 1. The radial velocity, tangential velocity, space velocity and proper motion of a star.

1.2 The Doppler principle

The underlying principle used in all radial velocity work was discovered by C. Doppler in 1842. If a source emits radiation of wavelength λ, then a receiver will receive radiation of wavelength λ only if the source and receiver are not moving relative to each other. If they are moving relative to each other with relative radial velocity, V, then the principle states that, for $V \ll c$,

$$\frac{\lambda' - \lambda}{\lambda} = \frac{V}{c} \qquad (1.2.1)$$

where λ' is the wavelength of radiation received

V is the relative radial velocity of source and receiver

c is the speed of light

If $\lambda' > \lambda$, the light is shifted to the red, and V is positive.

If $\lambda' < \lambda$, the light is blue-shifted, and V is negative.

The determination of the radial velocity of a star is then one of determining $\lambda' - \lambda \equiv \Delta\lambda$ as accurately as possible. Unfortunately, $\Delta\lambda$ is normally very small when one is working in the visual region of the spectrum. The method of measuring a radial velocity of a star is given in Section 5.3.

1.3 Binary stars

For many purposes, it is convenient to think of the sky as a huge sphere, with the earth situated at its center, so that, when one looks out into the night sky, one sees the stars as points of light projected onto this imaginary surface. If two stars are separated by a small angular distance, it is possible that they are not physically connected and are merely seen in the same line-of-sight. However, if the stars move together in the sky with the same proper motion, then it is likely that they form a binary system, a system held together by their mutual gravitational attraction. These stars each revolve around their common center of mass, much like the earth-moon system, each star radiating its own light as if the other were not present. Since both stars are visible, this type of stellar system is called a "visual binary".

If two stars form a binary system, but are at such a large distance from the observer that they appear as a single star, the system is termed a "spectroscopic binary". The fact that the system is binary is confirmed only by variations in radial velocity.

If the two stars in the binary system are of comparable luminosity, then spectra taken at various times during the orbital motion will reveal a doubling of the spectral lines. This doubling occurs because one of the stars is approaching the observer and the light is blue-shifted while at the same time, the other star is receding and the light is red-shifted. When the two stars cross the line-of-sight, the radial velocity of the stars with respect to the center of mass of the system is zero. The lines of both spectra have the same Doppler shift and, hence, appear as a set

of single lines. These stellar systems are called "double lined spectroscopic binaries".

If one star of a binary system is much more luminous than the other, then the faint star (the secondary) contributes no light to the observed spectrum. Its presence is inferred from the variation in the radial velocity of the brighter star (the primary) as it revolves around the center of mass of the system. In this case, the lines are single at all times, but they do shift about their zero velocity positions (the position where the radial velocity of the primary equals that of the center of mass). These systems are called "single lined spectroscopic binaries".

The angle of inclination, i, of a binary's orbital plane is the angle between the orbital plane and the plane at right angles to the line-of-sight. If this angle is non-zero, then changes in radial velocity are to be expected. Conversely, if no radial velocity changes are detected, then either the system is not a binary one, or the binary motion is so slow that the changes in radial velocity are below the level of detection, or the angle of inclination, $i, \approx 0°$.

The equation which relates the radial velocity of a star in its orbital motion to the elements of the orbit is given in Appendix A, Equation A.1.14.

Abt (1965) has suggested that the star μ^1 Bootis is a single lined spectroscopic binary. (The details are given in the following chapter.) The orbital elements were not well determined, as pointed out by Abt himself and also by Batten (1967). The purpose of the investigation undertaken herein was to determine the accuracy with which Abt's

(1965) orbital elements represent the radial velocity variation of the star.

1.4 Standard velocity stars

If the radial velocity of a star is constant whenever it is observed, and can be measured reasonably accurately, the star may be used as a radial velocity standard, hence, the name "standard velocity star". These stars have two very important uses. First, they provide a means of checking the spectrograph for a systematic velocity correction for any particular night's observations. Second, under special circumstances, they provide the means by which wavelength tables can be extended to non-solar type stars.

The objects in the solar system move through space in an orderly fashion discovered by Kepler and Newton, and, as a result, their velocities at any time can be calculated. Any spectrograms taken of them should reveal their dynamical velocities since they reflect the sun's light. To obtain a solar type wavelength table, the radial velocity measured using some lines is compared with the predicted dynamical radial velocity. Eventually a set of wavelengths will be found which will provide agreement between the observed and calculated radial velocities. It is possible to extend this wavelength table to slightly earlier (hotter) and later (cooler) stars, with the use of standard velocity stars of approximate solar type. The range in spectral types for which this is possible is F5 to K8 (Petrie, 1962, page 72). However, it is not possible to extend this system directly to spectral types much different from the sun since there are no dynamical velocity standards in the solar system of spectral types A, B, and M. The wavelengths of non-solar type spectra are determined in one of the two following ways, as outlined by the sub-commission on wavelengths of the International

Astronomical Union, (Adams et al., 1950).

(i) Galactic cluster membership.

Provided one or more stars in the cluster are solar type stars, their radial velocities can be determined using the solar wavelength table. The space motion of the cluster may be calculated from these radial velocities and from the positions of the stars. The space motion so derived may then be used to predict the velocities of the non-solar type members, and wavelengths in their spectra are chosen which duplicate these velocities.

(ii) Visual binary membership.

One member of the binary system must be a solar type star, hence, its radial velocity can be measured. By using only long period systems, one can assume that the radial velocities of the two stars are nearly the same and, therefore, the radial velocity of the second is known. Wavelengths in its spectrum are chosen such that they yield this velocity.

Application of both types of wavelength extensions to several systems provides a set of wavelengths which yield consistent velocities.

The latter type of system is pertinent to this particular discussion since, "the visual binary μ Bootis, composed of stars of types GO and late A, is a good example of a double star control." (Petrie, 1962, page 73) (μ^1 Bootis has since been reclassified FOV.)

The visual binary μ Bootis, used by Petrie, is made up of the primary, μ^1 Bootis or μ Bootis A, and the secondary, μ^2 Bootis or μ Bootis B. Their angular separation is 108 seconds of arc. μ^2 Bootis, which is seen as two stars through a large telescope, is itself

a visual binary with a known orbit (Baize, 1952). The star investigated in this work is the primary of the system, μ^1 Bootis, and unless otherwise specified, the abbreviation μ Boo refers to the primary, μ^1 Bootis, and not to the entire system.

CHAPTER 2

THE HISTORY OF μ BOO

The star μ Boo (HD 137391, R.A.$_{1900}$ $15^h\ 20^m.7$, Dec.$_{1900}$ +37° 44'), an F0 main sequence star of visual magnitude $4^m.3$, was measured for radial velocity by Campbell (1928). Between 1906 and 1911, six spectrograms of μ Boo were obtained with a three prism camera of dispersion 10.3 A/mm at Hγ. The heliocentric plate mean radial velocities ranged from -1.6 km/sec to -14.4 km/sec; the number of lines measured per plate ranged from five to thirteen. The unweighted mean radial velocity of μ Boo was tabulated as

$$-8.0 \pm 1.3 \text{ km/sec (p.e.m.)}$$

and the spectra were described as having "broad lines".

Four years later, Moore (1932) gathered together radial velocities of μ Boo from different observatories. Radial velocities from Ottawa (the mean radial velocity from three observations taken at 35 A/mm at Hγ was -21.7 ± 3 km/sec (p.e.m.)) and from Allegheny (the mean radial velocity from four observations also taken at 35 A/mm at Hγ was -14.6 ± 1.2 km/sec (p.e.m.), Jordan (1911)) were combined with the above Lick observations of Campbell to yield an adopted weighted mean radial velocity for μ Boo of

$$-9.6 \pm 1.0 \text{ km/sec (p.e.m.)}$$

Shortly after, Harper (1937) published his radial velocity catalogue for stars brighter than $6^m.5$. Since μ Boo fell into this category, two spectra were obtained, in 1921, at the Dominion

Astrophysical Observatory, (D.A.O.), with a dispersion of about 30 A/mm at Hγ. Harper found there were "numerous fair lines, though faint". Measuring 14 and 15 lines per plate, Harper obtained radial velocities of -8.9 km/sec and -9.0 km/sec. The adopted mean, with no error estimate given, was

-9.0 km/sec

More spectrograms of μ Boo were obtained by observers at the D.A.O. in the years 1944 to 1947, using the various cameras of the 72-inch telescope spectrograph. These were to be used by Petrie for his revision of the standard wavelength tables in use at the D.A.O.

Petrie's (1946) work involved setting up new wavelength tables for the solar type stars, spectral classes F4 to K8. The cameras investigated were the IIL (two prism, long focus, 11 A/mm at Hγ), IL (one prism, long focus, 22 A/mm at Hγ) and IM (one prism, medium focus, 30.1 A/mm at Hγ). McDonald (1948) extended this work to include the IS camera (one prism, short focus, 51 A/mm at Hγ).

Petrie (1947) extended the revision to stars of spectral types A0 to F2, for the IIL camera. Using members of galactic clusters and visual binaries as outlined in Chapter 1, he was able to extend the IIL wavelength table to non-solar type stars. Since μ Boo is a member of the visual binary A.D.S. 9626 and μ Bootis B has a solar type spectrum (Baize, 1952), the secondary was used by Petrie as a standard velocity "control star". From seven spectrograms, Petrie determined the mean radial velocity of μ Boo to be

-10.4 ± 0.4 km/sec (p.e.m.)

Extending the A type stellar wavelength revision to the single prism spectrographs of the D.A.O. (IM and IS), Petrie (1948) found the radial velocity of μ Boo, from nine spectrograms was

$$-7.6 \pm 1.0 \text{ km/sec (p.e.m.)}$$

Some years later, Slettebak (1955) studied the rotational velocities of the bright stars of spectral type A3-G0 and determined that the projected equatorial rotational velocity, $V_{eq} \sin i$, of μ Boo, is 90 km/sec. That is, μ Boo is rotating on its axis with an equatorial rotational velocity of at least 90 km/sec. As a comparison, the sun has an equatorial rotational velocity of approximately two km/sec. Hence, μ Boo is classed as a "moderately fast" rotator. Its speed of rotation is the principal reason for the broad lines found in its spectrum, as will be discussed later.

In 1965, Abt (1965) studied the frequency of occurrence of spectroscopic binaries among the normal A stars. Over a period of twenty-one months, he obtained thirteen spectrograms of μ Boo - four at a dispersion of 18 A/mm and nine at 20 A/mm. The resultant measured radial velocities, based on seven lines per plate, showed "no excessive variation". (The mean velocity and its probable error, from Abt's thirteen spectra, were (-15.9 ± 0.8) km/sec.) Combination of his data with all of those previously published (which also showed no excessive variation) nevertheless led Abt to the conclusion that μ Boo was a single lined spectroscopic binary. The conclusion was drawn after eleven least squares solutions were performed on the data. Clearly, if a star is a member of a spectroscopic binary system,

its radial velocity cannot be considered constant and as a result the star should not be used as a radial velocity standard.

Batten (1967), in his Sixth Catalogue of the Orbital Elements of Spectroscopic Binary Systems, assessed the quality of published orbits. The categories ranged from 'a' (definitive orbits) to 'e' (very poor orbits). Abt's orbital elements for μ Boo were graded 'd' (poor). Thus μ Boo was temporarily taken from the Victoria Standard Velocity star list, but observations were still taken for possible future work.

The spectroscopic orbital elements as given by Abt (1965) are probably not well determined, for reasons given by him, viz:

(i) the use of miscellaneous material gathered from various observatories

(ii) the lack of continuous observation over several years

(iii) the small velocity variation

(iv) the broad lines in the star's spectrum.

If the data obtained between 1963 and 1969 at the D.A.O. in Victoria only are used, the first two of the above four difficulties may be overcome. Little can be done with the other two, since they are intrinsic properties of the star. The old velocities of μ Boo (Petrie, 1947, 1948) would serve as checks on any binary period determined for μ Boo. Otherwise Petrie's velocities are useless because of objection (ii) above.

CHAPTER 3

INSTRUMENTS AND TECHNIQUES

3.1 The spectrograph

The main tool used by astronomers studying radial velocities is the spectrograph: a simplified diagram is shown in Figure 2. The prime purpose of such an instrument is to break up or disperse the original starlight into its component wavelengths, and to focus them onto some suitable recording device.

After entering the spectrograph through the slit, S, the light beam diverges. A collimator mirror, C, renders the beam parallel and diverts it to the grating, G. Older spectrographs had one or more prisms placed where the grating is situated. Gratings are becoming more popular than prisms because of their linear dispersion and relatively high resolving power. The gratings are blazed i.e. ruled at a fixed angle in order to concentrate a large percentage of the incident light into a single order around a predetermined wavelength. Higher and nearly linear dispersions can be obtained if gratings rather than prisms are used. Of course, more than one prism can be used to increase the dispersion (e.g. IIL camera, D.A.O. 11 A/mm at Hγ) but light losses become severe as the number of refractions increases. The grating or prism disperses the starlight so that rays of light of the same wavelength are parallel. The dispersed light falls on the camera mirror, C', which focusses the light onto the recording device, R, usually a photographic plate. The developed spectrographic plate provides a permanent record of the star.

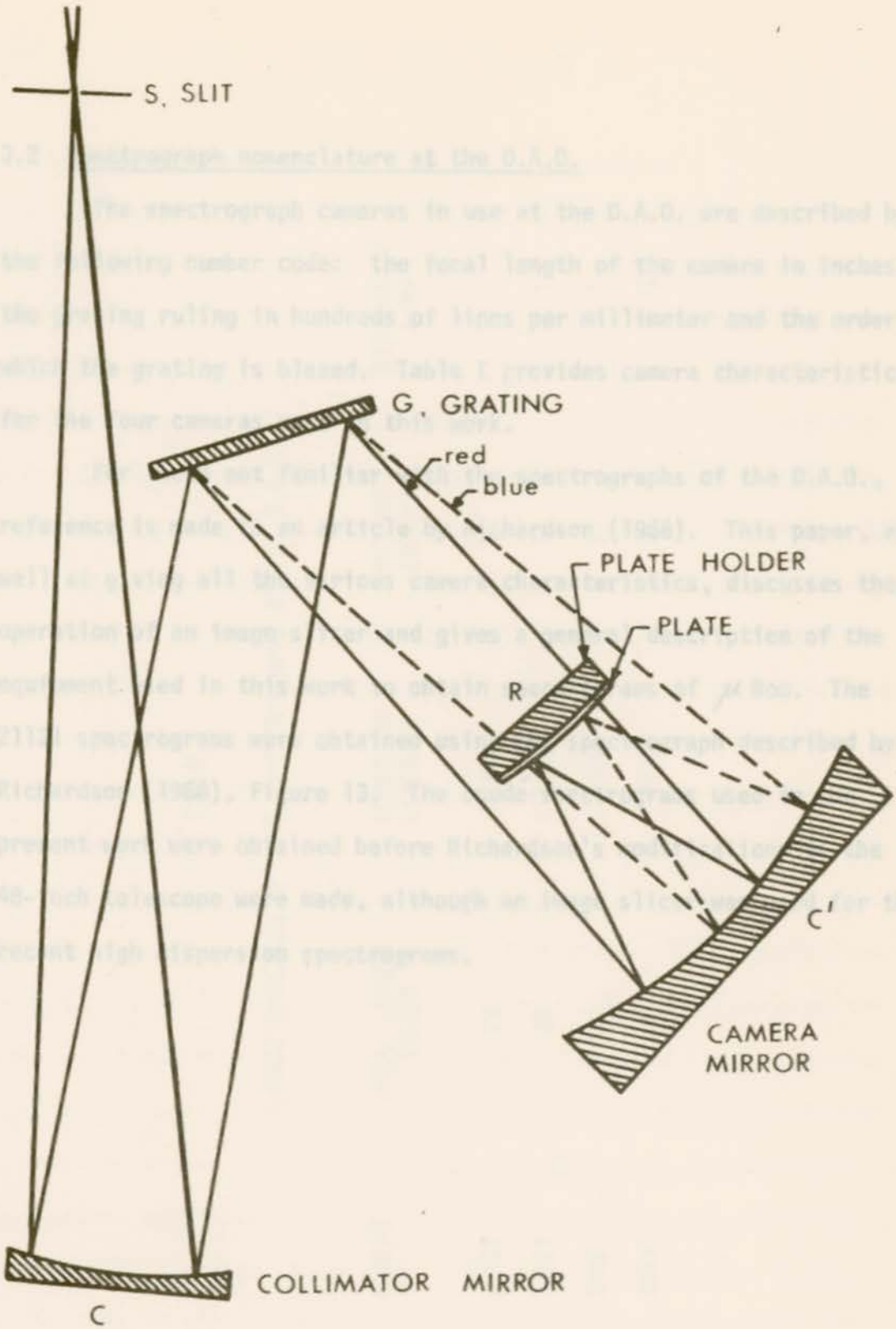

Figure 2. A typical spectrograph.

3.2 Spectrograph nomenclature at the D.A.O.

The spectrograph cameras in use at the D.A.O. are described by the following number code: the focal length of the camera in inches, the grating ruling in hundreds of lines per millimeter and the order in which the grating is blazed. Table I provides camera characteristics for the four cameras used in this work.

For those not familiar with the spectrographs of the D.A.O., reference is made to an article by Richardson (1968). This paper, as well as giving all the various camera characteristics, discusses the operation of an image slicer and gives a general description of the equipment used in this work to obtain spectrograms of μ Boo. The 21121 spectrograms were obtained using the spectrograph described by Richardson (1968), Figure 13. The coudé spectrograms used in the present work were obtained before Richardson's modifications to the 48-inch telescope were made, although an image slicer was used for the recent high dispersion spectrograms.

TABLE I

CHARACTERISTICS OF SOME SPECTROGRAPHS AT THE D.A.O.

CAMERA	FOCAL LENGTH INCHES	NUMBER OF LINES/MM	GRATING ORDER	DISPERSION A/MM
21121	21	1200	1	15.3
32121	32	1200	1	10.1
3282	32	800	2	6.5
3263	32	600	3	5.8

3.3 Observing technique

The method used to obtain some of the spectrograms used in this work is described in detail, primarily for those not familiar with the technique. The discussion will be confined to the 48-inch telescope at the D.A.O., since it was used most often.

The spectrograph is enclosed in a large coudé room (described by Richardson, 1968). Preparatory to observing with any camera, the focus and rotation of the plateholder are checked with a Hartmann focus test. The telescope can be set on a star automatically by entering the star's coordinates into the control console. The stellar image is centered in the field of view of the finding telescope with a guiding handset. Small adjustments place the starlight on the jaws of the slit or on the rectangular slot which forms the entrance to the image slicer (Richardson, 1968).

As the starlight enters the spectrograph, a small amount is diverted by a plane mirror into a photomultiplier. The current from the photomultiplier is integrated by a capacitor. A counter records the number of times the capacitor is charged and shorted to ground. The total count represents the exposure on the spectrogram. The counter sensitivity scale is chosen such that the count rate is approximately five counts per minute. A much slower count rate is not satisfactory since a non-zero dark current will affect the total count. A much faster rate is also unsatisfactory since the time required for the capacitor to discharge is then an appreciable fraction of the time required for it to charge and the spectrogram would appear more exposed than expected from the exposure count. The counter is reset when a

suitable count rate is found. With the spectrographic plate in place, the exposure is started by permitting starlight to fall on the image slicer. The observing record includes the time and the hour angle of the star, which are needed to calculate corrections to radial velocities (Appendix C), as well as the star's spectral type, plate emulsion, camera, and counter sensitivity.

Since intensities of stellar lines are often obtained from spectrograms by means of a microphotometer, it is necessary to have a calibration on the plate which relates density of exposure on the plate to intensity of light as a function of wavelength for the particular plate emulsion used. The calibrating device used at the D.A.O. consists of a standard lamp shining through a rotating step wheel (Wright, 1962, page 88). The intensity ratio of light from one step to the next is 1.58 (0.2 in the logarithm). Density can be related to relative intensity via this calibration. The calibration is applied at the same time as the stellar exposure.

In order to measure the radial velocity of the star from a spectrogram, it is necessary to place on the plate a comparison spectrum moving at zero velocity with respect to the spectrograph. The spectrograph of the 48-inch telescope is outfitted with an iron-argon tube which provides a set of standard lines with known wavelengths. The 72-inch telescope uses an iron arc. The comparison spectrum is applied more than once during the stellar exposure in order to minimize errors arising from small temperature changes in the spectrograph and from possible emulsion shifts during the exposure. For longer exposures, the arc is applied three times while for shorter exposures, twice is sufficient.

When the desired exposure count has been reached the exposure is stopped and the plate is developed in the appropriate developer.

All spectrograms obtained by the author using the 48-inch telescope at the D.A.O. were taken with the 32121 camera. Since 1968, an image slicer has been used instead of a slit, since it reduces the exposure time and avoids the necessity of trailing. Several spectrograms taken with a slit with other cameras (3282 and 3263) in previous years were also available for radial velocity measurement.

The plate emulsions used were Kodak IIaO, Kodak IIIO, and Kodak IIIaJ one night when five spectra were taken with the 72-inch telescope. Thackeray (1967) suggested the use of high contrast emulsions for three reasons:

(a) resolution of double lines,

(b) measurement of radial velocities of diffuse lines,

(c) detection of faint lines, especially the fainter components of spectroscopic binaries.

Since μ Boo has broad diffuse lines, it was thought that the use of a high contrast emulsion, such as IIIO, would increase the internal accuracy and ease with which a spectrogram could be measured. For this reason IIIO spectrograms were obtained whenever possible. However, exposure times with this emulsion were often greater than two hours. As a result, IIIO emulsion was used only if μ Boo was near the meridian and if the sky was very clear. Otherwise a IIaO emulsion was used. For a very low level of illumination and long exposure times, the effective sensitivity of a photographic plate is decreased so that more total exposure is needed to produce the desired density. This

loss in sensitivity, known as "reciprocity failure", can be reduced by using baked plates which require less exposure. Such an emulsion is designated by a "b", for example IIaOb. Frequently IIaOb plates were used instead of IIaO, particularly if the sky was partly cloudy. Appendix B gives a brief description of IIaO and IIIO emulsions.

3.4 Wavelengths

Batten of the D.A.O. prepared a table of wavelengths suitable for the A type stars to be used with the 32121 camera. He used as control objects those stars found in visual binary systems and open clusters, as outlined in Chapter 1. When the present work was started, Batten's table of wavelengths was in a preliminary state. The final table is in press (Batten et al., 1970).

Using Batten's table and a nicely exposed high contrast 32121 spectrogram of μ Boo, all the lines whose profiles were not asymmetric or obviously blended were measured in the usual way. The purpose of measuring extra lines was to determine if any of these lines could have been used with this particular spectral type. When the lines were measured on this spectrogram, not all the wavelengths were known. The lines from Batten's table were used to calculate a plate average velocity. All the velocities should have equalled the plate mean, but owing to measuring errors, they did not. It was possible to work backwards to obtain the approximate wavelengths of the measured features and to find their accurate wavelengths in "Solar Spectrum, Second Revision of Rowland's Preliminary Table of Solar Spectrum Wavelengths", (Moore et al., 1966). Many of the lines were rejected since they were unreliable for an F0 spectrum. The reason for this is explained below. The final stellar wavelengths used and their identifications are shown in Table II.

Many wavelengths given in Table II are the adjusted means of lines of different elements, both neutral and ionized, which are blended together to form the observed line. Unfortunately, the contribution of each line to a blend varies with spectral type and, as a result,

TABLE II

THE STELLAR WAVELENGTHS USED IN μ BOO, COUDÉ SPECTRA

WAVELENGTH ANGSTROMS	IDENTIFICATION	SOURCE	RANGE
3878.580	FeI	R.R.T.	
3933.682	CaII	A.H.B.	
4005.254	FeI	A.H.B.	
4030.680	MnI, FeI, TiI	adjusted	A3-F0
4045.815	FeI	R.M.T.	A0-F0
4063.578	FeI, MnI, GdII	adjusted	A0-F0
4101.737	Hδ	R.M.T.	A0-F0
4215.550	SrII, FeI, CrII, ZrII	adjusted	A3-F0
4325.775	FeI	R.R.T.	
4340.475	Hγ	R.R.T.	
4351.833	FeII	A.H.B. adjusted	
4549.544	FeI, TiII	R.R.T.	A0-F0

R.R.T. Rowland's Second Revised
A.H.B. A.H. Batten
R.M.T. Revised Multiplet Table

effective wavelengths vary with spectral type also. If this variation is unknown, the wavelength used for the particular line may be in error by an amount $\Delta\lambda$. This produces a systematic error, ΔV, in the velocity obtained from the blend, which is related to the wavelength error by

$$\Delta V = \frac{\Delta\lambda}{\lambda} \cdot c$$

according to the Doppler principle (see Figure 3). For example, consider a hypothetical line, of true wavelength 4000.000 A, for which the observer used a wavelength of 4000.050 A. Then the systematic error introduced into all measurements of this line is

$$\Delta V = \frac{0.050}{4000.000} \times 3\times10^5 \text{ km/sec} \approx 3.8 \text{ km/sec}$$

Usually the observer does not know he has adopted the incorrect stellar wavelength and, hence, does not realize the systematic error is present. It is necessary to determine whether or not the measured line velocity is consistent with the velocities of the other lines measured on the plate. The method used to test the consistency of the measured line velocities is given in Section 6.3.

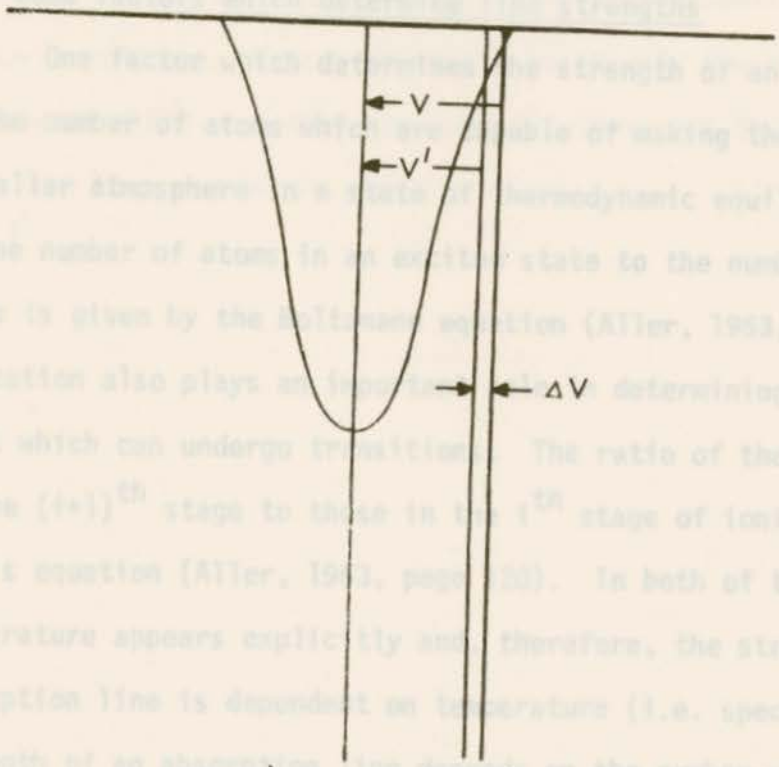

Figure 3. Systematic error in radial velocity, Δ V, due to incorrect adopted wavelength.

CHAPTER 4

VARIATION IN THE COMPOSITION OF BLENDS WITH SPECTRAL TYPE

4.1 Some factors which determine line strengths

One factor which determines the strength of an absorption line is the number of atoms which are capable of making the absorption. In a stellar atmosphere in a state of thermodynamic equilibrium, the ratio of the number of atoms in an excited state to the number in the ground state is given by the Boltzmann equation (Aller, 1963, page 112). Ionization also plays an important role in determining the number of atoms which can undergo transitions. The ratio of the number of atoms in the $(i+1)^{th}$ stage to those in the i^{th} stage of ionization is given by Saha's equation (Aller, 1963, page 120). In both of these equations, temperature appears explicitly and, therefore, the strength of an absorption line is dependent on temperature (i.e. spectral type). The strength of an absorption line depends on the number of atoms above the photosphere which do the absorbing. This number is determined not only by the excitation and ionization equations, but also by the depth to which one is able to see into the atmosphere. This depth is determined by the opacity of the stellar material. For large opacities, the number of atoms above the photosphere is small and, hence, absorption lines may be weak. As an example, consider the FeII lines in the star Sirius (Hynek, 1951, page 50). Even though the temperature of Sirius is greater than that of the sun and, therefore, more singly ionized iron atoms in Sirius than in the sun are expected, the FeII lines in the spectrum of Sirius are weaker than they are in the solar spectrum. This is so

because, at the temperature of Sirius, the hydrogen atoms are sufficiently excited and ionized to increase the opacity of the atmosphere of Sirius to a value much greater than that of the sun. The opacity increase is a result of absorption in the Paschen continuum and of electron scattering. Hence, there are relatively few atoms above a level beyond which we cannot see, and the lines are correspondingly weaker than they are in the sun.

4.2 A description of line blending as a function of spectral type

Consider a pair of lines of nearly equal wavelengths, λ_1 and λ_2, one of which decreases in strength with an increase in temperature, while the other increases. The variation of their combined profile and effective wavelength over the temperature range for which they are both present is illustrated in Figure 4. In this diagram the thin curves are the profiles of the individual lines, the thicker curves are the combined profiles, and the vertical stroke marks the effective wavelength of the blend.

In Figure 4, the individual line profiles are Gaussian, as expected for lines broadened by a Doppler motion of the absorbing atoms, whether this motion is thermal in origin or arises from large scale turbulent motions in the stellar atmosphere. In practise these turbulent motions often contribute more to the line broadening than does the random thermal motion of the atoms. Figure 4 does not include any attempt to depict a change of line width with changes of temperature.

Over a range of spectral types in which the effective wavelength of a blended line is changing, the line is useless for radial velocity measures since it will produce a systematic error of the type discussed in Section 3.4.

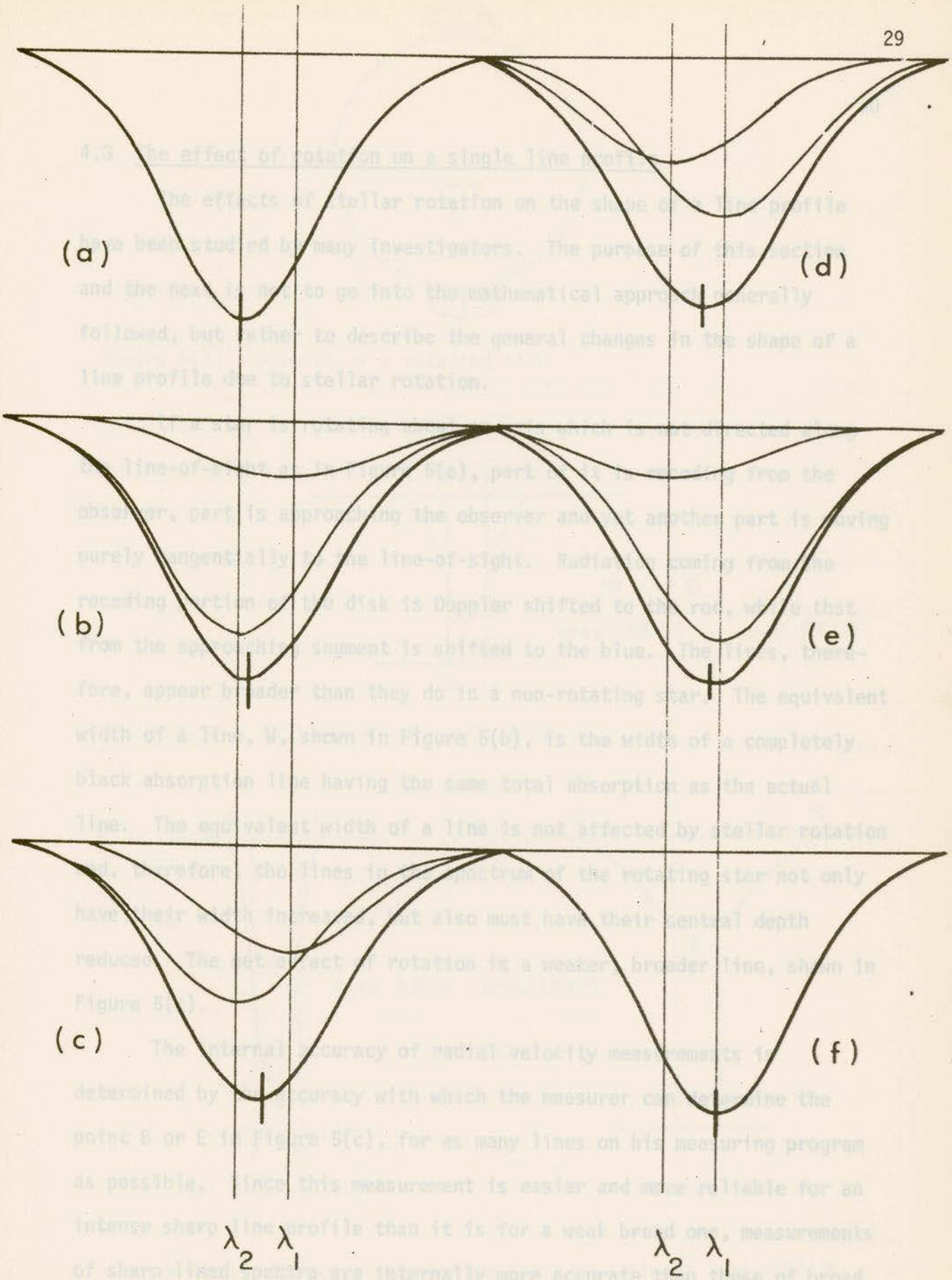

Figure 4. The blending of spectral lines.

4.3 The effect of rotation on a single line profile

The effects of stellar rotation on the shape of a line profile have been studied by many investigators. The purpose of this section and the next is not to go into the mathematical approach generally followed, but rather to describe the general changes in the shape of a line profile due to stellar rotation.

If a star is rotating about an axis which is not directed along the line-of-sight as in Figure 5(a), part of it is receding from the observer, part is approaching the observer and yet another part is moving purely tangentially to the line-of-sight. Radiation coming from the receding portion of the disk is Doppler shifted to the red, while that from the approaching segment is shifted to the blue. The lines, therefore, appear broader than they do in a non-rotating star. The equivalent width of a line, W, shown in Figure 5(b), is the width of a completely black absorption line having the same total absorption as the actual line. The equivalent width of a line is not affected by stellar rotation and, therefore, the lines in the spectrum of the rotating star not only have their width increased, but also must have their central depth reduced. The net effect of rotation is a weaker, broader line, shown in Figure 5(c).

The internal accuracy of radial velocity measurements is determined by the accuracy with which the measurer can determine the point B or E in Figure 5(c), for as many lines on his measuring program as possible. Since this measurement is easier and more reliable for an intense sharp line profile than it is for a weak broad one, measurements of sharp lined spectra are internally more accurate than those of broad

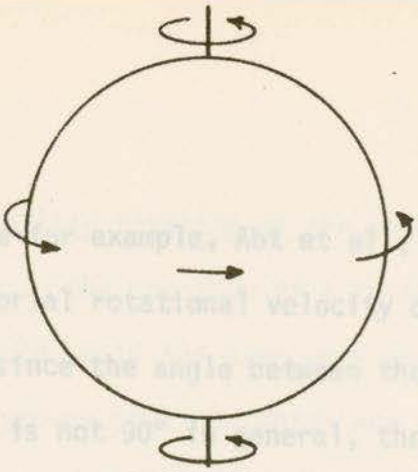

Figure 5(a). Diagram of a rotating star.

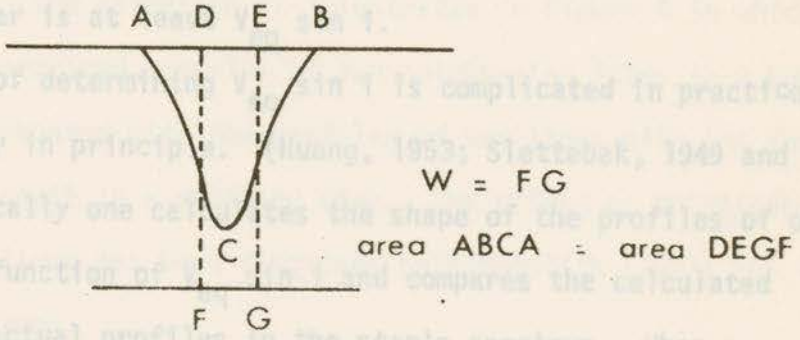

Figure 5(b). Equivalent width of a line, W.

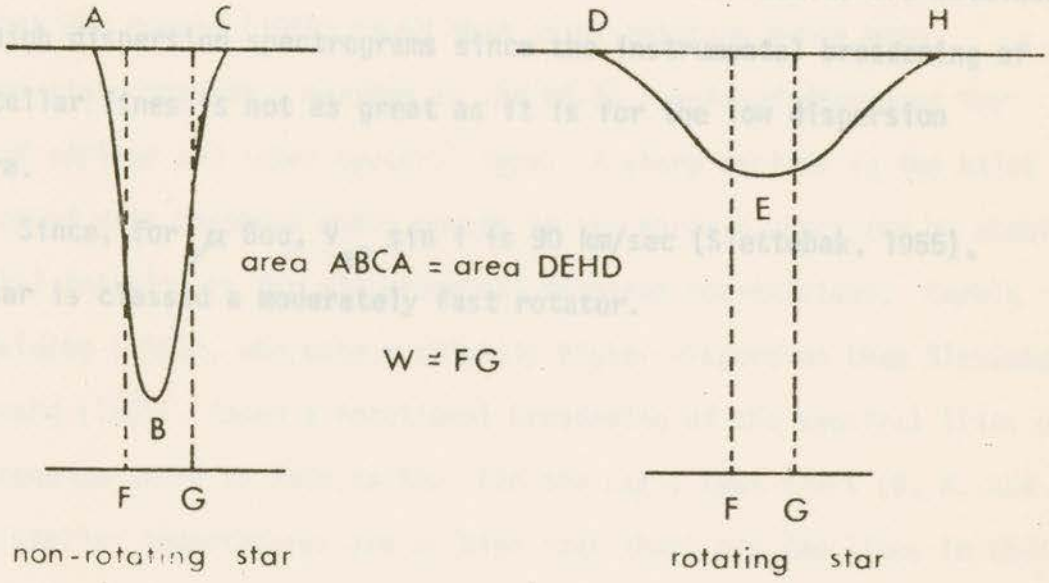

Figure 5(c). Effect of stellar rotation on a single line profile.

lined spectra. (See for example, Abt et al., 1969)

If the equatorial rotational velocity of a star rotating on its axis is V_{eq}, then, since the angle between the line-of-sight and the rotational axis, i, is not 90° in general, the effective velocity of rotation which broadens the lines is the projected equatorial rotational velocity, V_{eq} sin i. Since i remains completely indeterminate in the majority of cases, all one can say is that the equatorial rotational velocity of the star is at least V_{eq} sin i.

The method of determining V_{eq} sin i is complicated in practice, but moderately easy in principle. (Huang, 1953; Slettebak, 1949 and many others) Basically one calculates the shape of the profiles of one or two lines as a function of V_{eq} sin i and compares the calculated profiles with the actual profiles in the star's spectrum. When a sufficiently accurate match is made, the projected equatorial rotational velocity of the star has been determined. The best results are obtained with high dispersion spectrograms since the instrumental broadening of the stellar lines is not as great as it is for the low dispersion spectra.

Since, for μ Boo, V_{eq} sin i is 90 km/sec (Slettebak, 1955), the star is classed a moderately fast rotator.

4.4 The effect of stellar rotation on the observed spectrum

All the lines in the spectrum of a rotating star are thus broader than they would be if the star were not rotating. Therefore, many close pairs or groups of lines which are resolved in the spectrum of a non-rotating star become blended into a single broad profile in a rotating star. The profile may be asymmetrical and in general will have an uncertain effective wavelength. The blended line will also be awkward to measure. The situation is illustrated in Figure 6 in which the individual and combined profiles of two neighboring lines in a non-rotating star are compared with the profiles of two lines with the same difference in wavelength in a rotating star. The effect of rotational blending of nearby lines has been discussed by Binnendijk (1967) for the W Ursae Majoris systems.

Several investigators have studied the rotational velocity of stars as a function of both spectral type and luminosity class. Slettebak and Howard (1955) found that axial rotation among main sequence stars reaches a maximum in the B5-B7 range and decreases for stars of earlier and later spectral type. A sharp decline in the axial rotation of main sequence stars occurs in the early F stars and by about F5, axial rotation is for all practical purposes non-existent. Herbig and Spalding (1955), who used a slightly higher dispersion than Slettebak and Howard (1955), found a rotational broadening of the spectral lines of main sequence stars as late as F8. For the early type stars (O, B, and A) the stellar temperatures are so high that there are few lines in their visible spectra. At spectral types later than about F5, there are many lines in the stellar spectra, but they remain unblended by rotational

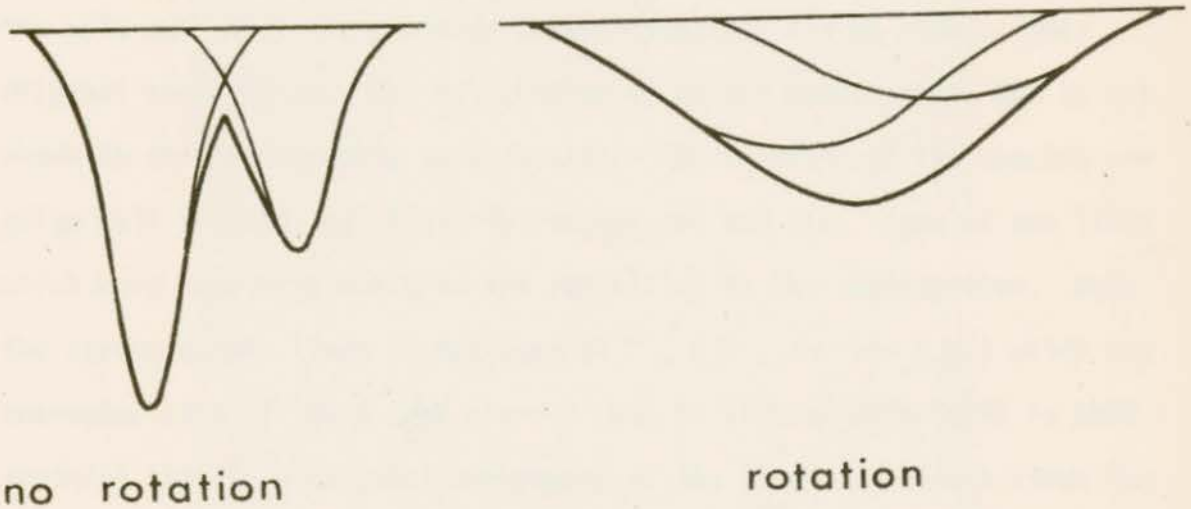

Figure 6. Effect of stellar rotation on the observed spectrum.

broadening, since the rotational velocities are low. The rotational blending of spectral lines is worst for the late A- early F type stars because there are many lines in their spectra and their rotational velocities are often sufficiently great to produce the blending. Since μ Boo is an FOV star, rotational blending of its spectral lines is expected.

CHAPTER 5

THE DATA

5.1 Typical spectrograms of μ Boo

Some typical spectrograms of μ Boo taken with the 72-inch telescope, 21121 camera are shown in Figure 7. The eight spectra illustrated were obtained in succession by moving the plateholder by fixed amounts in a direction perpendicular to the dispersion. The iron arc was applied to each spectrum during its exposure. The stellar image was trailed along the slit such that the spectrum is approximately 0.4 mm wide on the original spectrogram. The calibration is on the spectrogram, but is not shown in the photographic reproduction. The majority of the spectra are quite well trailed, particularly numbers one and six. Some of the lines which were regularly measured are identified in the reproduction. Note the strong Balmer lines of hydrogen ($H\gamma$, $H\delta$, $H\varepsilon$ and $H\zeta$) which are characteristic of the A type stars. ($H\varepsilon$ is blended with Ca(H) in this spectral type.) Rotational broadening of the lines is evident since the metallic lines are weak and broad. To demonstrate further the quality of the lines, spectra 2, 3, and 4 are enlarged again in Figure 8, where the low contrast which makes the positions of the lines hard to measure, is clearly evident.

The differences between camera dispersions are shown in Figure 9, where typical 21121, 32121 and 3282 spectra are shown, aligned approximately at λ 4200 A. All the emulsions are Kodak IIaO. The magnification of the photographic enlarger used in the three reproductions is the same. Naturally, the lines appear narrower on the low dispersion spectra

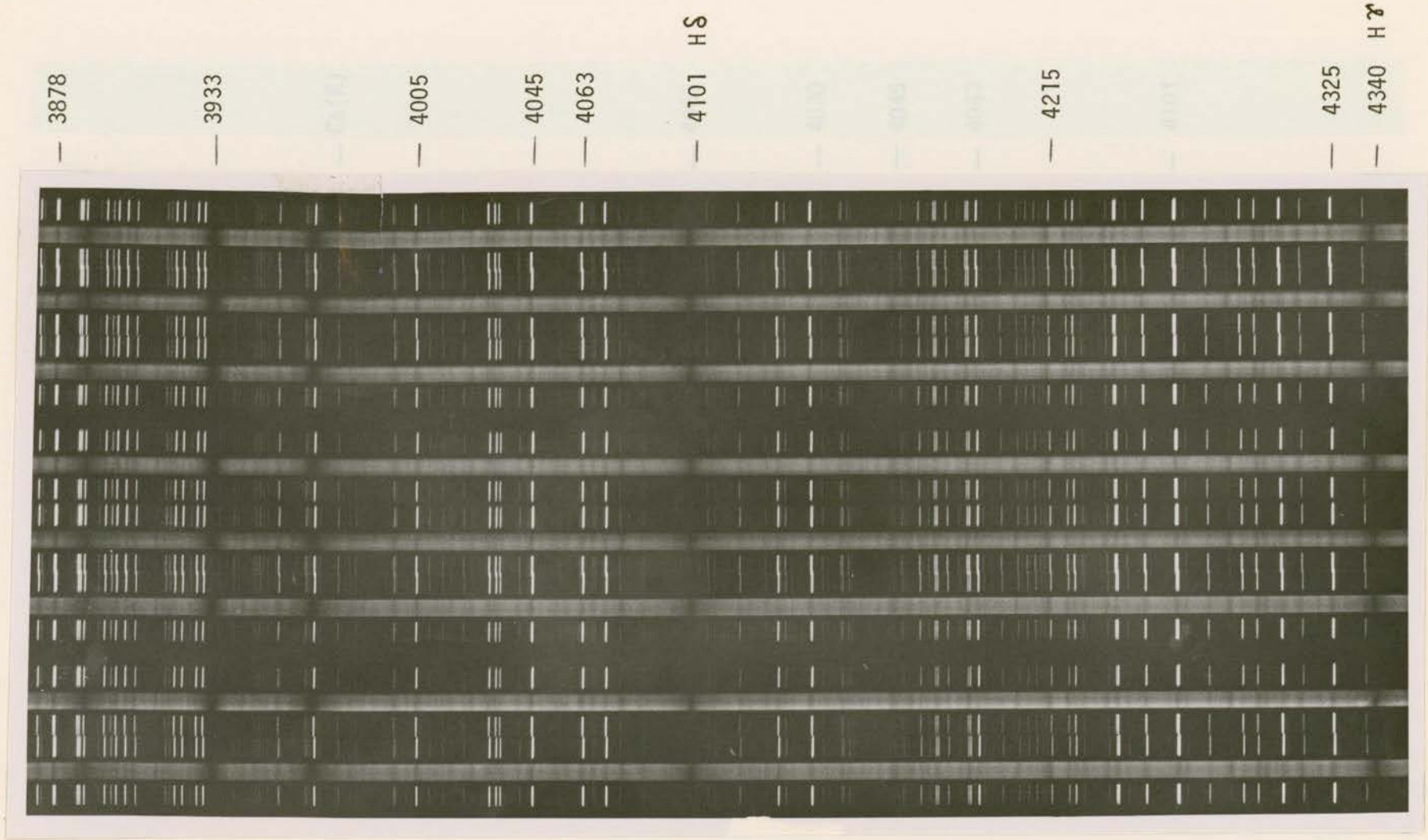

Figure 7. Photographic enlargement of eight 21121 spectrograms of μ Boo taken April 8, 1969.

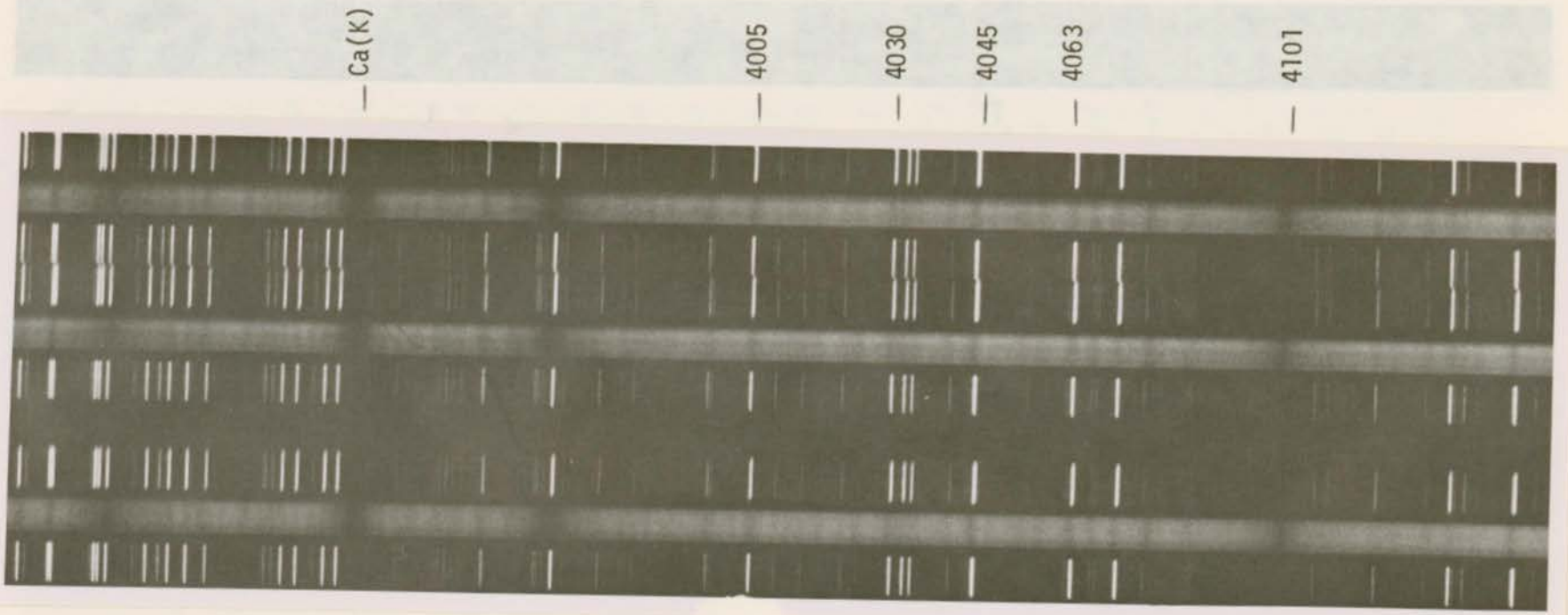

Figure 8. Further enlargement of 21121 spectrograms of μ Boo taken April 8, 1969 showing the poor quality of the spectral lines.

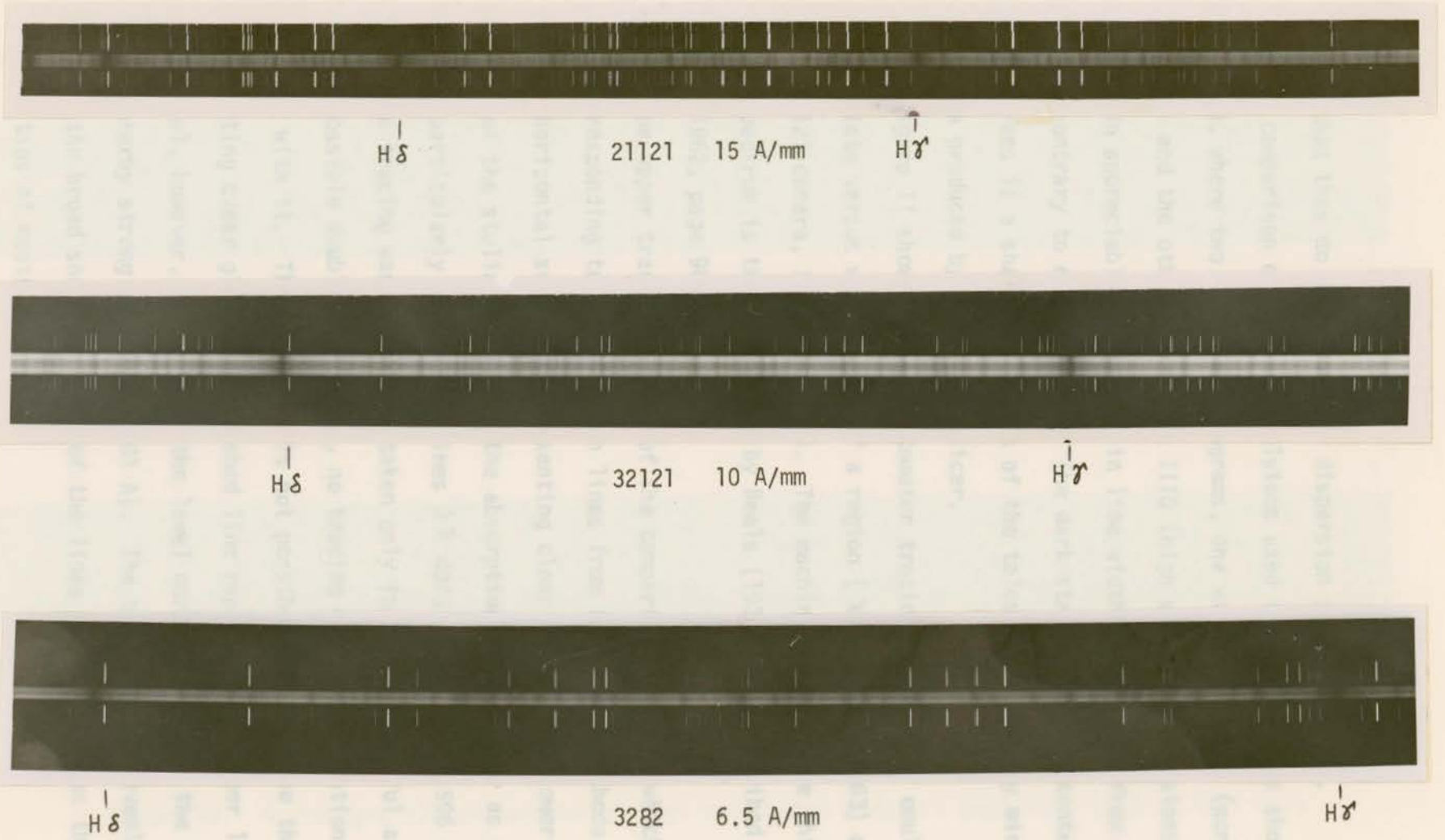

Figure 9. Effect of dispersion on three typical spectra of μ Boo: 21121, 32121 and 3282 spectra.

(21121) than they do on the higher dispersion spectra (3282).

A comparison of the two emulsions used in this work is shown in Figure 10, where two 32121 spectrograms, one with Kodak IIaO (normal contrast) and the other with Kodak IIIO (high contrast) emulsions are shown. No appreciable difference in line widths is evident from the prints, contrary to expectations. The dark strip along the center of the spectrograms is a shadowing effect of the telescope secondary mirrors on the image produced by the image slicer.

Figure 11 shows a microphotometer tracing (density of emulsion on the plate versus wavelength) of a region ($\lambda\lambda$ 4045 to 4063) of plate 3172 (32121 camera, IIIO emulsion). The machine used to give this trace of the spectrum is that developed by Beals (1936), and described by Wright (1962, page 90).

The upper tracing is that of the comparison spectrum which shows dips corresponding to the emission lines from the hollow cathode lamp between horizontal sections representing clear glass. The lower tracing is that of the stellar spectrum; the absorption lines appear as broad minima, particularly the strong lines $\lambda\lambda$ 4045.815 and 4063.596 of FeI. Since the tracing was originally taken only in an unsuccessful attempt to detect possible doubling of lines, no tracing of the calibration was included with it. Therefore, it is not possible to determine the level representing clear glass. The dashed line represents an upper limit to this level, however, since it is the level corresponding to the center of the nearby strong line Hδ (4101 A). The tracing thus reveals clearly the broad shallow nature of the lines and illustrates the difficulties of measuring them.

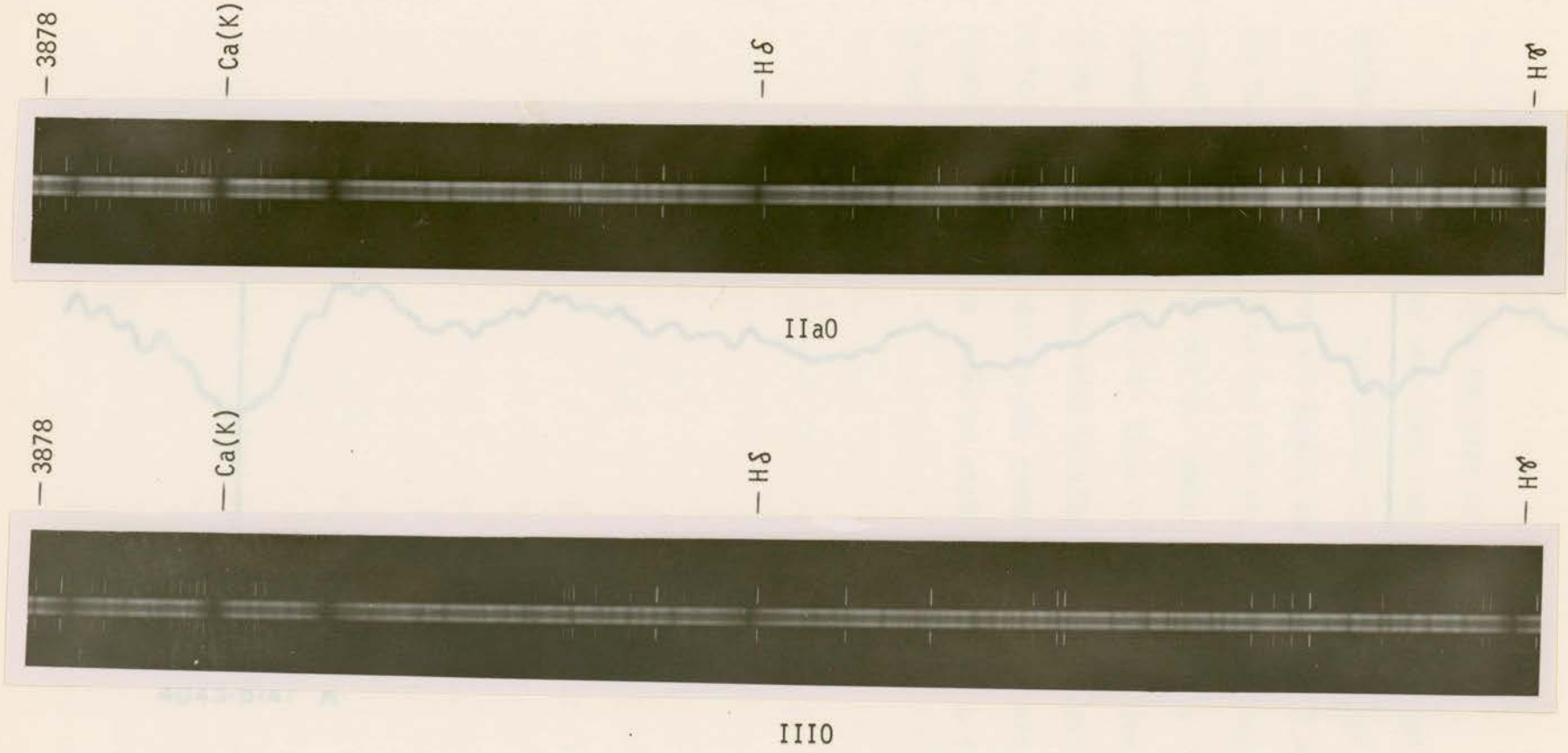

Figure 10. A photographic comparison of high and medium contrast emulsions used in this work.

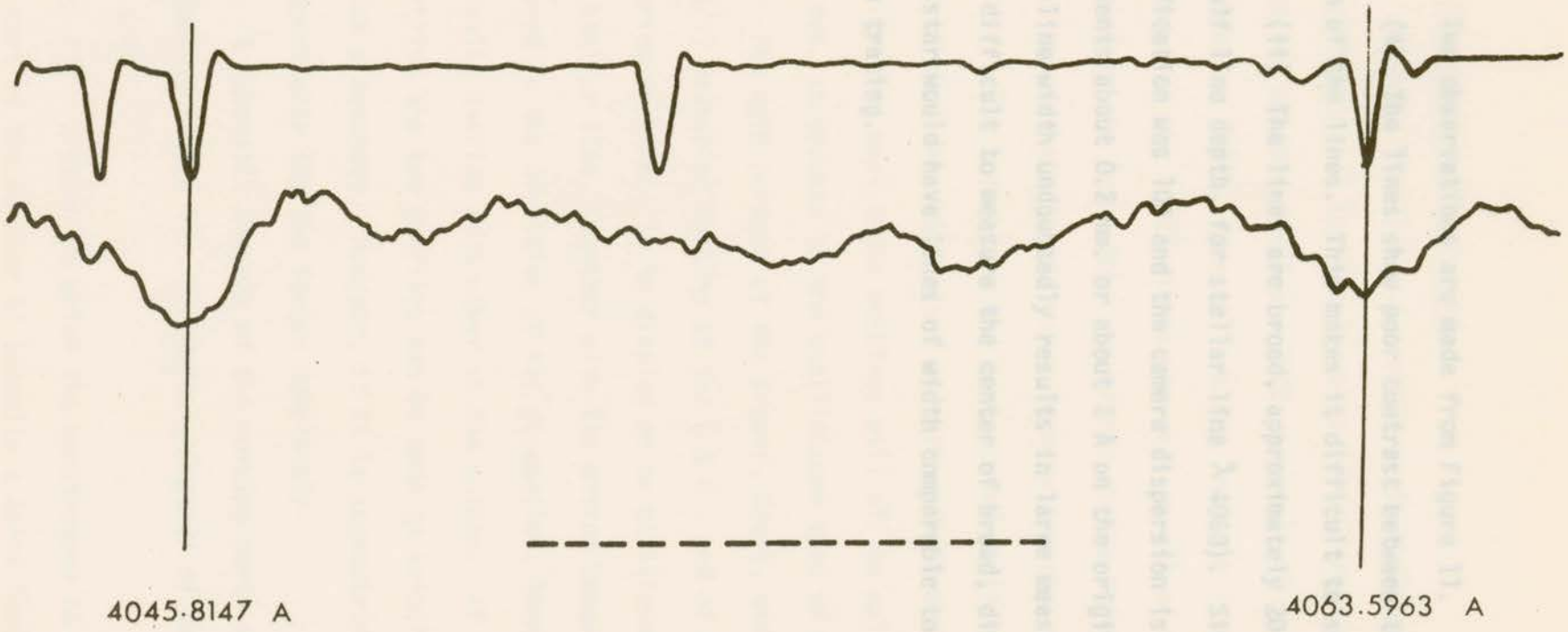

Figure 11. Intensitometer tracing of plate 3172 of μ Boo, between λ 4045 A and λ 4063 A.

Two observations are made from Figure 11.

(i) The lines show poor contrast between the continuum and the bottom of the lines. This makes it difficult to set on the features.

(ii) The lines are broad, approximately 20 mm. on the tracing (at half line depth, for stellar line λ 4063). Since the tracing magnification was 100 and the camera dispersion is 10 A/mm, this represents about 0.2 mm. or about 2 A on the original plate. This large line width undoubtedly results in large measuring errors, since it is difficult to measure the center of broad, diffuse lines. A sharp lined star would have lines of width comparable to the comparison lines in the tracing.

5.2 Measuring machines used

Andrews (1967) has described various plate measuring devices in use at the D.A.O. The machine used in this work to measure the high dispersion spectra (3263 and 3282 cameras) and some of the lower dispersion spectra (32121 camera) is shown in Plate 1 of his paper. The remainder of the 32121 plates, as well as all of the 21121 spectra were measured on the Zeiss Abbé comparator at the University of Victoria. It was assumed that there was a zero systematic error between the machines. The assumption has been proven valid by Scarfe who has measured the same sharp lined spectra on both machines. For the purposes of this work these machines will all be called visual measuring machines, as opposed to the oscilloscope type of machine described below.

The main purpose of the Brower, Grant, and Zeiss (abbreviated B.G.&Z.) measuring machine at the D.A.O., and of most oscilloscope measuring machines, is to display on an oscilloscope screen the profile of a stellar line, together with its mirror image. If the spectrogram is moved in the direction of its dispersion, then the two profiles will eventually overlap each other on the screen. If the star line is symmetric, the two profiles can be made to coincide almost completely by such a movement. However, if it is asymmetric, it is not possible to superimpose the two images completely.

A schematic diagram of the working parts of the B.G.&Z. machine is shown in Figure 12. The principal parts of the machine and their uses are:

(i) a bench on which the spectrogram to be measured is clamped. This part of the machine is actually a Zeiss Abbé comparator.

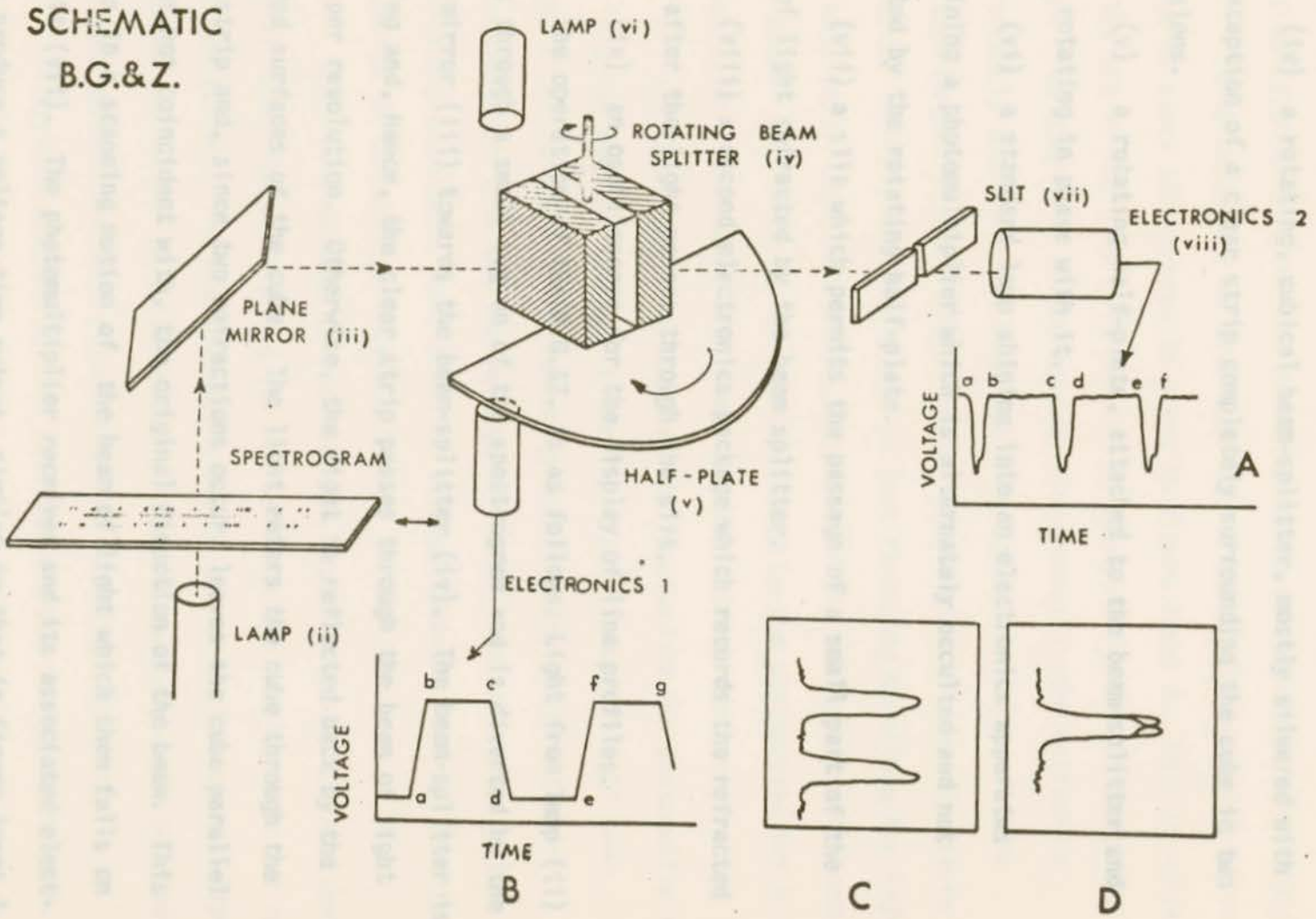

Figure 12. Schematic diagram of the B.G.&Z. oscilloscope machine.

(ii) a lamp which shines through the spectrogram.

(iii) a plane reflecting mirror.

(iv) a rotating, cubical beam-splitter, mostly silvered with the exception of a clear strip completely surrounding the cube in two dimensions.

(v) a rotating half-plate, attached to the beam-splitter and hence rotating in phase with it.

(vi) a standard lamp shining into an electronics apparatus containing a photomultiplier which is alternately occulted and not occulted by the rotating half-plate.

(vii) a slit which permits the passage of a small part of the beam of light refracted by the beam splitter.

(viii) a second electronics package which records the refracted light after the light passes through the slit.

(ix) an oscilloscope for the display of line profiles.

The operation of the B.G.&Z. is as follows. Light from lamp (ii) passes through a small region of the spectrogram and is diverted by the plane mirror (iii) towards the beam-splitter (iv). The beam-splitter is rotating and, hence, the clear strip passes through the beam of light twice per revolution. Otherwise, the light is reflected back by the silvered surfaces of the cube. The light enters the cube through the clear strip and, since two refractions occur, leaves the cube parallel to, but not coincident with, the original direction of the beam. This results in a scanning motion of the beam of light which then falls on the slit (vii). The photomultiplier receiver and its associated electronics produce a voltage-time output similar to that in figure inset A

Since the sweep across the slit (vii) is in the same direction, the line images given in figure inset A are exact repetitions of each other. This voltage is fed into the oscilloscope as the vertical input signal.

It is necessary to have some device which will produce a mirror image of every second profile given in figure inset A. This is achieved by the use of the lamp (vi) and the rotating half-plate (v). As the light from lamp (vi) shines towards electronics 1, the half-plate alternately chops off the beam and then leaves it unaltered. The voltage output of the photomultiplier electronics is shown in figure inset B. At 'a', the half-plate is just finishing occulting the light of lamp (vi). From 'a' to 'b', the edge of the half-plate cuts across the beam: the intensity of light received by the photomultiplier in electronics 1 increases with time, and the voltage increases. From 'b' to 'c', all the light from lamp (vi) is received by the photomultiplier. At 'c', the edge of the half-plate first cuts into the light beam. From 'c' to 'd', the light intensity entering the photomultiplier decreases with time and the voltage decreases. At 'd', lamp (vi) is completely occulted. Note that the voltage increase 'ab' is exactly opposite to the voltage decrease 'cd'.

When this voltage is fed into the oscilloscope as the horizontal signal, the line profile and its mirror image are displayed on the oscilloscope screen. The oscilloscope scans in one direction for the first profile and in the opposite direction for the second profile because the voltage applied has been reversed by the rotating half-plate.

A typical asymmetric line profile is shown in figure inset C. An asymmetric profile was drawn to show the reflected asymmetry. By moving

the spectrogram in the direction shown by the arrow, the two profiles can be made to coincide, as shown in figure inset D. Of course, one does not usually use asymmetric lines since it is not known what portion of the two images should be matched.

Comparison lines are measured by adjusting the mask (not shown, but situated between the cube and the slit) such that the stellar spectrum does not pass through the slit, but the comparison lines do.

When a spectrogram is measured, each line should be set upon three times, at least, and the average reading recorded. It is not necessary to measure both ways since the same two profiles should result if the plate were measured in the reverse direction. The remainder of the reduction to radial velocities is the same as for visual measurements.

5.3 Measurement of radial velocity and plate statistics

When one measures the radial velocity of a star from a spectrogram, he measures as accurately as possible the center of as many lines as are on his measuring program. (See for example Figure 7.) The measurer may or may not be able to measure all of the lines on his program, depending on the quality of the spectrogram and the type of star. In general, the lines will be shifted from their zero velocity position because of the relative non-zero radial velocity of the star (Equation (1.2.1)). The velocities obtained for each line should equal the plate velocity (either a weighted or unweighted average of all the line velocities) but measuring errors do occur, with the result that the line velocities scatter or disperse about this plate mean. This line-to-line scatter is called an "internal" error. Of course, it is assumed that the velocities of all the lines are the same. (For example, the iron lines do not have velocities different from those of the hydrogen lines.) The size of the internal error is a function of both the spectrograph dispersion and the width of the stellar lines, in the sense that low dispersion spectrograms and broad lined stars have larger internal errors associated with their measurement than do high dispersion spectrograms and sharp lined stars. (See for example Abt, 1968; Abt and Smith, 1969.)

The method used to measure a spectrogram has been described by Moore (1935). Each spectrogram was measured visually in the forward and reverse directions in the usual manner. The measurement of a single plate required about 1.5 hours. No more than two plates were measured on any day, since excessive eye fatigue resulted when more were attempted.

The reductions to radial velocities and plate statistics were done by hand, requiring about an hour. All the lines were given unit weight when measured and in the reductions.

Throughout this work, the subscript 'i' will always refer to lines and the subscript 'j' will always refer to plates. For each spectrum measured, j, the following statistics were calculated:

$$\bar{V}_j = \frac{\sum_{i=1}^{n_j} V_{ij}}{n_j} \quad \text{km/sec} \qquad (5.3.1)$$

$$\sigma_j = \sqrt{\frac{\sum_{i=1}^{n_j} (V_{ij} - \bar{V}_j)^2}{n_j - 1}} \quad \text{Km/sec} \qquad (5.3.2)$$

$$S.E.M._j = \frac{\sigma}{\sqrt{n_j}} \quad \text{Km/sec} \qquad (5.3.3)$$

where

$\bar{V}_j$ is the mean radial velocity of plate j with respect to the observer

V_{ij} is the velocity of the i^{th} line on the j^{th} plate

n_j is the number of lines measured on plate j

σ_j is the standard deviation of the line velocities on plate j

$S.E.M._j$ is the standard error of the mean of plate j

The plate mean radial velocity is the relative radial velocity of the source and observer. It is reduced to a heliocentric radial velocity as described in Appendix C. The final radial velocity of the star is recorded as

$$\bar{V}_{j_\odot} \pm S.E.M._j \quad \text{Km/sec}$$

Several plates were measured more than once by the author, both visually and with the oscilloscope machine, to provide consistency checks between the individual measurements (Section 8.3). Other measurers also measured several spectrograms (C. D. Scarfe measured visually while J. M. Fletcher used the B.G.&Z. machine), providing more data for more consistency checks (Section 8.3).

5.4 The measured radial velocity data

The radial velocity measurements, made visually by the author, of spectrograms of μ Boo are given in Table III. These will be called the 'Victoria data'. The measurements of twenty-nine 21121 spectra taken April 8, 1969 are not included in the table since they are discussed fully in Chapter 7. The column headings of Table III are self-explanatory. The method of obtaining the adjusted data in columns (6) and (7) is explained in Section 6.4.

One of the purposes of calculating the orbital elements of a binary star orbit is to be able to predict the radial velocity of the star at any time. Clearly, if those elements do not accurately predict the radial velocity of the star, then the elements must be in error. Since one of the objectives of this work was to determine the accuracy with which Abt's (1965) elements predict the radial velocity of μ Boo, the radial velocity of μ Boo as a function of time (i.e. the ephemeris) was calculated using his orbital elements.

TABLE III

RADIAL VELOCITIES OF μ BOO, MEASURED VISUALLY

(1) PLATE NUMBER	(2) JULIAN DATE 2400000.0+	(3) n_j	(4) RADIAL VELOCITY UNADJUSTED km/sec	(5) S.E.M. km/sec	(6) RADIAL VELOCITY ADJUSTED km/sec	(7) S.E.M. km/sec	(8) PLATE EMULSION	(9) CAMERA	(10) OBSERVER
(a) Coudé Plates									
692	38156.8333	7	-16.5	3.5	-14.5	2.4		3263	G
747	38169.7250	9	-14.3	2.8	-14.5	1.8		3263	An
830	38198.7819	9	-15.5	2.5	-17.5	1.9		3263	An
858	38221.8292	8	-14.6	4.5	-13.7	3.1		3263	R
874	38225.7188	9	-17.3	3.5	-16.5	1.7		3263	W
877	38226.7215	9	-18.0	4.0	-18.2	2.2		3263	An
1021	38302.6486	6	-16.8	3.6	-15.6	1.2		3263	Ba
2384	39206.9125	8	-12.2	2.5	-13.1	1.9		3282	H
2431	39231.9792	8	- 9.2	2.1	-10.4	1.2		3282	Ba
2498	39269.8646	8	-11.1	4.5	-11.0	1.5		3282	F
2515	39273.7875	8	-10.3	2.2	-12.5	3.0		32121	Sc
2583	39314.7285	8	-11.8	3.9	-11.7	1.1		3282	Ba
2624	39330.7056	7	-14.9	3.1	-13.2	1.3		3282	L
2633	39333.7083	8	-14.0	3.6	-13.3	1.3		3282	An
2634	39333.7292	8	-12.4	1.9	-12.1	1.7		3282	An
2639	39334.7181	9	-11.4	4.3	-10.2	1.8		3282	Sc
2691	39351.7556	10	-16.2	2.9	-15.4	1.3		3282	Sc
2890	39528.7936	6	-17.1	4.1	-16.9	2.2		3282	Ba
2890	39528.7936	8	- 8.9	4.6	- 8.6	3.4		3282	Ba
2891	39528.9917	8	-16.8	2.6	-13.9	1.1		3282	Ba

TABLE III (continued)

(1)	(2)	(3)	(4)	(5)	(6)	(7)	(8)	(9)	(10)
2891	39528.9917	9	- 9.1	3.4	-10.2	1.4		3282	Ba
2962	39554.0410	10	-12.9	3.9	-12.7	2.6	IIIO	32121	Sc
2962	39554.0410	11	- 9.4	3.5	- 9.6	1.3	IIIO	32121	Sc
2979	39555.0236	12	-12.9	3.3	-12.7	2.4		32121	Sc
2979	39555.0236	12	-14.3	3.6	-14.0	2.1		32121	Sc
3047	39612.8743	8	-10.9	3.8	-13.6	4.2	IIIO	32121	Sc
3077	39628.8604	9	-18.3	3.6	-16.8	1.6		32121	Ba
3118	39642.8979	8	-11.0	4.8	-11.4	2.9	IIIO	32121	F
3118	39642.8979	9	-11.5	4.9	-11.9	2.8	IIIO	32121	F
3172	39660.7583	10	-13.4	2.8	-14.7	2.0	IIIO	32121	Sc
3292	39708.7326	7	-12.1	3.8	-10.2	3.6	IIIO	32121	Sc
3769	39925.0083	10	- 9.7	3.1	- 9.6	3.1	IIIO	32121	Sc
3781	39936.0000	9	- 8.1	3.1	- 7.5	1.4	IIIO	32121	Sc
3807	39978.9146	10	-12.7	3.7	-12.6	4.4	IIIO	32121	Sc, Nh
3807	39978.9146	12	-11.9	3.6	-11.7	1.5	IIIO	32121	Sc, Nh
3807	39978.9146	11	-13.0	3.8	-12.2	1.5	IIIO	32121	Sc, Nh
3841	40004.8444	11	- 8.8	3.7	- 8.7	2.1	IIIO	32121	Nh
3850	40012.8854	10	-16.1	3.5	-16.2	1.4	IIIO	32121	Nh
3863	40036.7507	10	-11.9	3.4	-12.7	1.4		32121	Nh
3866	40036.9392	7	-12.7	5.5	-14.3	2.2		32121	Nh
3867	40036.9465	11	-11.2	4.2	-11.4	1.7		32121	Nh
3891	40058.7427	7	-13.4	6.4	-11.8	4.2	IIIO	32121	Nh
3937	40077.7215	10	- 6.2	3.6	- 5.9	2.8		32121	Nh
3980	40098.6653	11	-11.6	3.6	-11.7	1.3		32121	Ba
4056	40124.6441	11	- 9.3	3.4	- 9.4	1.7		32121	Nh
(b) Cassegrain Plates									
65240	40054.7263	6	-20.8	5.0				21121	Ba
65241	40054.7337	5	-15.3	5.6				21121	Ba

TABLE III (continued)

(1)	(2)	(3)	(4)	(5)	(6)	(7)	(8)	(9)	(10)
65274	40061.6989	8	-20.9	3.1				21121	An
65275	40061.7028	10	-16.4	3.2				21121	An
65284	40066.7299	5	-11.8	4.3			IIIaJ	21121	Sc, Nh
65285	40066.7351	6	-12.3	5.1			IIIaJ	21121	Sc, Nh
65286	40066.7410	6	-14.2	3.5			IIIaJ	21121	Sc, Nh
65287	40066.7472	11	-10.7	2.3			IIIaJ	21121	Sc, Nh
65288	40066.7538	9	-15.4	1.9			IIIaJ	21121	Sc, Nh

Plate emulsion, IIaO or IIaOb unless otherwise specified

OBSERVER CODE:

G	= F. Gutmann ;	An	= D.H. Andrews
R	= E.H. Richardson;	W	= K.O. Wright
Ba	= A.H. Batten ;	H	= R.E. Huffman
F	= J.M. Fletcher ;	Sc	= C.D. Scarfe
L	= E.K. Lee ;	Nh	= R.J. Niehaus

5.5 Calculation of the ephemeris

It is shown in Appendix A that the radial velocity, V, of a binary star is related to the elements of its orbit in the following way:

$$V = \gamma + K e \cos\omega + K \cos(v+\omega) \qquad \text{(A.1.14)}$$

where the symbols are defined in Appendix A. The true anomaly, v, which can be calculated using the following equations, is a complicated function of time, t. If T is the time of periastron passage,

$$M = \mu(t-T) = E - e\sin E \qquad (5.5.1)$$

$$\tan\left(\frac{v}{2}\right) = \sqrt{\frac{1+e}{1-e}}\ \tan\left(\frac{E}{2}\right) \qquad (5.5.2)$$

where M = mean anomaly

$\mu = 2\pi/\text{period}$

E = eccentric anomaly defined in Figure 13, below (after Van de Kamp, 1964)

These two equations may be solved for v in terms of t. However, the Allegheny tables (Schlesinger and Udick, 1912) provide the value of v for M in intervals of one degree and e in values of 0.01. These tables may be used to find v, and hence the radial velocity, as a function of time, using the known values of μ, T, and e.

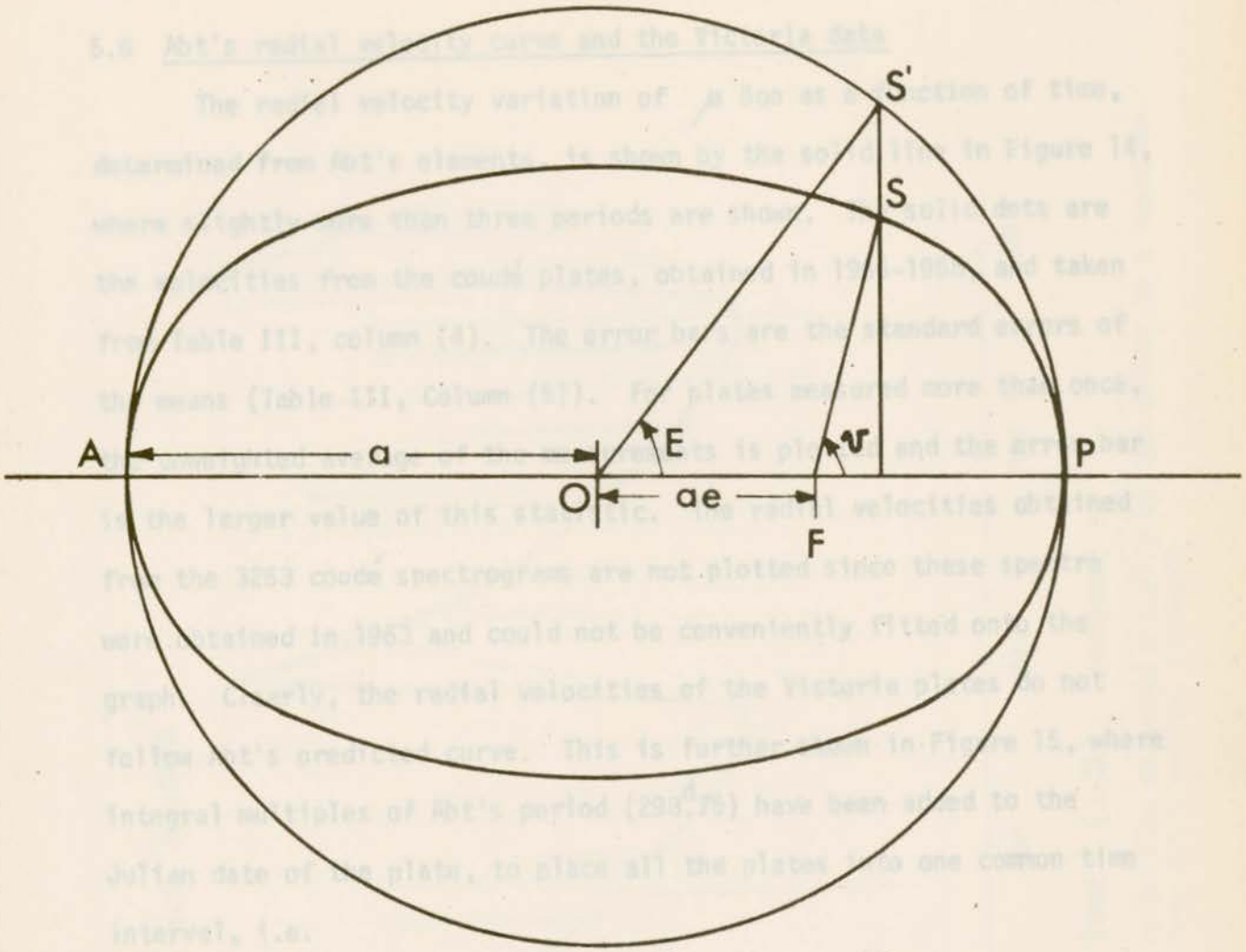

The star S moves in an elliptic orbit PSA about the focus F. The center of the ellipse, at O, is also the center of the auxiliary circle, PS'A, of radius 'a', which is tangent to the ellipse at the ends of the major axis, AP. A line perpendicular to PA passes through S and projects onto the auxiliary circle at S'. The eccentric anomaly, E, is defined to be the angle POS'; the true anomaly, v, is defined to be the angle PFS. They are related by Equation (5.5.2) in the text.

Figure 13. Relationship between the eccentric anomaly, E, and the true anomaly, v, in an elliptic orbit.

5.6 Abt's radial velocity curve and the Victoria data

The radial velocity variation of μ Boo as a function of time, determined from Abt's elements, is shown by the solid line in Figure 14, where slightly more than three periods are shown. The solid dots are the velocities from the coudé plates, obtained in 1966-1968, and taken from Table III, column (4). The error bars are the standard errors of the means (Table III, Column (5)). For plates measured more than once, the unweighted average of the measurements is plotted and the error bar is the larger value of this statistic. The radial velocities obtained from the 3263 coudé spectrograms are not plotted since these spectra were obtained in 1963 and could not be conveniently fitted onto the graph. Clearly, the radial velocities of the Victoria plates do not follow Abt's predicted curve. This is further shown in Figure 15, where integral multiples of Abt's period ($298^{d}.75$) have been added to the Julian date of the plate, to place all the plates into one common time interval, i.e.

$$2439850 < \text{J.D.} < 2440230$$

The 3263 velocities are included in Figure 15. Two points should be noted:

(i) The variation in plate means is not large and, hence, it is possible that the radial velocity of μ Boo is indeed constant, and the scatter of the plate mean velocities about this constant velocity is due to measuring errors.

(ii) The errors of the plate measurements are possible larger than would be expected, owing to possible wavelength errors. Systematic effects described in Section 3.4 would thereby be introduced. The root

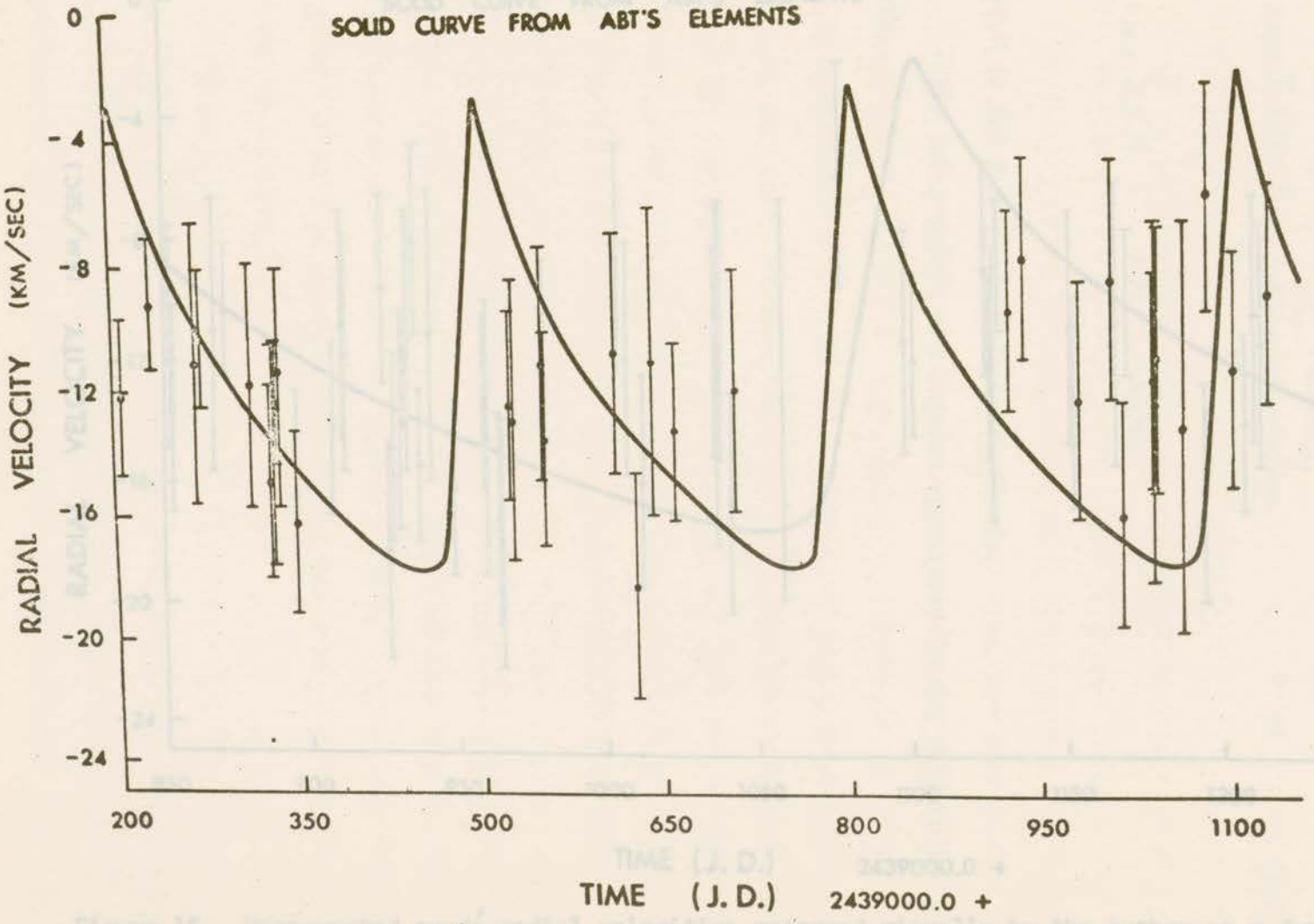

Figure 14. Uncorrected coudé radial velocities measured visually by the author as a function of time. Solid curve is derived from Abt's orbital elements.

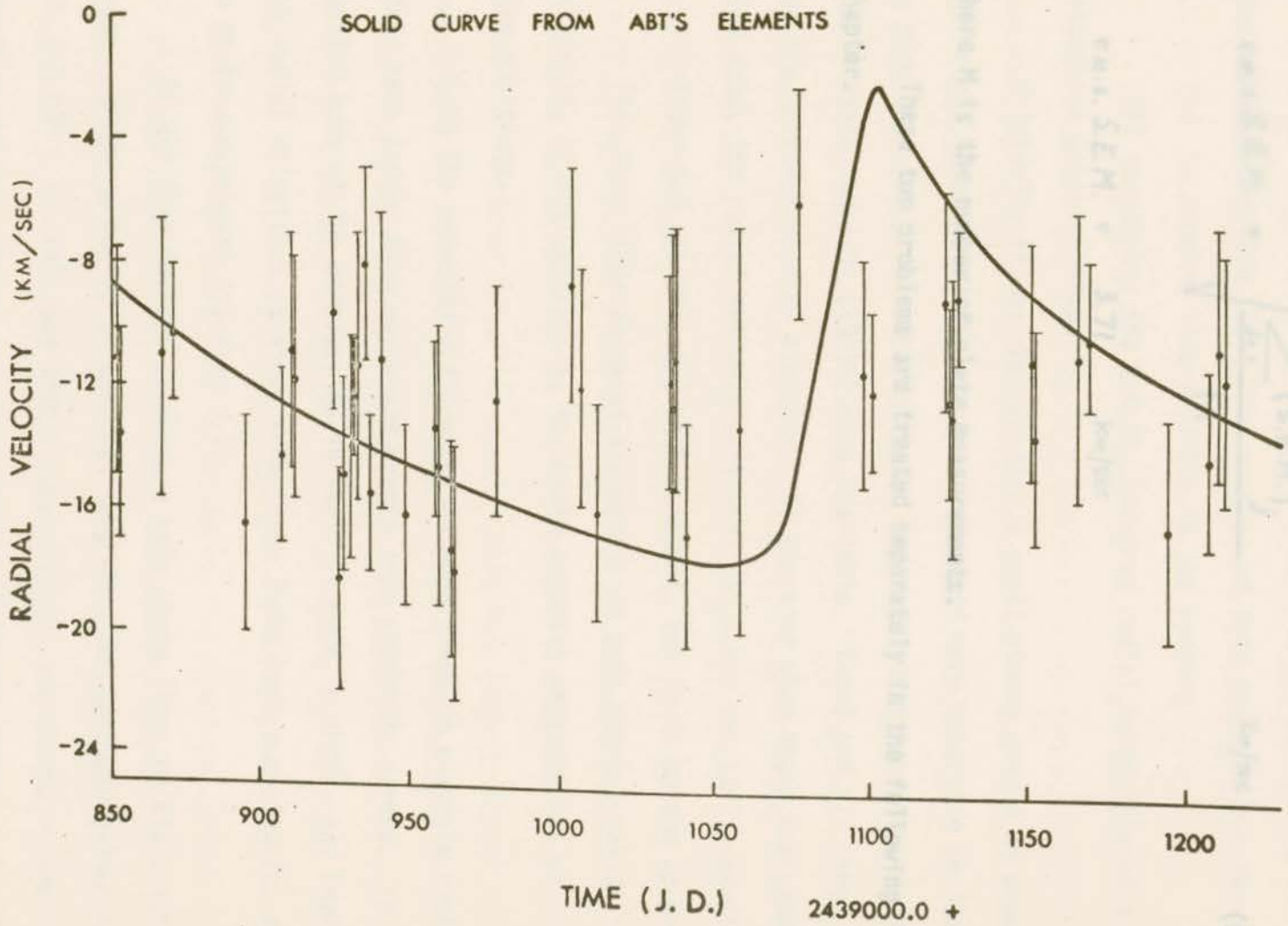

Figure 15. Uncorrected coudé radial velocities measured visually by the author as a function of phase in Abt's orbit.

mean square standard error of the mean, r.m.s.S.E.M. is

$$\text{r.m.s. S.E.M.} = \sqrt{\frac{\sum_{j=1}^{M} (\text{S.E.M.})_j^2}{M}} \quad \text{Km/sec} \qquad (5.6.1)$$

$$\text{r.m.s. S.E.M.} = 3.71 \quad \text{Km/sec}$$

where M is the number of plate measurements.

These two problems are treated separately in the following chapter.

5.7 The B.G.&Z. measurements of J. M. Fletcher and of the author

Mr. J. M. Fletcher of the D.A.O. staff kindly measured some spectrograms of μ Boo with the B.G.&Z. oscilloscope machine at the D.A.O. (described in Section 5.2). The purpose of this exercise was two-fold:

(i) to examine line profiles in the spectra

(ii) to compare the B.G.&Z. measured radial velocities with velocities measured visually.

Originally it was thought that a small binary period of about ten days might be detected if the plates measured were separated in time by no more than about one hundred days. Seven spectrograms taken between J.D. 2439269 and J.D. 2439351 were available. These and six other spectra were measured by Fletcher. At the time when these measurements were made, the radial velocity variation of μ Boo was still undecided.

After two spectrograms were measured, two facts became apparent:

(i) Many lines appeared asymmetric to some degree, making it difficult, if not impossible, to obtain accurate measurements of the line positions.

(ii) The velocity differences between lines on a single plate was often much larger than one would expect from measuring errors. This implied some of the wavelengths in Table II were in error, and therefore, the radial velocities obtained from these lines have a systematic error in their measurement (Section 3.4).

It was then decided to measure only three lines on all spectrograms. Since μ Boo is of spectral type F0V, the hydrogen Balmer lines Hδ and Hγ ($\lambda\lambda$ 4101 and 4340 A respectively) are strong in the spectrum and were chosen for measurement. A strong neutral iron line

which often appeared very symmetric to the eye was also used (λ 3878 A). If the radial velocity of μ Boo is varying, then each of these three lines should produce the same radial velocity curve, separated only in systemic velocity, if the wavelengths are incorrect. (See Binnendijk, 1967.)

With only three lines measured on each plate, the formal errors of measurement, i.e. σ_j, S.E.M.$_j$, are bound to be large, and will be artificially large if wavelengths are incorrect. Thus it is difficult to estimate the measurement error associated with the radial velocity of a single line. More will be said, in Chapter 8, about this internal error, but for now it is sufficient to say that an error as large as 2.5 to 3.0 km/sec could be obtained with this type of broad lined star. It must be kept in mind that the lines are very broad and the emulsion is often very grainy, (Figure 11).

It was noticed, after several plate measurements, that the radial velocities determined from Hδ and Hγ generally agreed with each other, while at other times there was a vast difference between them. There were apparently no minor plate defects near Hγ (for example an emulsion shift) because the two comparison lines ($\lambda\lambda$ 4325 and 4348 A) fell on the smooth correction curves for the spectrograms in question. One suggestion is that a weak line in the wing of Hγ (a TiII line, λ 4337.916 A from Moore's Multiplet table) has a varying effect on the Hγ profile, caused by varying degrees of exposure between the plates. A less exposed plate would tend to increase the importance of this titanium line in the broad violet wing of Hγ .

The velocity of the FeI line, λ 3878, differed from that obtained

for Hδ by an amount that varied very little from plate-to-plate, but that was much larger than the scatter of the velocities of either line. The adopted wavelength of λ 3878 is undoubtedly incorrect.

The line velocities, corrected to the sun, for the plates measured by Fletcher are given in Table IV. The column headings are self-explanatory. Plates 2583 and 3077 were each measured twice by Fletcher and the velocities in Table IV are the averages of the two measures. The individual velocities were used for the measuring error analysis described in Chapter 8. Plates 65274 and 65275 were obtained only five minutes apart and, therefore, the velocities given for the three lines are averages of the two plates. It is assumed that the velocity of the star did not vary in the five minute interval.

The range of velocities of any particular line from plate-to-plate is so small that any of the lines would be a reasonably good 'standard velocity line', when measured with the B.G.&Z. However, it was found that if the Hδ velocities are gathered into a time interval representing one period of $25^{d}.96$, then they follow very closely a nearly sinusoidal variation of total amplitude about 7 km/sec. (This can be done by defining the phase, ϕ, as the decimal part of

$$(\text{J.D.}_{\text{observation}} - \text{J.D.}_{\text{plate 2498}}) = nP + \phi$$

where n is an integer.)

The largest difference, |curve - measurement| , was about one km/sec. From these data, it appeared that the radial velocity of Hδ was varying. Unfortunately, the range was small and the other lines measured and

TABLE IV

HELIOCENTRIC RADIAL VELOCITIES OF SELECTED LINES MEASURED BY FLETCHER WITH THE OSCILLOSCOPE MACHINE OF THE D.A.O.

VELOCITIES IN KM/SEC

PLATE	WAVELENGTHS (A)			CAMERA
	3878.580	4101.737	4340.475	
2498	-21.7	- 7.3	- 5.2	3282
2583	-20.3	- 9.7	- 9.6	3282
2624	-17.4	- 2.6	-10.8	3282
2633	-20.8	- 6.5	- 4.7	3282
2634	-22.8	- 7.6	- 7.1	3282
2639	-22.3	- 7.1	- 6.6	3282
2691	-18.4	- 3.9	- 9.7	3282
3077	-18.4	-10.7	- 9.1	32121
3850	-22.7	- 9.5	-12.4	32121
3891	-18.3	- 4.9	- 2.8	32121
65274-5	-18.7	- 6.8	-10.0	21121
3980	-20.9	- 7.3	- 7.6	32121

combination of the three lines, showed no such periodic behaviour with this period. To clarify the variation further, the author measured the radial velocity of several plates of μ Boo on the B.G.&Z.

These plates had all been taken at times corresponding approximately to the phases of maximum and minimum in the velocity curve, and thus provided a test of its validity. Seventeen spectra in all were measured by the author using the B.G.&Z. machine. Some of the plates had already been measured by Fletcher - these duplicate measurements provide more data for the consistency checks of Chapter 8. As many lines as possible, from Table II, were measured since it was felt desirable to compare the author's B.G.&Z. measurements with the author's visual measurements as well as with Flethcer's measurements.

The author's oscilloscope radial velocity data for the same three lines are shown in Table V. When these Hδ velocities are plotted on the previous graph exhibiting sinusoidal variation, they do not follow the curve and, hence, destroy the observed variation. It is concluded that the variation arose purely by chance and the velocity of any particular line is constant. This constant velocity and the standard deviation for each of the three lines is:

$$\bar{V}_i = \frac{\sum_{j=1}^{M} V_{ij}}{M} \qquad (5.7.1)$$

TABLE V

HELIOCENTRIC RADIAL VELOCITIES OF SELECTED LINES MEASURED BY THE AUTHOR WITH THE OSCILLOSCOPE MACHINE OF THE D.A.O.

VELOCITIES IN KM/SEC

PLATE	WAVELENGTHS (A)			CAMERA
	3878.580	4101.737	4340.475	
2384	-20.4	- 8.6	-12.0	3282 slit
2583	-22.9	- 9.0	-11.9	3282 slit
2633	--	- 4.6	- 9.1	3282 slit
2634	-21.7	- 6.1	- 5.7	3282 slit
2639	-24.3	--	- 6.1	3282 slit
3077	-19.6	-12.9	-11.9	32121 slit
3118	-12.3	- 4.0	--	32121 slit
3769	-15.0	- 4.5	- 8.4	32121 IS
3781	-16.9	- 5.0	- 6.9	32121 IS
3807	-15.3	- 8.6	- 7.6	32121 IS
3841	-20.0	- 8.3	- 4.9	32121 IS
3863	-21.4	- 7.7	- 5.4	32121 IS
3866	-27.9	- 4.2	- 9.1	32121 IS
3867	-15.3	- 9.4	- 4.2	32121 IS
65286	-18.8	-19.8	-12.3	21121 slit
65287	-21.2	-15.4	- 6.0	21121 slit
65288	-17.6	-10.9	12.1	21121 slit

IS = image slicer

$$\sigma_i = \sqrt{\frac{\sum_{j=1}^{M} (V_{ij} - \bar{V}_i)^2}{M-1}} \qquad (5.7.2)$$

$$S.E.M_i = \frac{\sigma_i}{\sqrt{M}} \qquad (5.7.3)$$

where $\bar{V}_i$ is the average radial velocity of line i

M is the number of plates on which the line was measured (combining data from Tables IV and V)

These results are found in Table VI. This is a plate-to-plate estimate of the error and is called an 'external' error. In order for the statistics of Table VI to have any meaning, it must be remembered that a constant velocity has been assumed for each of the three lines.

It is worth noting that in Table V, occasionally a line velocity is very different from what is expected; for example the Hγ measurement on plate 65288, the Hδ measurement on plate 65286, or the λ 3878 measurement of plate 3866. There are, of course, two explanations:

(i) the velocity of the line is variable. This is unlikely since, in each case, there are one or more spectra taken only a few minutes away which show 'normal' line velocities. Also, other lines on the same plate are not variable and there is no reason to suspect the above lines are any different.

TABLE VI

RADIAL VELOCITY STATISTICS OF SELECTED LINES
MEASURED WITH THE OSCILLOSCOPE MACHINE
OF THE D.A.O.

	WAVELENGTH (A)			
	3878.580	4101.737	4340.475	
$\bar{V}_i$	-19.76	- 7.96	- 7.32	km/sec
σ_i	3.22	3.70	4.62	km/sec
S.E.M.$_i$	0.61	0.70	0.88	km/sec
M	28	28	28	

(ii) measuring errors. This is quite likely since the author had not used the oscilloscope machine previously and it is possible that a slightly incorrect setting was made or that the wrong part of a slightly asymmetric profile was measured. Such large discrepancies did not occur in Table IV probably because Fletcher has had a great amount of experience with this particular machine.

It is easy to see that wavelength errors exist, especially for λ 3878. The two hydrogen line mean velocities are essentially the same, but the iron line yields velocities approximately 11 km/sec more negative than the hydrogen lines. This large difference lends support to the somewhat arbitrary adjustments performed later in Sections 6.3 and 6.4.

CHAPTER 6

STATISTICS

6.1 Introduction

It is clear that the variation in the measured radial velocity of μ Boo is not large (Table III, page 53; Figure 14, page 59), and that the estimates of the internal errors of measurements (Table III, column (5)) are large so that they tend to mask any possible variation.

It has also been shown in the last chapter that the incorrect wavelength for the iron line (λ 3878.580 A) has probably been adopted. (The same can possibly be said about the two hydrogen lines, H δ and H γ used in the last chapter.) Many of the wavelengths used for the radial velocity measurements of μ Boo (Table II) have a useful range ending with F0. Since μ Boo is of spectral type F0V, it is possible that some of these wavelengths do not apply to this particular star because many neighboring lines are rotationally blended together. Therefore, the possibility that some of the wavelengths are incorrect must be considered. If this is true, then systematic errors in the line velocities occur (Section 3.4) and, as a result, the internal plate statistics (σ_j and S.E.M.$_j$) are no longer true estimates of random measuring errors. Such non-random effects would invalidate any statistical test for variability which uses the internal error as an estimator of the scatter of the velocities.

6.2 Use of the sharp lined star μ Orionis to find lines that might be blended in μ Boo

To investigate further the degree to which lines are blended together by the axial rotation of μ Boo, the spectrum of the sharp-lined late A-type star μ Orionis was examined. A well exposed spectrogram taken in 1966 by Scarfe was measured for radial velocity, by the author, using the Abbé comparator at the University of Victoria. The position of all features in the spectrum of μ Orionis near the wavelengths used in μ Boo were measured as accurately as possible. By using the plate mean radial velocity, calculated from nine lines of Batten's wavelength table, it was possible to work backwards and determine the approximate wavelengths of the other lines measured. A search in Moore's Multiplet Table (Moore, 1945) provided accurate laboratory wavelengths of the unidentified lines. The measured lines were considered identified if one of the laboratory wavelengths resulted in a velocity approximating the plate mean. These lines numbered twenty-seven. In some cases, two or three transitions of different elements were separated only by a few hundredths of an Angstrom. Since the spectrograph could not resolve these transitions even if they all did occur, they were labelled "blended". These features could still be contributing to the blending in μ Boo, however. The plate velocity measured by the author using the twenty-seven identified lines and the original nine lines was, within measuring errors, equal to that measured by Scarfe who used wavelength tables supplied for the 3263 and IIM cameras.

The result found in this investigation was that, in nearly every case, in the spectrum of μ Orionis, there were some absorption features at wavelengths very close to those wavelengths used in μ Boo. The lines in the spectrum of μ Boo are undoubtedly blends of these individual lines.

6.3 Calculation of line residuals

We now look at a method by which we determine whether the measured line velocities on a plate all differ randomly from the plate mean, or whether some of them are systematically affected by wavelength errors.

Each line velocity, V_{ij}, on a particular plate, j, differs from the plate mean, $\bar{V}_j$, by a residual, R_{ij}, where

$$R_{ij} = \left(V_{ij} - \bar{V}_j \right) \quad \text{Km/sec} \qquad (6.3.1)$$

The above calculations are performed for every line (i running from one to about twelve) on every coudé plate measurement (j running from one to M). Each line has an overall residual, R_i, and a residual dispersion, σ_i, as follows:

$$R_i = \frac{1}{M} \sum_{j=1}^{M} R_{ij} \quad \text{Km/sec} \qquad (6.3.2)$$

$$\sigma_i = \sqrt{\frac{\sum_{j=1}^{M} (R_{ij} - R_i)^2}{M-1}} \quad \text{Km/sec} \qquad (6.3.3)$$

$$\text{S.E.M.}_i = \frac{\sigma_i}{\sqrt{M}} \quad \text{Km/sec} \qquad (6.3.4)$$

where M is the number of plate measurements.

If all the wavelengths are correct, then we expect R_{ij} to be positive as often as it is negative, i.e. that all $R_i \approx 0$ km/sec. Then σ_i is a measure of random measuring errors associated with the i^{th} line.

If, however, one or more of the wavelengths are incorrect, then we do not expect all $R_i \approx 0$ km/sec. Furthermore, the non-random errors in the line velocity measurements, which the wavelength errors produce, will show up in the residuals, R_{ij}. Naturally, if not all the wavelengths are correct, then the plate means $\overline{V}_j$, may be somewhat in error, and, as a result, each residual R_{ij} does not wholly reflect errors in wavelengths. Averaging R_{ij} over M measurements should determine whether or not a wavelength error exists for any particular line.

6.4 Analysis of line residuals for coudé spectrograms and the t-test

The calculated line residuals, (6.3.1), are given in Tables VII, VIII, and IX, where the calculations were performed for the three coudé cameras separately. Blanks in the tables indicate those lines that were, for some reason, not measured on those plates. Columns (2) through (13) are the wavelengths of the lines used (Table II, page 23). The plates which were measured more than once are included in the tables as separate measurements. In the lower portion of the tables, the overall line residuals, R_i, and their dispersion statistics, given by Equations (6.3.2), (6.3.3) and (6.3.4) are shown. The variable 't' and the letters 'Y' and 'N' are defined below.

It is now necessary to decide whether or not each $R_i \pm \sigma_i$ is significantly different from zero (the value expected if correct wavelengths were used). To do this, a "t-test" is applied to the mean residuals, R_i. The t-test is used to determine whether the apparent difference between two means is real, or could have occurred by chance. Examples of its use are given by Lacey (1953). The null hypothesis used in all the calculations in this work is that each of the mean residuals, R_i, is zero, and any deviation from this value is a matter of chance. Using the t-test, one must determine the probability that the observed deviations, R_i, could have occurred by chance. It is implicitly assumed in this test that the line residuals are Normally distributed with standard deviation σ_i, about the overall line residual, R_i. The variable 't' is formally defined as:

$$t = \frac{\bar{x} - \mu}{\sigma_{\bar{x}}} \qquad (6.4.1)$$

TABLE VII

LINE RESIDUALS, 32121 SPECTRA, NO ADJUSTMENTS

RESIDUAL (LINE - MEAN) KM/SEC

(1)	(2)	(3)	(4)	(5)	(6)	(7)	(8)	(9)	(10)	(11)	(12)	(13)
						WAVELENGTH (A)						
PLATE NUMBER	3878	3933	4005	4030	4045	4063	4101	4215	4325	4340	4351	4549
2515	- 7.1		- 2.3	0.8	0.8		4.5	12.3			- 6.2	- 2.6
2962	- 6.5		24.3	- 4.4	- 8.1	2.6	2.1	18.7	-10.6		- 8.3	-10.0
2962	- 9.5	- 2.4	20.9		-13.0	-10.9	3.9	16.7	-12.6	7.1	0.2	- 0.1
2979	- 6.1	- 8.7	26.3	- 5.5	- 0.1	-18.7	5.5	7.6	-17.1	10.3	7.6	- 1.5
2979	- 7.5	1.6	27.2	- 7.7	- 1.5	-19.3	5.6	1.9	-11.5	6.1	6.2	- 1.5
3047	14.3		11.8	-10.9	- 8.5		-15.0	3.0		6.0	- 1.0	
3077	- 9.1		19.8	- 9.8	- 9.0	- 5.1	1.8		- 8.3		10.7	9.4
3118	- 7.6		18.6	-12.6	-20.1	- 5.0	11.4	11.9	3.1			
3118	5.2	-20.4	17.3		-19.1	-10.4	10.2		- 8.9	13.2	13.1	
3172	- 6.1		3.0	- 8.4	- 8.3		4.4	10.8	- 5.7	15.3	4.1	- 9.4
3292	- 5.2				- 6.0	1.6	-13.4	15.7	- 3.1		10.1	
3769	- 6.9		- 8.2	1.9	0.4	-14.5	8.9	5.7	- 10.7		16.0	7.7
3781	- 7.0		10.4	- 2.4	-11.7	- 2.3	- 0.6	10.8			-10.1	12.7
3807	- 3.4		-24.3	1.7	-11.1	7.7	15.2	6.4	- 6.8		6.5	8.0
3807	- 8.1	-10.9	15.3	- 2.9	-19.4	-10.3	16.6	11.4	-14.7	5.7	13.4	3.9
3807	- 8.9	- 9.4	20.3	2.1	-16.0	- 7.6	11.5	9.7	-17.0		12.5	3.1
3841	-13.6	-16.5	14.2	7.3	- 4.8	- 2.5	- 2.5	22.8	-12.9	6.0		2.2
3850	- 9.0			- 1.7	-10.0	-14.4	10.3	20.3	- 8.2	3.7	- 0.5	9.7
3863	- 9.5	-16.4	4.0		-13.4		9.7	15.5	- 7.9	8.6	5.0	4.0

TABLE VII (continued)

(1)	(2)	(3)	(4)	(5)	(6)	(7)	(8)	(9)	(10)	(11)	(12)	(13)
3866					-19.9		2.6	14.7	-21.6	8.3	8.9	7.3
3867	- 6.0	-18.0	15.8		-18.4	- 4.8	11.5	15.8	-18.5	9.9	2.5	10.5
3891	- 2.7	- 7.2	19.5			-15.7	27.5		-16.0		- 5.5	
3937	- 4.7	- 4.8	4.2		-20.6	13.3	0.1	13.5	-13.1	1.6		12.3
3980	-12.5	- 2.2	18.3		-12.0	- 8.3	3.7	15.0	-19.1	5.4	7.5	4.3
4056	-12.2	2.7	11.6		-16.2	- 4.9	- 1.1	17.0	-16.4	5.3	10.2	4.4
R_i	- 6.66	- 8.66	12.18	- 3.50	-11.08	- 6.48	5.38	12.60	-11.70	7.50	4.68	3.72
σ_i	5.22	7.55	12.21	5.68	6.84	8.47	8.84	5.39	5.81	3.56	7.45	6.44
S.E.M.$_i$	1.06	2.09	2.60	1.46	1.40	1.89	1.77	1.15	1.24	0.92	1.59	1.44
M	24	13	22	15	24	20	25	22	22	15	22	20
t	6.28	4.16	4.68	2.40	7.91	3.43	3.04	10.96	9.43	8.15	2.94	2.58
	Y	Y	Y	Y	Y	Y	Y	Y	Y	Y	Y	Y

TABLE VIII

LINE RESIDUALS, 3282 SPECTRA, NO ADJUSTMENTS

RESIDUAL (LINE - MEAN) KM/SEC

(1)	(2)	(3)	(4)	(5)	(6)	(7)	(8)	(9)	(10)	(11)	(12)	(13)
					WAVELENGTH (A)							
PLATE NUMBER	3878	3933	4005	4030	4045	4063	4101	4215	4325	4340	4351	4549
2384	- 6.7	2.5	3.9				3.1	8.5	-10.6	6.4		- 7.0
2431	-10.4	- 1.8	4.9		- 4.7		8.0	2.7		4.3		- 3.0
2498	-14.6	5.0	19.4		-10.2		8.2		-14.8	10.0		- 2.8
2583	-17.3	4.2	14.9		- 7.8		8.0		-11.1	7.0		2.1
2624	-10.2	9.8		- 2.9	- 6.8		8.1		- 5.1	7.3		
2633	- 6.7	5.6	6.4	0.4	- 9.9		13.7		-16.9	7.5		
2634	-11.9	2.4	4.7		- 1.3	- 1.3	3.4			2.7		1.0
2639	-13.9	6.1	22.7	- 1.2	- 9.0	-10.5	3.5		-11.9	14.5		
2691	- 7.3	4.5	7.8	3.8	-12.8	- 4.0	8.5	4.9	-15.7		9.9	
2890		- 4.4			- 3.0	-15.8	11.6	1.5		9.9		
2890		- 2.9			-10.3	-18.1	6.4	22.8	- 9.9	5.8	6.3	
2891	- 5.7	5.4			- 5.7	- 9.3	11.3		- 4.3	2.5		5.5
2891	-11.1	4.4	16.8		-11.4	-11.6	1.8			- 1.5	12.4	0.4
R_i	-10.52	3.14	11.23	0.03	- 7.74	-10.09	7.35	8.08	-11.14	6.37	9.53	- 0.54
σ_i	3.73	3.99	7.20	2.85	3.52	5.97	3.62	8.65	4.37	4.15	3.07	4.07
S.E.M.$_i$	1.12	1.11	2.40	1.43	1.01	2.26	1.00	3.87	1.46	1.20	1.77	1.54
M	11	13	9	4	12	7	13	5	9	12	3	7
t	9.39	2.83	4.68	0.02	7.36	4.46	7.35	2.09	7.63	5.31	5.38	0.35
	Y	Y	Y	N	Y	Y	Y	N	Y	Y	Y	N

TABLE IX

LINE RESIDUALS, 3263 SPECTRA, NO ADJUSTMENTS

RESIDUAL (LINE - MEAN) KM/SEC

(1)	(2)	(3)	(4)	(5)	(6)	(7)	(8)	(9)	(10)	(11)	(12)	(13)
					WAVELENGTH (A)							
PLATE NUMBER	3878	3933	4005	4030	4045	4063	4101	4215	4325	4340	4351	4549
692	- 5.5	4.0	6.9		2.6	- 2.9			-16.8	11.5		
747	-18.2	11.1	- 1.5		- 2.6	2.2	1.9		- 4.0	2.7	8.6	
830		-14.0	- 5.2	- 3.3	2.4	- 2.0	6.2		- 0.9	7.0	10.1	
858	-14.1	2.1			-11.7	- 8.6	9.9	17.2	- 9.6	14.7		
874	-21.3	- 4.0	10.8		- 2.5	4.9	9.5	1.3	- 9.0	10.6		
877	-20.3	- 9.4			- 3.7	4.2	9.3	13.8	-12.7	10.5	8.5	
1021	-14.9				4.4	- 2.4	7.6		- 3.3	8.5		
R_i	-15.72	- 1.70	2.75	- 3.3	- 1.59	- 0.66	7.40	10.77	- 8.04	9.36	9.07	
σ_i	5.76	9.24	7.38		5.44	4.75	3.03	8.37	5.65	3.80	0.90	
S.E.M.$_i$	2.35	3.77	3.69		2.06	1.80	1.23	4.83	2.14	1.44	0.52	
M	6	6	4		7	7	6	3	7	7	3	
t	6.69	0.45	0.75		0.77	0.37	6.02	2.23	3.76	6.50	17.44	
	Y	N	N		N	N	Y	N	Y	Y	Y	

where $\bar{X}$ is the observed sample mean (R_i km/sec)

μ is the true population mean (0 km/sec)

$\sigma_{\bar{x}}$ is the standard error of the mean of the observed sample ($\sigma_i/\sqrt{M}$)

In our case, we use the absolute value of t, thus

$$t = \frac{|R_i|}{\sigma_i/\sqrt{M}} = \frac{|R_i|}{S.E.M._i} \qquad (6.4.2)$$

Hence, t is the amount in standard deviation of the mean units by which the overall residual differs from the value implied by the null hypothesis (0 km/sec).

The variable $t = \frac{\bar{x}-\mu}{\sigma_{\bar{x}}}$ is not distributed Normally, but is distributed according to a frequency function known as "Student's t distribution". (Lacey, 1953, page 102). The standard deviation of the distribution does not occur in its equation (in the Gaussian distribution for example, it does), but the number of cases, M, does and, hence, is a parameter of the distribution. Particular probability values will, therefore, depend on the number of cases making up the mean ($\bar{X}$) whose significance is to be tested. One would, therefore, need an infinite number of tables of t, one for each M. Rather than do that, a single table with fixed probabilities (0.05 and 0.01) is used, i.e. the results are significant at the 5% level if the probability of obtaining as discrepant a difference is less than 0.05 or the results are significant at the 1% level if the probability of obtaining the discrepant result is less than 0.01. Examples of such a table used

are found in Lacey (1953, Table C) and Alder et al. (1968, Table II). The calculated values are compared to the tabulated values for M-1 degrees of freedom.

Application of the t-test to each of the mean residuals in Tables VII, VIII and IX resulted in significant differences at the 5% level in the majority of cases. (The last line of the three tables show Y⇒ significant and N⇒ not significant.) A generous level of 5% (rather than 1%) was used since the R_i are only an approximate indication of a discrepancy, stemming from the fact that $\bar{V}_j$ and, hence, R_{ij} may be in error.

Since some of the overall residuals were non-zero, it was assumed that the non-zero residuals had arisen from the use of incorrect wavelengths. This was a reasonable assumption in the light of the μ Orionis investigation. For those lines for which R_i proved to be significantly different from zero, an empirical correction was made to the velocities by subtracting R_i from all the velocities of the i^{th} line. For those lines for which R_i was not significantly different from zero, no correction at all was made.

These adjustments will remove, <u>on the average</u>, the contributions to the line velocities from systematic wavelength errors. Ideally the incorrect wavelengths themselves should be adjusted, but by adjusting the velocities, essentially the same correction is made. The velocities, obtained from different lines will be more consistent than before and the mean obtained from these lines will have a small formal error which should be a reliable estimate of the error of measurement. The resulting plate mean velocity will probably not be reliable, owing to

the semi-arbitrary nature of the adjustments. However, the variation of the adjusted means from plate-to-plate should not be greatly changed. The adjusted unweighted plate mean is given by

$$\bar{V}_{j_{adj.}} = \sum_{i=1}^{n_j} \frac{V_{ij\,adj}}{n_j}$$

$$= \sum_{i=1}^{n_j} \frac{(V_{ij} - R_i)}{n_j} = \sum_{i=1}^{n_j} \frac{V_{ij}}{n_j} - \sum_{i=1}^{n_j} \frac{R_i}{n_j}$$

$$\bar{V}_{j_{adj}} = \bar{V}_{j_{unadj}} - \left(\sum_{i=1}^{n_j} \frac{R_i}{n_j} \right)$$

This equation is correct if R_i is taken to be identically zero for those lines for which it was found not to be significantly different from zero. Now $\sum_{i=1}^{n_j} R_i/n_j \approx 0$ if all line residuals are used, (e.g. 32121 camera Table VII, $\sum_{i=1}^{12} \frac{R_i}{12} \approx -0.1$ km/sec) and the adjusted and unadjusted velocities yield the same plate mean.

But most plates, not all 12 lines were measured, therefore, $\sum_{i=1}^{n_j} R_i/n_j$ was not necessarily zero and, in these cases, the new plate mean differed from the old plate mean. The largest differences occurred when $\left| \sum_{i=1}^{n_j} \frac{R_i}{n_j} \right|$ for some j was large, i.e. whenever lines with overall residuals of the same sign were omitted in the original measurement.

After every line velocity had been adjusted, the entire process was repeated, i.e. new $\bar{V}_j$, σ_j, S.E.M.$_j$, R_{ij}, R_i, σ_i, t were calculated. The results are given in Tables X, XI, and XII for the three cameras separately. The tables are set out in the same format as the three previous tables. The new plate means and their standard errors are found in Table III, columns (6) and (7) (page 53).

We make three observations:

(i) All R_i are equal to zero, statistically, as given by a further application of the t-test.

(ii) The internal error per plate has been reduced considerably by this adjustment by residuals. The root-mean-square standard errors of the means for the unadjusted and adjusted data are given in Table XIII below. The new r.m.s.S.E.M.'s are more indicative of the true measuring errors with wavelength errors eliminated.

(iii) The plate-to-plate scatter has not been reduced artificially by this process, as is shown in Table XIV below.

The adjusted velocities do not fit Abt's velocity curve for μ Boo, as is shown in Figure 16. As in Section 5.6 (page 58), the velocities were assembled into a time interval representing about 1¼ periods and are shown in Figure 17.

TABLE X

LINE RESIDUALS, 32121 SPECTRA, ONE ADJUSTMENT

RESIDUAL (LINE - MEAN) KM/SEC

(1)	(2)	(3)	(4)	(5)	(6)	(7)	(8)	(9)	(10)	(11)	(12)	(13)
						WAVELENGTH (A)						
PLATE NUMBER	3878	3933	4005	4030	4045	4063	4101	4215	4325	4340	4351	4549
2515	1.7		-12.3	6.4	14.0		1.2	1.9			- 8.8	- 4.1
2979	0.4	0.8	13.9	- 2.2	10.8	-12.4	- 0.1	- 5.2	- 5.6	2.6	2.7	- 5.4
2979	- 0.9	10.2	14.9	- 4.3	9.5	-12.9	0.1	-10.8	0.1	- 1.5	1.4	- 5.3
3077	- 3.9		6.1	- 7.8	0.6	- 0.1	- 5.1		1.9		4.5	4.2
3863	- 2.0	- 6.9	- 7.4		- 1.5		5.1	3.7	- 4.6	1.9	1.1	1.1
3866					- 7.3		- 1.3	3.6	- 8.4	2.3	5.7	5.1
3867	0.8	- 9.2	3.7		- 7.2	1.8	6.2	3.3	- 6.7	2.5	- 2.1	6.9
3937	1.7	3.6	- 8.3		-10.8	18.5	- 5.6	0.6	- 1.7	- 6.2		8.3
3980	- 5.7	6.6	6.2		- 0.8	- 1.7	- 1.6	2.5	- 7.3	- 2.0	2.9	0.7
4056	- 5.4	11.5	- 0.3		- 5.0	1.7	- 6.4	4.5	- 4.6	- 2.1	5.5	0.8
2962	0.0		11.9	- 1.1	2.8	8.9	- 3.5	5.9	0.9		-12.2	-13.9
2962	- 2.7	6.4	8.8		- 1.8	- 4.2	- 1.4	4.2	- 0.8	- 0.3	- 4.4	3.7
3047	23.6		2.3	- 4.7	5.3		-17.7	- 6.9		1.2	- 3.0	
3118	- 0.5		- 5.4	- 8.7	- 8.6	1.9	6.4	- 0.3	15.2			
3118	12.2	-13.4	- 3.0		- 7.7	- 3.6	- 3.7		3.1	6.0	9.7	
3172	1.9		- 7.9	- 3.6	4.1		0.3	- 0.5	7.3	9.1	0.5	-11.8
3292	- 0.4				3.2	6.2	-20.7	1.2	6.7		3.5	
3769	- 0.3		-20.5	5.3	11.4	- 8.1	3.4	- 7.0	0.9		11.2	3.9
3781	- 0.9		- 2.4	0.5	- 1.2	3.6	- 6.6	- 2.4	1.0			8.4

TABLE X (continued)

(1)	(2)	(3)	(4)	(5)	(6)	(7)	(8)	(9)	(10)	(11)	(12)	(13)
3807	3.2		-36.6	5.1	- 0.1	14.1	9.7	- 6.3	4.8		1.7	4.2
3807	- 1.6	- 2.4	2.9	0.4	- 8.5	- 4.0	11.0	- 1.4	- 3.2	- 2.0	8.5	0.0
3807	- 3.0	- 1.5	7.3	4.8	- 5.7	- 2.9	5.3	- 3.7	- 6.1		7.0	- 1.4
3841	- 7.0	- 7.9	- 4.1	10.7	6.2	3.9	- 8.0	10.1	- 1.3	- 1.6		- 1.6
3850	- 2.2			1.9	1.2	- 7.6	5.0	1.2	3.6	- 3.7	- 5.1	6.1
3891	2.6	- 0.1	5.7			-10.8	20.5		- 5.9		-11.8	
R_i	0.48	- 0.18	- 1.11	0.18	0.12	- 0.39	- 0.30	- 0.08	- 0.07	0.41	0.88	0.49
σ_i	6.19	7.70	11.88	5.56	7.00	8.31	8.62	5.00	5.68	3.86	6.58	6.16
S.E.M.$_i$	1.26	2.14	2.52	1.43	1.43	1.86	1.72	1.07	1.18	1.00	1.44	1.38
M	24	13	22	15	24	20	25	22	23	15	21	20
t	0.38	0.08	0.44	0.13	0.08	0.21	0.17	0.07	0.06	0.41	0.61	0.36
	N	N	N	N	N	N	N	N	N	N	N	N

TABLE XI

LINE RESIDUALS, 3282 SPECTRA, ONE ADJUSTMENT

RESIDUAL (LINE - MEAN) KM/SEC

(1)	(2)	(3)	(4)	(5)	(6)	(7)	(8)	(9)	(10)	(11)	(12)	(13)
						WAVELENGTH (A)						
PLATE NUMBER	3878	3933	4005	4030	4045	4063	4101	4215	4325	4340	4351	4549
2384	4.2	0.3	- 6.5				- 3.4	9.4	1.4	0.9		- 6.1
2431	1.3	- 3.7	- 5.1		4.2		1.8	3.9		- 0.9		- 1.8
2498	- 4.3	1.7	8.0		- 2.7		0.6		- 3.9	3.4		- 3.0
2583	- 7.0	0.9	3.5		- 0.3		0.4		- 0.2	0.4		1.9
2624	- 1.5	4.9		- 4.7	- 0.9		- 1.1		4.2	- 0.9		
2633	3.1	1.7	- 5.6	- 0.4	- 2.9		5.5		- 2.1	0.3		
2634	- 1.7	- 1.0	- 4.2		6.1	8.5	- 4.3			- 4.0		0.7
2639	- 4.7	1.7	10.2	- 2.5	- 2.6	- 1.7	- 5.2		- 2.1	6.9		
2691	2.4	0.6	- 4.2	3.0	- 5.9	5.3	0.3	4.1	- 5.4		- 0.4	
2890		- 7.6			4.6	- 5.8	4.1	1.4		3.4		
2890		- 6.3			- 2.9	- 8.3	- 1.3	22.5	0.9	- 0.9	- 3.3	
2891	1.6	- 0.5			- 0.8	- 2.1	1.1		4.0	- 5.7		2.7
2891	0.4	2.3	6.6		- 2.7	- 0.5	- 4.6			- 6.9	3.9	1.4
R_i	- 0.56	- 0.38	0.30	- 1.15	- 0.57	- 0.66	- 0.47	8.26	- 0.36	- 0.33	0.19	- 0.60
σ_i	3.59	3.53	6.69	3.28	3.65	5.88	3.30	8.48	3.33	3.92	3.60	3.17
S.E.M.$_i$	1.08	0.98	2.23	1.64	1.05	2.22	0.91	3.79	1.11	1.13	2.08	1.19
M	11	13	9	4	12	7	13	5	9	12	3	7
t	0.51	0.39	0.13	0.71	0.54	0.30	0.52	2.17	0.32	0.29	0.09	0.50
	N	N	N	N	N	N	N	N	N	N	N	N

TABLE XII

LINE RESIDUALS, 3263 SPECTRA, ONE ADJUSTMENT

RESIDUAL (LINE - MEAN) KM/SEC

(1)	(2)	(3)	(4)	(5)	(6)	(7)	(8)	(9)	(10)	(11)	(12)	(13)
					WAVELENGTH (A)							
PLATE NUMBER	3878	3933	4005	4030	4045	4063	4101	4215	4325	4340	4351	4549
692	8.2	2.0	4.9		0.6	- 4.9			-10.8	0.1		
747	- 2.3	11.3	- 1.3		- 2.4	2.4	- 5.3		4.2	- 6.5	- 0.3	
830		-12.0	- 3.2	- 1.3	4.4	0.0	0.8		9.1	- 0.4	3.0	
858	0.7	1.2			-12.6	- 9.5	1.6	16.3	- 2.5	4.4		
874	- 6.4	- 4.8	10.0		- 3.3	4.1	1.3	0.5	- 1.8	0.4		
877	- 4.5	- 9.2			- 3.5	4.4	2.1	14.0	- 4.5	1.3	- 0.4	
1021	- 0.3				3.3	- 3.5	0.9		3.6	- 0.2		
R_i	- 0.77	- 1.92	2.60	- 1.3	- 1.93	- 1.00	0.23	10.27	- 0.38	- 0.13	0.77	
σ_i	5.11	8.51	6.02		5.66	5.19	2.75	8.54	6.57	3.25	1.93	
S.E.M.$_i$	2.09	3.48	3.01		2.13	1.96	1.12	4.93	2.48	1.23	1.11	
M	6	6	4		7	7	6	3	7	7	3	
t	0.37	0.55	0.86		0.90	0.51	0.21	2.08	0.15	0.11	0.69	
	N	N	N		N	N	N		N	N	N	

TABLE XIII

ROOT MEAN SQUARE STANDARD ERRORS OF THE MEANS, COUDÉ SPECTRA

CAMERA	UNADJUSTED r.m.s.S.E.M. km/sec	ADJUSTED r.m.s.S.E.M. km/sec
32121	3.88	2.55
3282	3.46	1.72
3263	3.52	2.12

TABLE XIV

EXTERNAL DISPERSION STATISTICS, COUDÉ SPECTRA

CAMERA	$\bar{V}_u$	σ_u	$\bar{V}_a$	σ_a	
32121	-11.72	2.52	-11.79	2.51	km/sec
3282	-12.62	2.86	-12.23	2.26	km/sec
3263	-16.12	1.43	-15.88	1.72	km/sec

$\bar{V}_u$ = weighted, unadjusted, overall average velocity

$\bar{V}_a$ = weighted, adjusted, overall average velocity

σ_u = weighted, unadjusted, standard deviation of velocities

σ_a = weighted, adjusted, standard deviation of velocities

Weighted statistics calculated according to Equations 6.6.1 and 6.6.2 below.

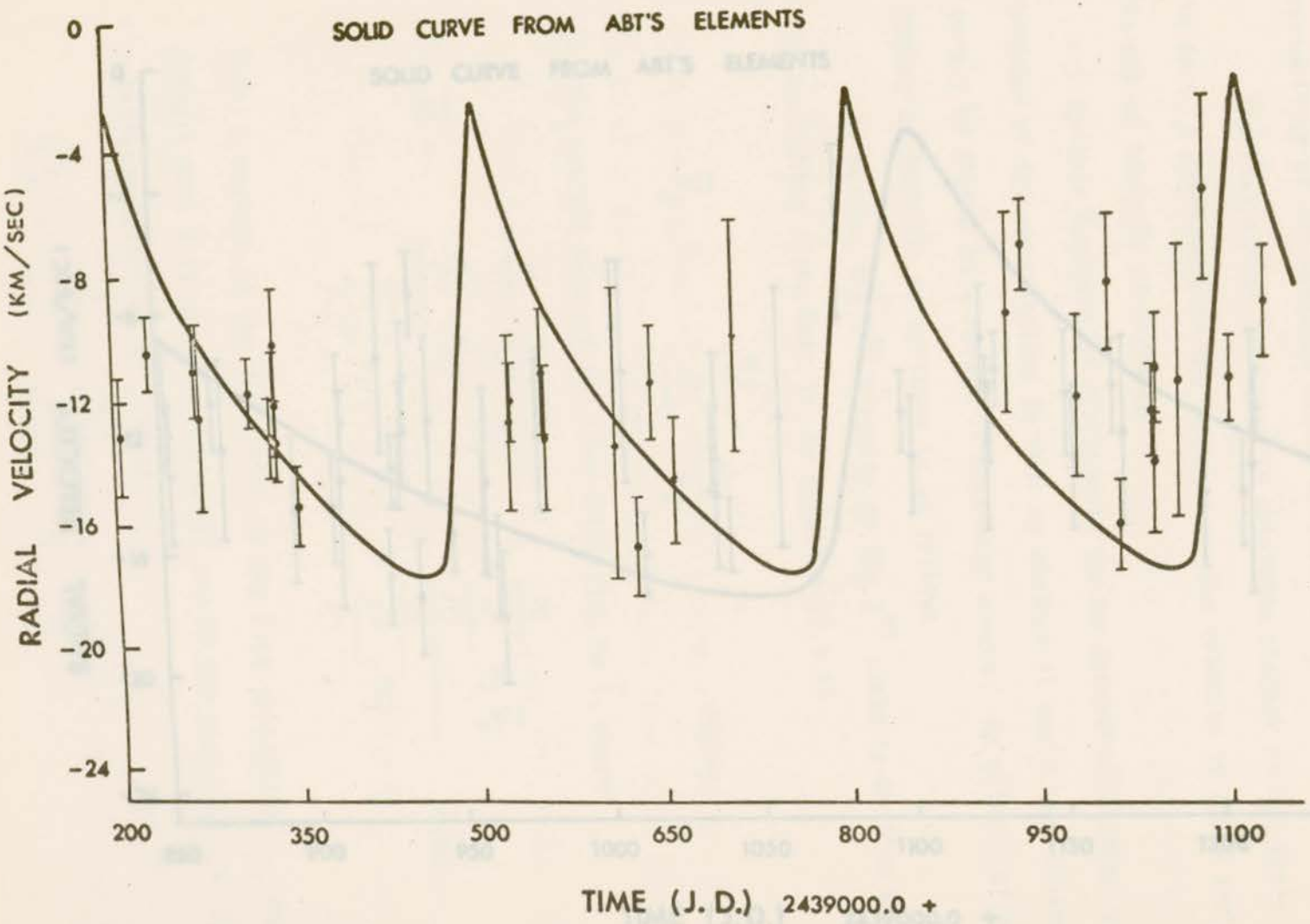

Figure 16. Corrected coudé radial velocities measured visually by the author as a function of time. Solid curve is derived from Abt's orbital elements.

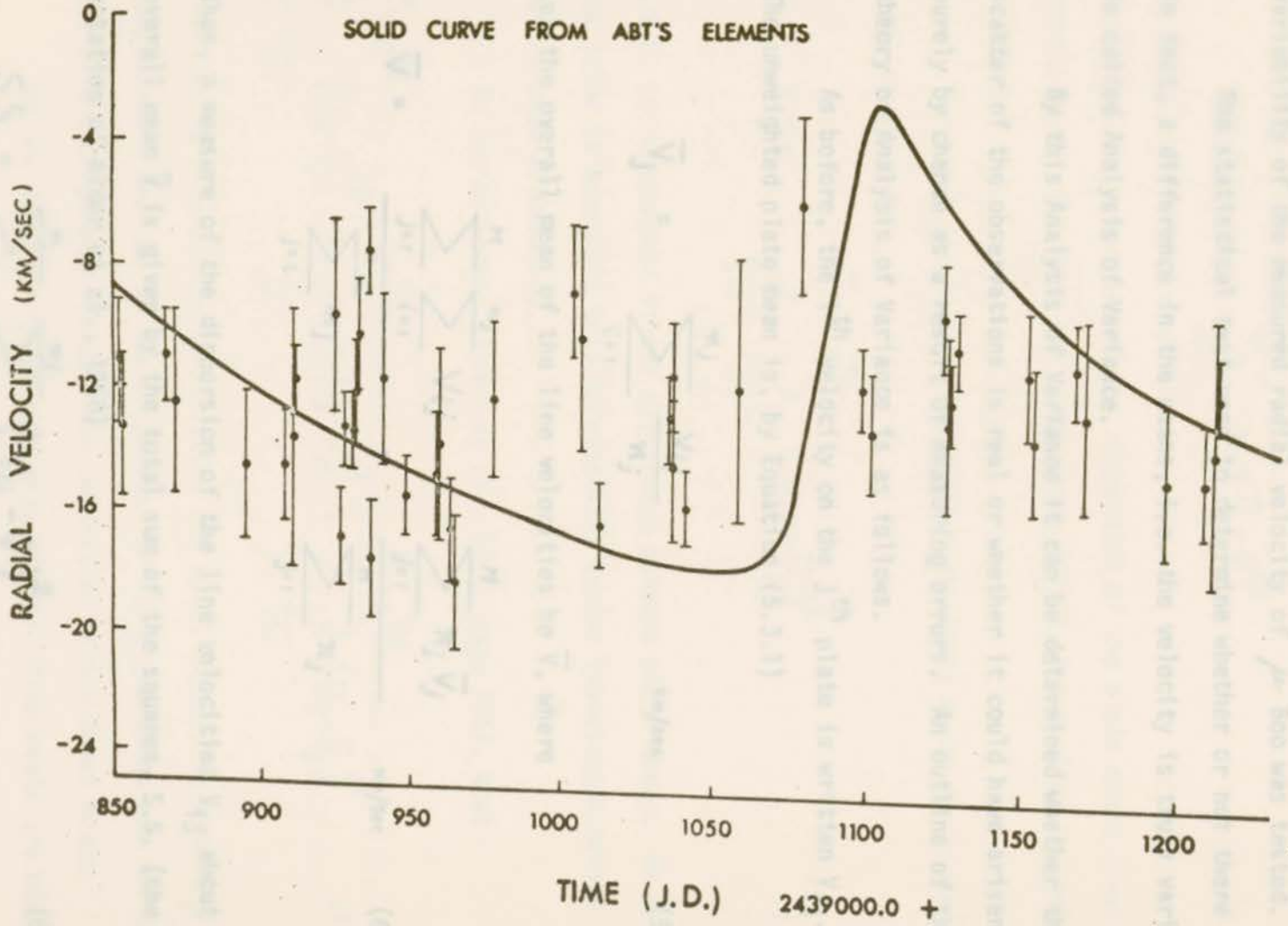

Figure 17. Corrected coudé radial velocities measured visually by the author as a function of phase in Abt's orbit.

6.5 Analysis of Variance

With the large r.m.s.S.E.M. in the Victoria data eliminated, the variability of the measured radial velocity of μ Boo was tested.

The statistical test used to determine whether or not there is, in fact, a difference in the means, i.e. the velocity is truly variable, is called Analysis of Variance.

By this Analysis of Variance it can be determined whether the scatter of the observations is real or whether it could have arisen purely by chance as a result of measuring errors. An outline of the theory of Analysis of Variance is as follows.

As before, the i^{th} velocity on the j^{th} plate is written V_{ij}. The unweighted plate mean is, by Equation (5.3.1)

$$\bar{V}_j = \sum_{i=1}^{n_j} \frac{V_{ij}}{n_j} \quad \text{km/sec} \qquad (5.3.1)$$

Let the overall mean of the line velocities be $\bar{V}$, where

$$\bar{V} = \frac{\sum_{j=1}^{M} \sum_{i=1}^{n_j} V_{ij}}{\sum_{j=1}^{M} n_j} = \frac{\sum_{j=1}^{M} n_j \bar{V}_j}{\sum_{j=1}^{M} n_j} \quad \text{Km/sec} \qquad (6.5.1)$$

Then, a measure of the dispersion of the line velocities V_{ij} about the overall mean $\bar{V}$ is given by the total sum of the squares, S.S. (the notation of Alder et al., 1968)

$$S.S. = \sum_{j=1}^{M} \sum_{i=1}^{n_j} \left(V_{ij} - \bar{V} \right)^2 \qquad (6.5.2)$$

The individual plate means, $\bar{V}_j$, also disperse about the overall mean with a between-means dispersion of

$$S.S.T. = \sum_{j=1}^{M} n_j (\bar{V}_j - \bar{V})^2 \qquad (6.5.3)$$

Thus S.S.T. is a measure of the dispersion of the plate means about the overall mean. The less the plate means differ, the smaller the value of S.S.T.

The total dispersion of the line velocities about their plate means is given by

$$S.S.E. \quad \sum_{j=1}^{M} \sum_{i=1}^{n_j} (V_{ij} - \bar{V}_j)^2 \qquad (6.5.4)$$

S.S.E. is independent of any difference between plate means. As such, its value is dependent only on measuring errors (wavelength errors having been eliminated).

It can be shown, (Alder et al., 1968, page 265), that

$$\sum_{j=1}^{M} \sum_{i=1}^{n_j} (V_{ij} - \bar{V})^2 = \sum_{j=1}^{M} n_j (\bar{V}_j - \bar{V})^2 + \sum_{j=1}^{M} \sum_{i=1}^{n_j} (V_{ij} - \bar{V}_j)^2 \qquad (6.5.5)$$

That is, it is possible to partition the total dispersion into two components - one due to the dispersion of the plate means and the other due to the dispersion of the line velocities within those means.

We now make the hypothesis that all the plate means are equal,

i.e. $\bar{V}_1 = \bar{V}_2 = \bar{V}_3 = \bar{V}_4 = \ldots = \bar{V}_M$. It is this hypothesis which must be tested. Since the means are assumed to be the same, they supposedly have the same unknown standard deviation, σ. This standard deviation, σ, or the population variance, σ^2, can be estimated in two ways.

(i) The line velocity measurements V_{ij} can be "pooled", i.e.

$$\sigma^2 = \frac{\sum_{j=1}^{M} \sum_{i=1}^{n_j} (V_{ij} - \bar{V}_j)^2}{\sum_{j=1}^{M} n_j - M} \qquad (6.5.6)$$

or,

$$\sigma^2_{int} = \frac{S.S.E.}{N_T - M} \qquad (6.5.7)$$

where the total number of lines measured is N_T and

$$N_T = \sum_{j=1}^{M} n_j \qquad (6.5.8)$$

(ii) The variance of the plate means, weighted according to the number of lines measured on the plates, can be calculated, i.e.

$$\sigma^2_{ext} = \frac{\sum_{j=1}^{M} n_j (\bar{V}_j - \bar{V})^2}{M-1} \qquad (6.5.9)$$

The Analysis of Variance test then consists of comparing these two estimates of σ^2. Since these estimates are estimates of the same

variance, their ratio should not differ significantly from unity.

The ratio

$$F = \frac{\sigma^2_{ext}}{\sigma^2_{int}} \qquad (6.5.10)$$

has a distribution known as the F distribution characterized by two degrees of freedom, M-1 and N_T-M. (Alder et al., 1968, Chapter 16; Cramer, 1955, page 127 and 247).

If the hypothesis that the plate means are equal is not true, i.e. the M plates are taken from populations of differing means, then σ^2_{ext} will be considerably greater than σ^2_{int}, because of the greater dispersion of the plate means about the overall mean. If σ^2_{ext} is so large compared to σ^2_{int} that the F value so calculated is greater than $F_{.05}$, (5% level of significance) for the appropriate degrees of freedom, then the plate means must be considered different and, therefore, it must be concluded that there is at least one pair of means which differ significantly. If $\sigma^2_{ext} < \sigma^2_{int}$, the result is always considered insignificant and the dispersion of the plate means about the overall mean would be no more than that expected ordinarily from a set of M values, all of which are taken from the same population.

The calculation of σ^2_{int} is simplified by using

$$\sigma^2_{int} = \frac{\sum_{j=1}^{M}\sum_{i=1}^{n_j}(V_{ij}-\bar{V}_j)^2}{N_T - M} = \frac{\sum_{j=1}^{M}(n_j-1)\sigma_j^2}{N_T - M} \qquad (6.5.11)$$

since the σ_j have already been calculated as individual plate statistics (Equation (5.3.2)).

In order to apply this statistical test, the internal errors on the plates must be random and, therefore, the line velocities must, if possible, be free from wavelength errors. The adjusted velocities derived in the previous section satisfy this criterion and, therefore, the analysis can be applied to them. If the 32121, 3282 and 3263 data of Tables X, XI and XII are grouped, the following results are obtained.

$$\overline{V} = \frac{-5066.9}{406} = -12.48 \text{ km/sec}$$

$$\sigma^2_{ext} = \frac{2894.85}{44} = 65.79 \text{ (km/sec)}^2$$

$$\sigma^2_{int} = \frac{16386.39}{361} = 45.34 \text{ (km/sec)}^2$$

$$F = \frac{65.79}{45.34} = 1.45$$

For 44 and 361 degrees of freedom, $F_{.05} \approx 1.50$. Thus, we may accept the hypothesis that the plate means do indeed come from the same population and are thus all equal.

6.6 The radial velocity of μ Boo from coudé plate measurements

The mean velocity of μ Boo is the population mean, $\bar{V}$. The velocity statistics, weighted according to the number of lines measured on the plates, are calculated as follows:

$$\bar{V} = \frac{\sum_{j=1}^{M} n_j \bar{V}_j}{\sum_{j=1}^{M} n_j} \quad \text{km/sec} \qquad (6.6.1)$$

$$\sigma = \sqrt{\frac{\sum_{j=1}^{M} n_j (\bar{V}_j - \bar{V})^2}{\sum_{j=1}^{M} n_j} \left(\frac{M}{M-1}\right)} \quad \text{km/sec} \qquad (6.6.2)$$

$$\text{S.E.M.} = \frac{\sigma}{\sqrt{M}} \quad \text{km/sec} \qquad (6.6.3)$$

For the coudé data of Table III, (adjusted velocities), the results, using the above three equations, are

$$\bar{V} = \frac{-5066.9}{406} = -12.48 \text{ km/sec} = -12.5 \text{ km/sec}$$

$$\sigma = \sqrt{\frac{2894.85}{406}\left(\frac{45}{44}\right)} = 2.70 \text{ km/sec}$$

$$\text{S.E.M.} = \frac{2.40}{\sqrt{45}} = 0.40 \text{ km/sec}$$

6.7 Comparison of the data with the error curve

An alternate method of determining whether or not the variation in the measured radial velocity is real is given by Aitken (1964, page 155)

> "...an observer has accumulated many plates of a star which apparently shows variable radial velocity without being able to determine any period. It (the method proposed by Schlesinger, 1915, quoted by Aitken) consists in constructing a frequency curve for the velocities by "dividing the total range exhibited by the measured velocities into successive groups of equal extent, say 3 km each, and then counting the number of velocities that fall within these groups. Regarding these numbers as ordinates, we plot them and join the ends by a smooth curve." This curve is compared with the well-known error curve; if the two are the same, within reasonable limits, we may conclude that the differences in the measured velocities are due to errors of observation, and afford no support for the assumption that the star is a spectroscopic binary."

A velocity increment of 2 km/sec has been used with the data in Table III, column (6) (i.e. the data in Figure 17, page 91). The resultant histogram is shown in Figure 18, where the frequency of occurrence of the measured radial velocity, V, is plotted versus the radial velocity. The solid curve is the Normal probability curve given by

$$\text{Frequency} = \frac{32.58}{\sqrt{2\pi}} \exp\left(-\frac{z^2}{2}\right) \qquad (6.7.1)$$

where

$$z \equiv \frac{V-\bar{V}}{\sigma}$$

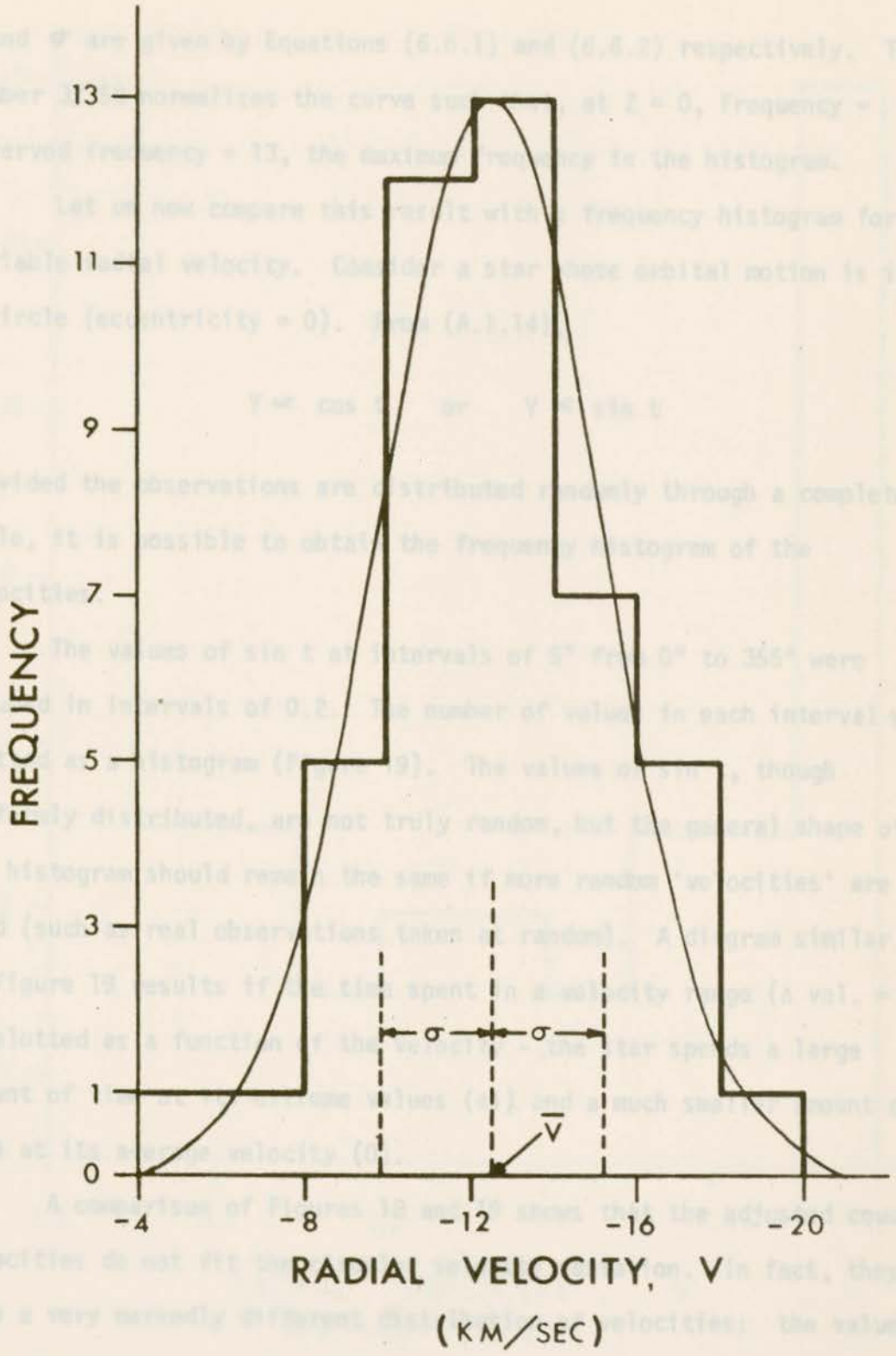

Figure 18. Frequency histogram for adjusted coudé radial velocities. Solid curve is a normal curve, with parameters defined in the text.

$\bar{V}$ and σ are given by Equations (6.6.1) and (6.6.2) respectively. The number 32.58 normalises the curve such that, at Z = 0, Frequency = observed frequency = 13, the maximum frequency in the histogram.

Let us now compare this result with a frequency histogram for a variable radial velocity. Consider a star whose orbital motion is in a circle (eccentricity = 0). From (A.1.14),

$$V \propto \cos t \quad \text{or} \quad V \propto \sin t$$

Provided the observations are distributed randomly through a complete cycle, it is possible to obtain the frequency histogram of the velocities.

The values of sin t at intervals of 5° from 0° to 355° were grouped in intervals of 0.2. The number of values in each interval was plotted as a histogram (Figure 19). The values of sin t, though uniformly distributed, are not truly random, but the general shape of the histogram should remain the same if more random 'velocities' are used (such as real observations taken at random). A diagram similar to Figure 19 results if the time spent in a velocity range (Δ vel. = 0.1) is plotted as a function of the velocity - the star spends a large amount of time at its extreme values (±1) and a much smaller amount of time at its average velocity (0).

A comparison of Figures 18 and 19 shows that the adjusted coudé velocities do not fit the circular velocity variation. In fact, they show a very markedly different distribution of velocities: the values group around the average velocity and there are few at large deviations from this average. The coudé velocities fit the error curve very well,

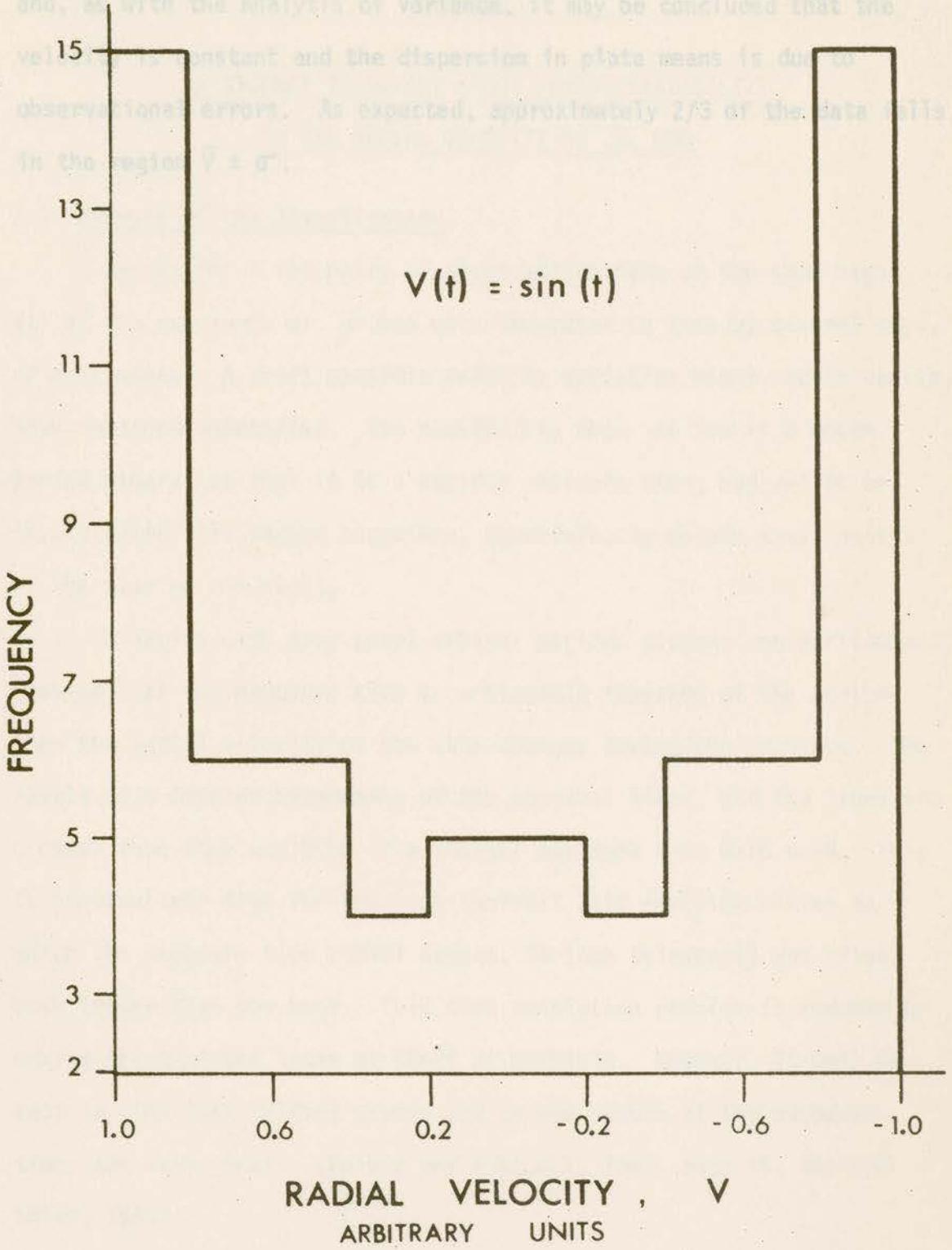

Figure 19. Frequency histogram for a sinusoidal velocity variation.

and, as with the Analysis of Variance, it may be concluded that the velocity is constant and the dispersion in plate means is due to observational errors. As expected, approximately 2/3 of the data falls in the region $\bar{V} \pm \sigma$.

CHAPTER 7

AN ATTEMPT TO DETECT SHORT PERIOD VARIABILITY IN THE RADIAL VELOCITY OF μ BOO

7.1 Purpose of the investigation

Except for a few pairs of observations made on the same night, all of the exposures of μ Boo were separated in time by several days, or even weeks. A short periodic velocity variation might, quite easily, have remained undetected. The possibility that μ Boo is a short period binary, or that it is a rapidly variable star, had yet to be investigated. It seemed necessary, therefore, to obtain many spectra of the star on one night.

Binaries with very short orbital periods present one particular problem. If the exposure time is a sizeable fraction of the period, then the radial velocity of the star changes during the exposure. The result is a Doppler broadening of the spectral lines, and the lines are broader than they would be if a shorter exposure time were used. This is particularly true for the high contrast IIIO emulsion plates for which the exposure time (32121 camera, 48-inch telescope) was often much longer than one hour. This time resolution problem is reduced by making the exposure times as short as possible. However, it must be kept in mind that guiding errors may become severe if the exposure times are very short. (Petrie and Fletcher, 1967, page 45; Abt and Smith, 1969)

There are three practical ways of achieving this goal of short exposure times. One could use a larger telescope, a camera of lower

dispersion, or a faster emulsion than previously used. It was decided that the 72-inch telescope, 21121 camera, IIaO emulsion combination would be used.

7.2 The observations

On the night of April 8, 1969, Dr. C. D. Scarfe and Mr. J. E. Penfold obtained thirty spectra of μ Boo on four plates using the above apparatus. Of these thirty spectra, twenty-nine are useable, since the first spectrum was not exposed to the iron arc.

The exposure times ranged from two to four minutes, with three minute exposures occurring most often. About two hours were required for the exposures, during which time μ Boo moved from 0^h26^m West to 2^h16^m West of the Meridian. Approximately ten minutes were required to change each spectrographic plate. The Julian date of the exposures ranged from 2440319.9563 to 2440320.0319. Although two hours of continuous observations would probably not cover the full period of variation, they might still provide radial velocities that show systematic motion of a binary or pulsatory nature.

Photographic reproductions of some of the spectra are given in Chapter 5, Figures 7 and 8.

7.3 The data

The quality of the spectrograms varied greatly. The first seven spectra, plates 66714 through 66720, were generally poorly trailed, while the next eight (Figure 7, page 37) were well trailed, followed by eight more poorly trailed spectra. The last six were well trailed, but differed appreciably in exposure.

The spectra were all taken with one instrument and, hence, were homogeneous, with the exception of possible guiding errors. Therefore, steps were taken to ensure that the radial velocities obtained from these spectra would be as consistent as possible. To this end, all of the spectra were measured by one person (the author) on one machine (the Zeiss Abbé comparator) at the University of Victoria. The wavelengths used for this work are given in Table XV.

TABLE XV

STANDARD WAVELENGTHS USED FOR
21121 RADIAL VELOCITIES

Wavelength Å	Wavelength Å	Wavelength Å	Wavelength Å
3878.580	3933.682	4005.254	4030.680
4045.815	4063.564	4071.698	4101.787
4271.532	4325.775	4340.475	4351.833

Not all of the spectra were equally exposed, with the result that accurate radial velocity measurements of the spectral lines were difficult. Nevertheless, as many lines as possible were measured on every plate. After several plates had been measured, it was noticed that at least the same six standard lines were measured on every plate, along with other lines. It was decided that these six lines ($\lambda\lambda$ 3878, 3933, 4045, 4101, 4271, 4340 A), if measured on all plates, would be used to yield a consistent plate velocity. In this manner it was hoped that the effect of any errors in wavelengths would be the same for every exposure.

The spectra were measured in the forward and reverse directions and reduced as usual. The approximate times for measurement and reduction per plate were similar to those mentioned previously for the higher dispersion spectrograms. Very often it was found that, especially for the broad lines, the sum of the micrometer forward and reverse readings was not the same as it was for the comparison lines. This indicated that the measurer's eyes did not see the center of the line profile. The measurement of the plate in both directions, and the method of reduction resulted in the center of the line being used, and the radial velocity obtained from the line should be reliable.

Plate statistics were calculated for all lines measured (generally 10 or 11) and for the above six lines, according to Equations (5.3.1), (5.3.2) and (5.3.3). All lines were given unit weight in the reductions.

Since the calculations involved in computing plate statistics for a large number of plates are laborious and always subject to minor

errors, a computer program was written to do the job. Some of the results are given in Table XVI. The column headings are self explanatory.

The first results from these data are shown in Figure 20, where radial velocity (Table XVI, column (4)) is plotted as a function of time. For these data, the root mean square standard error of the mean, from Equation (5.6.1), was

$$\text{r.m.s.S.E.M.} = 3.48 \text{ km/sec}$$

The radial velocity determined from the same six lines (Table XVI, column (6)) as a function of time, is shown in Figure 21. For these data, for M = 28 (since λ 4271 was not measured on plate 66714), it was found that

$$\text{r.m.s.S.E.M.} = 3.97 \text{ km/sec}$$

These rather large values suggested that the velocities were again affected by errors in the wavelengths. Therefore, for the same six lines on all plates, velocity residuals were calculated as outlined in Section 6.3. The t-test was applied to each of the six overall residuals, R_i, with the level of significance set at 2%. Each line velocity was adjusted as previously described, depending on whether or not $t_{obs.}$ was significant at the above level. The results, in Table XVII, show that only the K line of calcium (λ3933) did not need to be adjusted, since its overall residual (0.29 km/sec) was statistically equal to zero. After one adjustment had been made, new plate statistics and residuals were calculated. The new plate means differed from the old ones by only

TABLE XVI

RADIAL VELOCITIES FROM 21121 PLATES

OF μ BOO TAKEN APRIL 8, 1969

(1) PLATE NUMBER	(2) JULIAN DATE 2440319.+	(3) n_j	(4) VELOCITY ALL LINES km/sec	(5) S.E.M. km/sec	(6) VELOCITY 6 LINES UNADJUSTED km/sec	(7) S.E.M. km/sec	(8) VELOCITY 6 LINES ADJUSTED km/sec	(9) S.E.M. km/sec
66714	0.9604	8	- 6.51	3.84				
66715	0.9618	9	-13.76	3.26	-14.95	4.10	-14.90	2.82
66716	0.9646	9	-12.52	1.99	-11.91	2.85	-11.86	1.85
66717	0.9667	11	-13.05	2.27	- 9.90	3.48	- 9.85	2.01
66718	0.9694	10	-11.05	3.14	-10.74	4.41	-10.69	3.03
66719	0.9708	12	-12.94	4.21	-13.36	3.77	-13.31	4.52
66720	0.9729	12	-12.31	2.79	-12.14	4.48	-12.09	2.31
66721	0.9806	11	-12.10	3.27	-10.53	4.26	-10.48	2.09
66722	0.9833	12	-15.59	2.96	-17.26	4.09	-17.21	2.54
66723	0.9854	11	-11.66	3.58	-14.83	3.31	-14.78	2.03
66724	0.9875	12	-13.67	4.64	-13.29	5.43	-13.24	3.76
66725	0.9903	11	-13.08	2.67	-12.95	3.97	-12.90	2.96
66726	0.9924	12	-11.43	3.01	-10.45	2.37	-10.40	1.22
66727	0.9944	12	-12.75	3.06	-12.76	3.14	-12.71	2.09
66728	0.9965	12	-10.65	2.97	- 9.31	3.69	- 9.26	3.58
66729	1.0035	9	-10.92	2.78	-10.70	3.75	-10.65	1.27
66730	1.0049	9	- 6.31	4.07	- 7.82	3.41	- 7.77	2.15
66731	1.0063	9	-10.83	3.79	-11.68	3.75	-11.63	0.89
66732	1.0083	11	-13.88	2.99	-15.62	2.94	-15.57	4.55

TABLE XVI (continued)

(1)	(2)	(3)	(4)	(5)	(6)	(7)	(8)	(9)
66733	1.0097	7	-13.62	4.18	-11.86	4.48	-11.81	2.54
66734	1.0118	10	-10.60	3.84	- 9.21	4.64	- 9.16	3.06
66735	1.0132	10	-16.21	3.57	-17.81	4.49	-17.76	2.35
66736	1.0146	11	-17.98	2.55	-16.94	3.57	-16.89	1.70
66737	1.0215	10	-14.08	3.37	-12.95	3.54	-12.90	1.67
66738	1.0236	11	-14.48	5.10	-14.74	4.94	-14.69	2.10
66739	1.0257	11	-12.33	3.80	-12.58	3.12	-12.53	1.28
66740	1.0278	12	-11.88	3.59	-11.27	4.94	-11.22	2.84
66741	1.0299	12	-16.80	3.06	-12.55	4.29	-12.50	1.92
66742	1.0319	11	-13.55	3.30	-11.83	4.29	-11.78	2.57

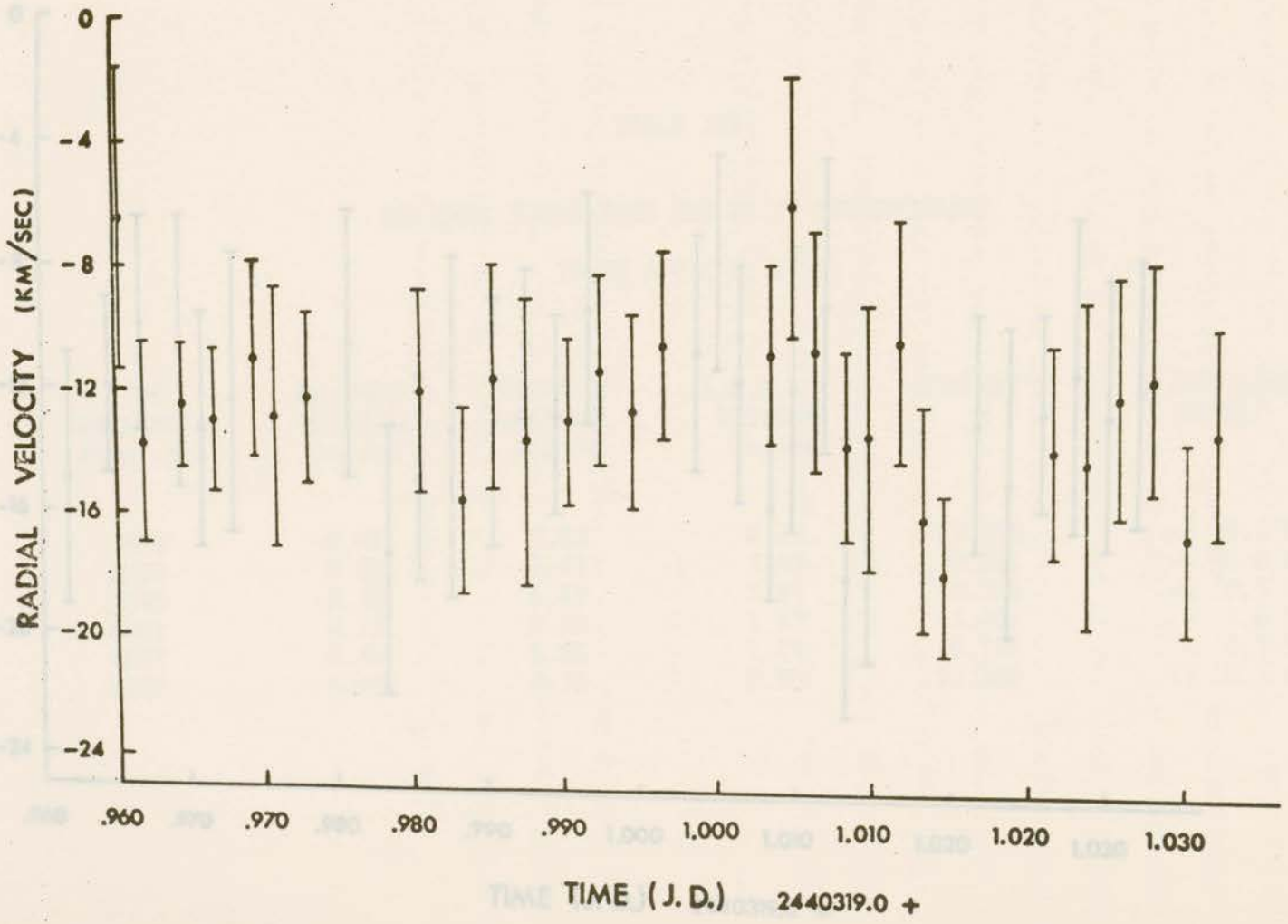

Figure 20. Radial velocity of μ Boo as a function of time, 21121 spectra taken April 8, 1969. Values are means of all measured lines.

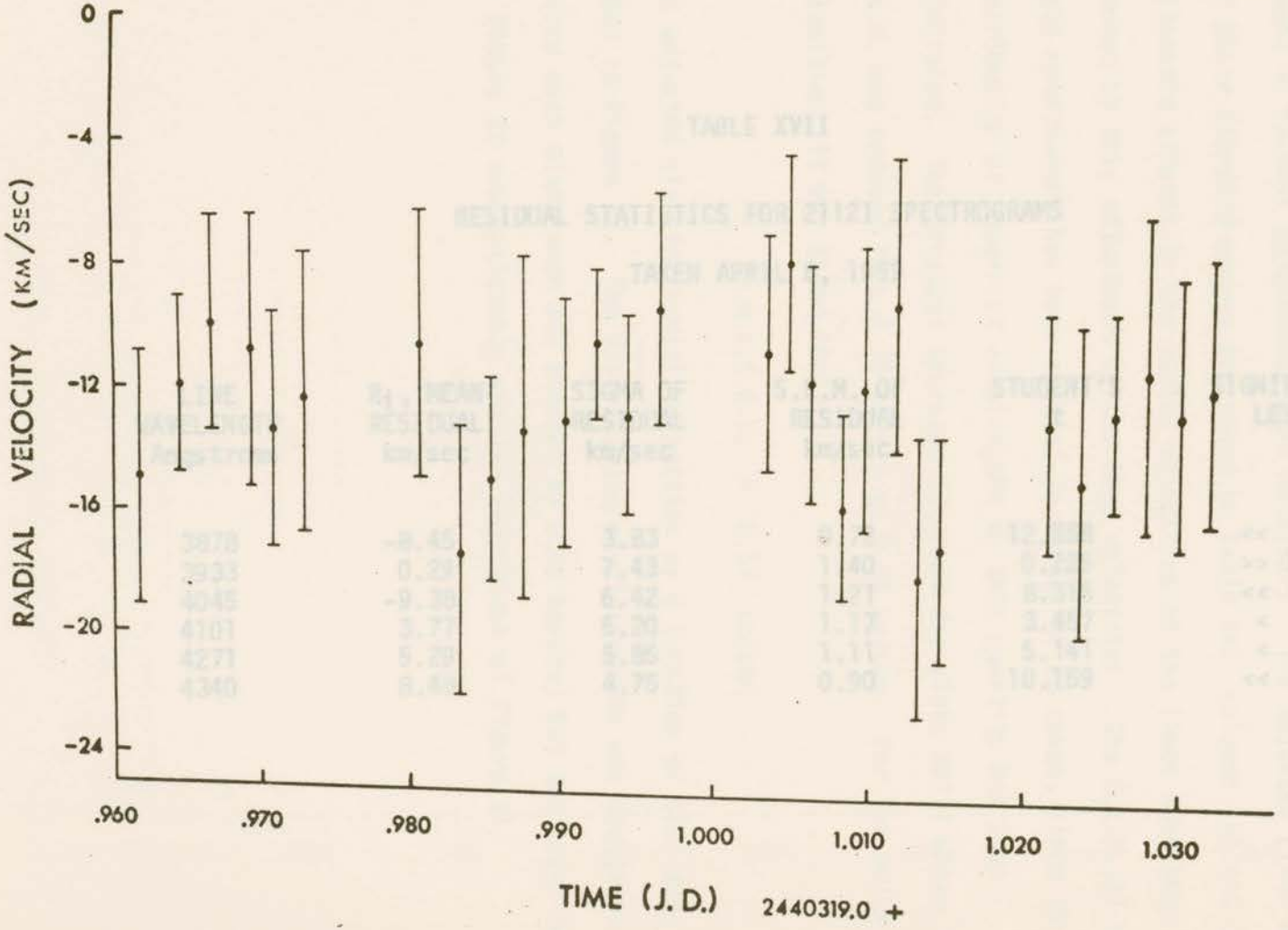

Figure 21. Radial velocity of μ Boo as a function of time, 21121 spectra taken April 8, 1969. The velocities are the uncorrected means of the same six lines for each plate.

TABLE XVII

RESIDUAL STATISTICS FOR 21121 SPECTROGRAMS

TAKEN APRIL 8, 1969

LINE WAVELENGTH Angstroms	R_i, MEAN RESIDUAL km/sec	SIGMA OF RESIDUAL km/sec	S.E.M. OF RESIDUAL km/sec	STUDENT'S t	SIGNIFICANCE LEVEL
3878	-8.45	3.83	0.72	12.558	<< 0.1 %
3933	0.29	7.43	1.40	0.226	>> 10.0 %
4045	-9.38	6.42	1.21	8.316	<< 0.1 %
4101	3.77	6.20	1.17	3.457	< 1.0 %
4271	5.29	5.86	1.11	5.141	< 0.1 %
4340	8.48	4.75	0.90	10.159	<< 0.1 %

$$\frac{0.29}{6} \text{ km/sec} \approx 0.05 \text{ km/sec}$$

Further application of the t-test to the new overall line residuals showed no further adjustments were necessary. The adjusted plate means and their standard errors are found in Table XVI, columns (8) and (9). Systematic effects in the radial velocities of the lines have been removed by this adjustment of the line velocities. The S.E.M. of each plate measurement has been reduced in 26 out of 28 cases, since the contribution of incorrect wavelengths to this quantity has been eliminated. The greatest decrease occurred for plate 66731 where the S.E.M. was reduced from 3.75 km/sec to 0.89 km/sec. For the adjusted velocities, it was found that

$$\text{r.m.s.S.E.M.} = 2.58 \text{ km/sec}$$

The adjusted six-line radial velocities as a function of time are shown in Figure 22. The distribution of plate means was unaltered (since each plate mean was changed by 0.05 km/sec) but the error bars of Figure 22 are noticeably smaller than those of Figure 21.

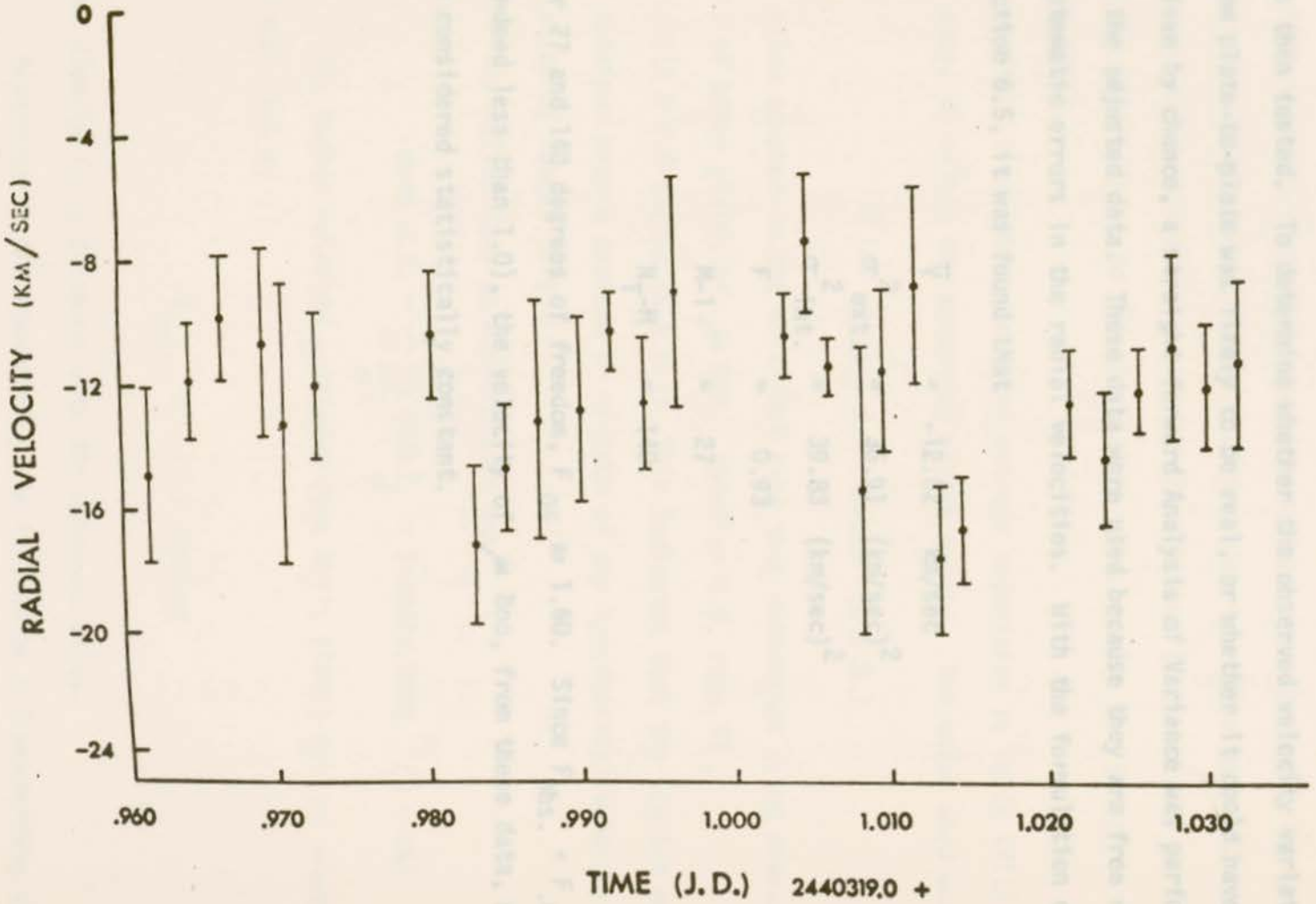

Figure 22. Corrected radial velocity of μ Boo as a function of time, 21121 spectra taken April 8, 1969.

7.4 Analysis of Variance

The variability of the radial velocity over the two hour period was then tested. To determine whether the observed velocity variation from plate-to-plate was likely to be real, or whether it could have arisen by chance, a straight-forward Analysis of Variance was performed on the adjusted data. These data were used because they are free of systematic errors in the radial velocities. With the formulation of Section 6.5, it was found that

$$\bar{V} = -12.52 \text{ km/sec}$$

$$\sigma^2_{ext.} = 36.91 \text{ (km/sec)}^2$$

$$\sigma^2_{int.} = 39.83 \text{ (km/sec)}^2$$

$$F = 0.93$$

$$M-1 = 27$$

$$N_T-M = 140$$

For 27 and 140 degrees of freedom, $F_{.05} \approx 1.60$. Since $F_{obs.} < F_{.05}$ (indeed less than 1.0), the velocity of μ Boo, from these data, must be considered statistically constant.

7.5 The measured radial velocity

Since there was no evidence that the velocity was varying during the time interval covered by the observations, the mean velocity of the plates was considered to be the stellar velocity. This mean and its standard error were found using all the measured lines as well as using the six lines common to all the plates. The results are listed in Table XVIII.

It is clear that the three average velocities in Table XVIII are the same, to within the measuring errors quoted. The value used was

$$\bar{V} = -12.6 \pm 0.5 \text{ km/sec (S.E.M.)}$$

The value adopted is not different from that determined using measurements of other plates of μ Boo. (Section 6.6, page 97, $\bar{V} = -12.5 \pm 0.4$ km/sec (S.E.M.)) This indicates that the spectra were not obtained near a maximum or minimum of any hypothetical velocity variation of longer period.

The Julian date at mid-exposure was

$$\text{mean J.D.} = \frac{1}{M}\sum_{j=1}^{M}(\text{J.D.})_j = 2440319.9982 \quad (M = 28)$$

The radial velocity predicted from Abt's (1965) orbital elements for that time is

$$V_{calc.} \approx -17.1 \text{ km/sec}$$

which clearly fails to agree with the observed value.

According to the reasoning given in Section 6.7 concerning the

TABLE XVIII

COMPARATIVE RADIAL VELOCITIES FROM DIFFERENT SETS OF STELLAR LINES

		CASE I ALL LINES MEASURED	CASE II SAME 6 LINES MEASURED	CASE III SAME 6 LINES 1 ADJUSTMENT	
$\bar{V}$	=	-12.75	-12.57	-12.52	km/sec
σ^2	=	5.86	6.15	6.15	$(km/sec)^2$
σ	=	2.42	2.48	2.48	km/sec
S.E.M.	=	0.45	0.48	0.48	km/sec
M	=	29	28	28	

frequency histogram for these velocity data, the histogram should approximate a Normal curve, with the mean value of the velocity occurring most often. Using a velocity increment of 2 km/sec, Figure 23 was obtained. Even though the sample size was small (M = 28), this histogram approximates a Normal curve very well.

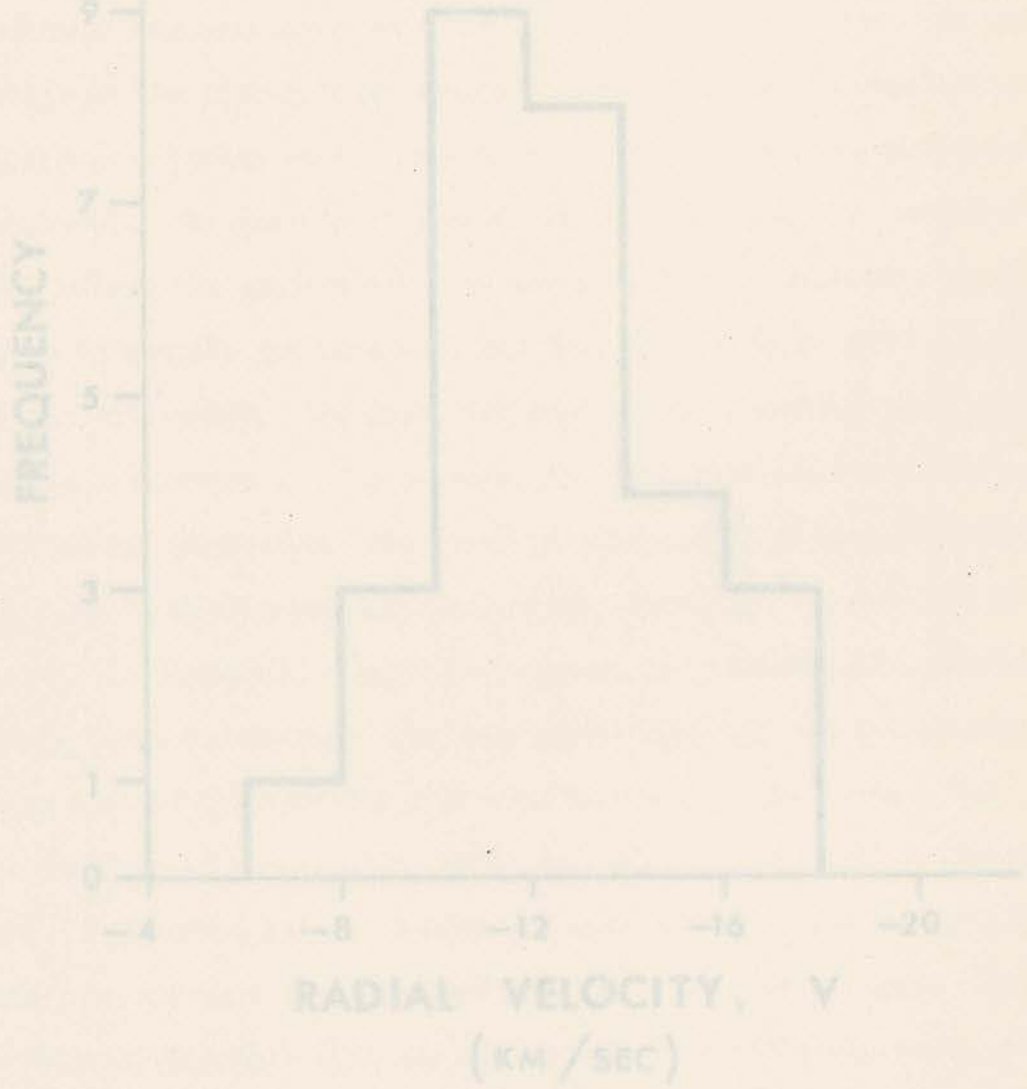

Figure 23. Frequency histogram for corrected velocities of 21121 spectra taken April 8, 1969.

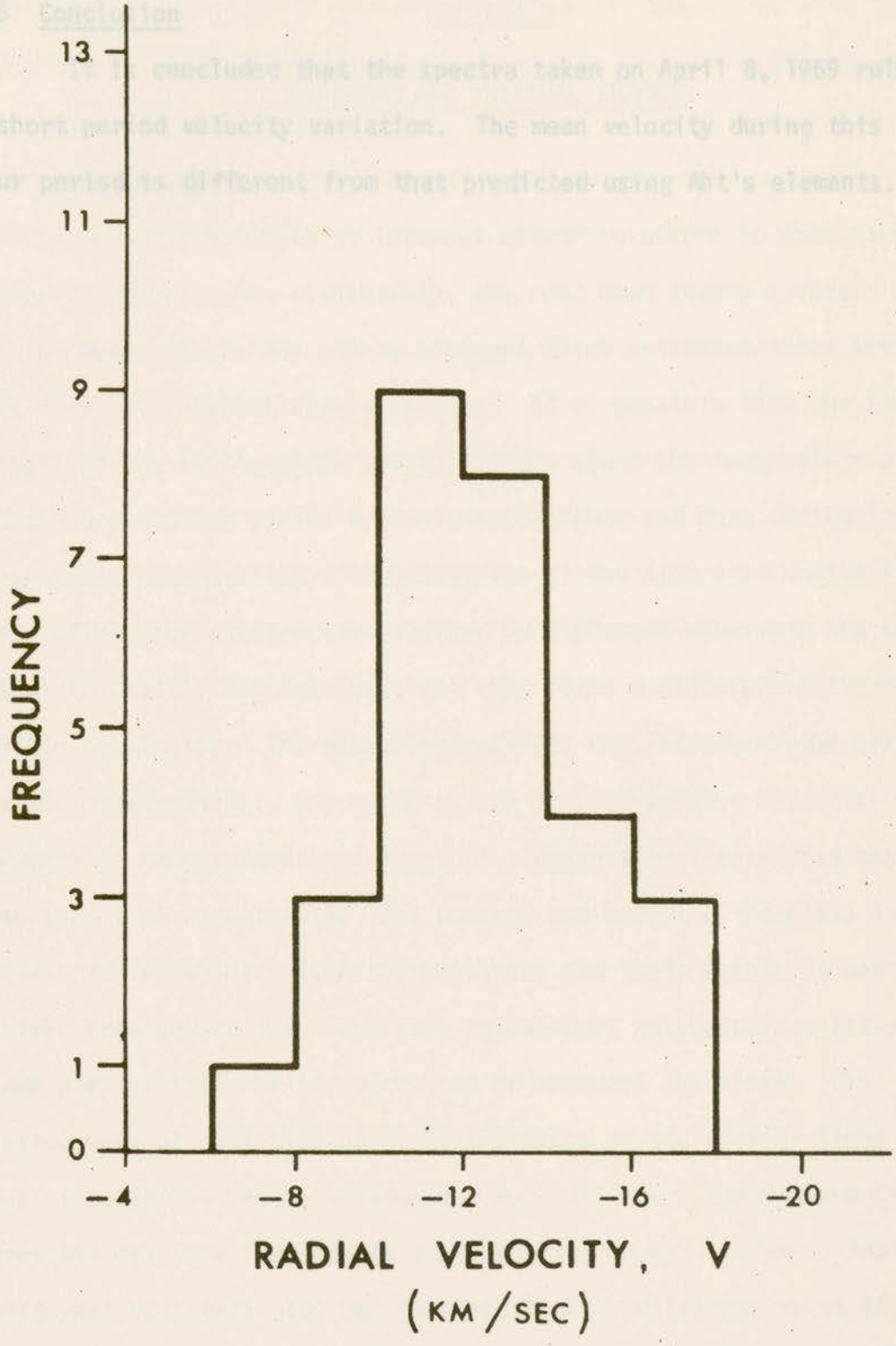

Figure 23. Frequency histogram for corrected velocities of 21121 spectra taken April 8, 1969.

7.6 Conclusion

It is concluded that the spectra taken on April 8, 1969 rule out a short period velocity variation. The mean velocity during this two hour period is different from that predicted using Abt's elements.

CHAPTER 8

EXTERNAL AND INTERNAL ERRORS

8.1 Introduction

Our only estimate of internal measuring errors is the standard error of the mean or, alternately, the root mean square standard error of the mean. These may not be adequate error estimates since they do not take into account several errors. It is possible that the focal length of the spectrograph camera changes since the temperature of the spectrograph often varies from night-to-night, and even during long exposures. The quality of spectrograms of the same star varies since, very often, the spectra are obtained by different observers who do not guide in exactly the same way, and thus cause a different illumination of the collimator. The measuring machines may introduce some errors in the measurements. For example, the Abbé comparator measuring scale depends on temperature; the screw of a conventional measuring machine may vary from time-to-time (oil content and amount of backlash in the screw, for example). Even the measurers and their method of measuring differ from day-to-day. The same person does not measure exactly the same part of the profiles each time he measures the lines. The seriousness of this type of error increases as the stellar lines which one is measuring become broader and more diffuse. The measurer's eyesight may vary from day-to-day depending on eye fatigue. Two different observers also may measure slightly different parts of the line profiles. For a broad lined star, such as μ Boo, we might expect that the actual uncertainty of setting on the center of a weak

line (such as the iron lines measured) or of a strong line (such as the broad hydrogen lines) is more than the errors introduced by temperature changes in the spectrographs etc.

Several estimates of the errors of measurement are required and, from these, a better idea of the accuracy with which the spectra can be measured is obtained. In order to provide this greater number of error estimates, several consistency checks have been devised, and are presented in Section 8.3.

It has already been shown that the observed scatter in plate velocities could be explained by internal errors. (This is essentially the Analysis of Variance test.) If the true error of a plate measurement is underestimated by the internal errors, then the scatter of the data is even more easily explained.

8.2 External errors

An external error is an estimation of the variation, from plate-to-plate, of the measured radial velocities. It is assumed that the radial velocity of the star is constant, and that the observed differences in measured velocities are then due to observational and measuring errors.

Consider the measurements, described in Chapter 5, of the same three lines ($\lambda\lambda$ 3878, 4101, and 4340 A) on many spectrograms, made using the oscilloscope machine. The measured radial velocities of one line (e.g. Hδ) are not the same, due to the errors of measurement. The individual line velocities scatter, from plate-to-plate, with a standard deviation σ_i, about their respective overall means and this gives an estimate of the errors involved when measurements of one of the lines are made. The dispersion of the velocities is independent of the wavelengths used; however, the overall means do depend on the wavelengths adopted, since it is the wavelength used which determines the 'mean Doppler shift' used in radial velocity determinations. If the three overall line velocity means are very different from one another, then this is a further indication that one or more of the adopted wavelengths may be incorrect.

Visual measurements of the same three lines on many plates are also available for comparison. By using the visual measurements of the same plates as above, it is possible to obtain another set of statistics for these three lines. Each measured radial velocity is given unit weight and the dispersion statistics are calculated according to Equations (5.7.1), (5.7.2) and (5.7.3). In Table XIX the statistics

for the three lines, measured with the oscilloscope machine and visually, are given.

Except for Hγ, the standard error of a single measurement, σ_i, is smaller for the B.G.&Z. measurements than it is for the visual measurements. If it is assumed that the very positive velocity of Hγ on plate 65288, as measured with the B.G.&Z. machine (Table V, page 67) is, for some reason, incorrect (a reasonable assumption since the difference $|\text{line} - \text{mean}|_{H\gamma} > 4\sigma_{H\gamma}$) and if the measurement is omitted, then the standard error of a single measurement of Hγ (i.e. $\sigma_{H\gamma}$) is reduced to 2.77 km/sec. Furthermore, the overall mean velocity of Hγ is $\bar{V} = (-8.04 \pm 0.53)$ km/sec (S.E.M.) and it is equal to the overall mean of Hγ.

In this case, then, it is possible to measure all of the three lines on a plate more accurately using the oscilloscope machine than it is using a visual machine.

A second estimate of the plate-to-plate scatter is obtained by using the plate mean radial velocities, $\bar{V}_j$. The data are given in Tables III and XVI. The unweighted velocity statistics are given by

$$\bar{V} = \frac{\sum_{j=1}^{M} \bar{V}_j}{M} \quad \text{km/sec} \qquad (8.2.1)$$

$$\sigma = \sqrt{\frac{\sum_{j=1}^{M} (\bar{V}_j - \bar{V})^2}{M-1}} \quad \text{km/sec} \qquad (8.2.2)$$

TABLE XIX

EXTERNAL MEASURING ERRORS FOR SELECTED LINES,

MEASURED VISUALLY AND WITH THE B.G.&Z.

	RADIAL VELOCITIES VISUAL MEASUREMENTS WAVELENGTH (A)			RADIAL VELOCITIES B.G.&Z. MEASUREMENTS WAVELENGTH (A)			
	3878	4101	4340	3878	4101	4340	
$\bar{V}_i$	-21.39	- 4.65	- 4.02	-19.76	- 7.96	- 7.32 *	km/sec
σ_i	4.91	6.13	4.43	3.22	3.70	4.67 *	km/sec
S.E.M.$_i$	0.96	1.18	1.10	0.61	0.70	0.88 *	km/sec
M	26	27	16	28	28	28	

* see text for discussion of $H\gamma$, B.G.&Z. statistics

$$S.E.M. = \frac{\sigma}{\sqrt{M}} \qquad (8.2.3)$$

The weighted velocity statistics are given by Equations (6.6.1), (6.6.2) and (6.6.3). The results are gathered together in Table XX. It is clear that there is very little difference whether weighted or unweighted statistics are used.

The statistics in Table XX which provides the estimate of the external scatter is "σ", since this is the standard error of a single plate measurement. The coudé velocities tend to scatter about their means with a slightly larger dispersion than do the Cassegrain velocities, and one possible explanation of this is as follows. The Cassegrain 21121 spectra were taken in succession on one night and it is expected that the observational errors (guiding, changes in spectrograph temperature, etc.) are minimal in this case. The coudé velocities, on the other hand, are measured from plates of three different dispersions spread over four observing seasons, taken by different observers under vastly different conditions. It is not surprising, therefore, that the errors of observation are slightly larger than they are with the Cassegrain velocities.

A second explanation of the differences between the coudé and Cassegrain velocities is the fact that the 3263 velocities are more negative than the 32121 and 3282 velocities. A t-test applied to the 32121, 3263 unweighted, unadjusted velocities indicates the means differ

TABLE XX

EXTERNAL MEASURING ERRORS FOR SPECTROGRAMS OF μ BOO

CAMERA		UNADJUSTED VELOCITIES		ADJUSTED VELOCITIES	
		UW	W	UW	W
32121	$\bar{V}$	-11.74	-11.72	-11.83	-11.79
	σ	2.52	2.52	2.52	2.51
	S.E.M.	0.50	0.50	0.50	0.50
	M	25	25	25	25
3282	$\bar{V}$	-12.70	-12.62	-12.31	-12.23
	σ	2.89	2.86	2.31	2.26
	S.E.M.	0.80	0.79	0.64	0.63
	M	13	13	13	13
3263	$\bar{V}$	-16.14	-16.12	-15.79	-15.88
	σ	1.39	1.43	1.68	1.72
	S.E.M.	0.52	0.54	0.64	0.70
	M	7	7	7	7
32121, 3282, 3263	$\bar{V}$	-12.70	-12.57	-12.58	-12.48
	σ	2.90	2.87	2.70	2.70
	S.E.M.	0.43	0.43	0.40	0.40
	M	45	45	45	45
21121 6 line	$\bar{V}$	-12.57	-12.57	-12.52	-12.52
	σ	2.48	2.48	2.48	2.48
	S.E.M.	0.47	0.47	0.47	0.47
	M	28	28	28	28
21121 all line	$\bar{V}$	-12.64	-12.75	*	*
	σ	2.51	2.42	*	*
	S.E.M.	0.47	0.45	*	*
	M	29	29	*	*

NOTE: $\bar{V}$, σ, S.E.M. are measured in km/sec

UW = unweighted
W = weighted
* = adjustments for all wavelength velocities for the 21121 spectra taken April 8, 1969 were not made

at the 1% probability level, i.e. the probability of obtaining as discrepant a result from a random sample is very small (< 0.01). It is possible that the wavelengths adopted for the 32121 camera do not apply to the 3263 camera. This is unlikely since they seem to apply to the 3282 camera, which has approximately the same dispersion as the 3263 spectrograph (Table I, page 17). An alternative explanation of the negative 3263 velocities is evident if the times when the spectra were taken are compared. The 3263 spectra were obtained much earlier (approximately 3 years) than the 3282 and 32121 spectra. It is possible that the radial velocity changed during this long interval of time, indicating a binary star with a long period and probably a small amplitude. If, on the other hand, the 3263 velocities are very different from the other coudé velocities, we would expect a secondary peak in the coudé radial velocity frequency histogram (Figure 18, page 100). The 3263 velocities did not produce such a secondary peak. Also, the Analysis of Variance (Section 6.5), when applied to all of the coudé velocities, did not indicate variability in the radial velocity of μ Boo. However, a long period variation (P > 6 years) cannot be ruled out at present.

8.3 Internal errors

When a star's radial velocity is measured using many lines, not all the lines give the same result. However, it is assumed that the velocities of all the lines are in fact the same and that the spread in the measured velocities is due to measuring errors. A measure of the line-to-line dispersion of the velocities is an estimate of the internal error associated with the plate measurement. Its value is given by Equation (5.3.2). A second internal error estimate is the standard error of the mean, given by Equation (5.3.3). Another estimate of the internal measuring error is the root mean square standard error of the mean, taken over M measurements and given by Equation (5.6.1). The values found previously are collected in Table XXI, below.

Many spectra were measured more than once, by different people and with different types of machines for internal consistency checks. By using these duplicate measurements, it is possible to give a better error estimate to the measured velocities. The five checks below are based on the following reasoning. Observer A measures the radial velocity of n_j' lines on a spectrogram. Observer B, using the same wavelength table, measures n_j'' lines on the same spectrogram. If both people measure the same part of the line profile (i.e. the center) then the radial velocity of each line they measure in common should be equal. In general, they are not, and an estimate of the inequality of the velocity measurements is an estimate of the measuring error. For each line, i, that the two observers measure in common, the difference Δ_i is formed where

TABLE XXI

ROOT MEAN SQUARE STANDARD ERRORS OF THE MEANS

OF MEASURED RADIAL VELOCITIES

		r.m.s.S.E.M. km/sec	M
COUDÉ VELOCITIES			
Unadjusted	32121, 3282, 3263	3.71	45
Adjusted	32121, 3282, 3263	2.27	45
CASSEGRAIN VELOCITIES, spectra taken April 8, 1969			
Unadjusted,	all wavelengths	3.48	29
Unadjusted,	six wavelengths	3.97	28
Adjusted ,	six wavelengths	2.58	28

M is the number of measurements making up the r.m.s.S.E.M.

$$\Delta_i = V_i(A) - V_i(B) \qquad (8.3.1)$$

The estimate of the error of measurement for plate j, which is used in this work, is the root mean square difference, D_j, where

$$D_j = \sqrt{\frac{\sum_{i=1}^{N_j} (\Delta_i)^2}{N_j}} \qquad (8.3.2)$$

and N_j is the number of lines on plate j which observers A and B measure in common.

The use of this differential method of comparison eliminates all wavelength problems, since the same wavelength table is used by the measurers. The error found, D_j, will be indicative of the accuracy with which the spectral lines can be measured for radial velocities.

The r.m.s. difference, D_j, is an average measuring error associated with the measurement of a single line on a particular plate, j. An estimate of the measuring error associated with the plate, E_j, can also be made by dividing D_j by $\sqrt{N_j}$. It has been said that many spectra have been measured more than once by different measures (eg. the author and Scarfe measured visually the same six spectrograms.) Each of these j plate measurements produces a r.m.s. difference. Arguing one step further, the averages of D_j and E_j are even better estimates of

the measuring errors than any particular one of them, since the quality of the plates differs from plate-to-plate. For example, a very good spectrogram may result in a small r.m.s. difference, indicating that both measurers have measured the same radial velocity for at least the majority of lines. To quote this value alone as the error estimate would be incorrect and misleading, since other spectra of differing quality were measured by the two people. Hence, the best error estimates available are the average values, D and E, of D_j and E_j, averaged over the number of plates measured in common. If A and B are the same person, then the value of D and E indicates the accuracy with which he can duplicate his measurements, perhaps with two different types of machines.

The average r.m.s. difference, D, and the average internal error of a single plate, E, as well as the average number of lines measured per plate, $\bar{N}$, by both observers, are given in Table XXII below. The first check compares visual measurements made by the same person while the last one compares measurements made by one person with an oscilloscope machine. The remainder of the entries results from different people using the two types of machines.

The details of each section are now discussed.

(i) The author measured visually five spectrograms twice and one spectrogram three times. A simple weighting system was adopted: for the five spectra measured twice, a weight of 2 was given to each D_j and E_j; for the spectrum measured three times, each D_j and E_j was given unit weight, so that the total weight for this spectrogram was 3. The weighted values for the errors, D and E are in Table XXII.

TABLE XXII

A COMPARISON OF INTERNAL MEASURING ERRORS

OBTAINED FROM SPECTRA OF μ BOO

	SOURCE OF ERROR ESTIMATE	D km/sec	E km/sec	M	$\bar{N}$
(i)	RJN visual; RJN visual	8.10	2.89	8	9
(ii)	RJN visual; CDS visual	10.59	2.53	6	9
		5.35	2.09	6	7
(iii)	RJN visual; RJN BG&Z	7.76	3.16	20	6
(iv)	RJN BG&Z ; JMF BG&Z	2.34	1.19	7	4
(v)	JMF BG&Z ; JMF BG&Z	1.25	0.73	2	3

D the average r.m.s. difference in line measurements

E the average internal error of a single plate measurement

M the number of pairs of measurements compared

$\bar{N}$ the average number of lines measured in common per plate

RJN R.J. Niehaus is the measurer
CDS C.D. Scarfe is the measurer
JMF J.M. Fletcher is the measurer
BG&Z Brower, Grant, and Zeiss oscilloscope measuring machine

(ii) Scarfe measured visually six 3282 spectrograms which the author had measured. A comparison of the line velocity measurements resulted in the errors given in the table. On several line measurements |RJN - CDS| > 15 km/sec. This indicates that the same line center was not measured by both people. If these individual velocity differences are omitted, the new error estimates, given in line 3 of the table, are obtained. The more reliable estimate is probably the former, since the measurements are valid. This further demonstrates the difficulties encountered in obtaining very accurate radial velocities from the spectra of μ Boo.

(iii) A large number of spectra were measured by the author with the B.G.&Z. machine. Many of the results are given in Section 5.6. The B.G.&Z. measurements were compared with the author's visual measurements and the values for the average weighted errors, D and E (weighted as in (i) above) are given in the table. The error is perhaps large indicating that the measurer did not measure the same part of the line profile when measuring visually and with an oscilloscope machine.

(iv) Some plates were measured with the B.G.&Z. machine both by the author and Fletcher. On one plate, seven lines were measured in common; on another, eight. On three others, only three lines were measured by Fletcher; the reasons were given in Section 3.5. The resultant error estimates are given in the table. Note that they are smaller than the visual measurements in (i) and (ii) above.

(v) Two spectrograms were measured twice each by Fletcher with the B.G.&Z. Only three lines per plate were measured, making a total

of six lines. The errors are given in Table XXII. They are small compared to the other measuring errors for three reasons: (a) Fletcher has had much experience with this particular measuring machine, (b) a single measurer tends to set on the same part of a profile more consistently than two different people do, and (c) it is possible that the good result occurred by chance, since it is based on few observations.

It was found that the most reliable error estimates in this section are those given in (ii) and (iv), since both were obtained from different measurers using the same type of machine in each case. It appears the measurement with the oscilloscope machine produces somewhat more consistent velocities.

8.4 A comparison of IIa0 and III0 emulsions

In Section 3.3, the arguments for using either Kodak IIa0 or III0 emulsions were given. As a by-product of the present work, it was possible to provide some evidence in this matter, at least with regard to the accuracy of measurement. The standard deviation of the plate, σ_j, was used as an estimate of the accuracy with which the line velocities are measured. Since the use of incorrect wavelengths introduces systematic errors into the measured velocities, the corrected velocities were used. In order to avoid possible small differences between spectrographs, only the 32121 IIa0 and III0 spectra were used in this comparison (because only the 32121 camera was used to obtain III0 spectrograms). It was assumed that the adjustments to the line velocities, which were calculated from all 32121 measurements, would apply separately to the IIa0 and III0 spectra.

Using the data of Table X, page 85 (the top half of which is IIa0 measurements and the bottom half, III0 measurements) the following results were obtained:

$$\text{r.m.s. } \sigma_{III0} = 8.36 \text{ km/sec}$$

$$\text{r.m.s. } \sigma_{IIa0} = 6.51 \text{ km/sec}$$

These results were based on 15 and 10 plate measurements respectively.

The difference between the values is small, and in a sense opposite to what was expected. From these twenty-five measurements, it appears that it is not possible to measure III0 emulsion spectra more accurately than IIa0 emulsion spectra.

CHAPTER 9

SUMMARY AND CONCLUSIONS

This spectroscopic study of μ Boo was undertaken to determine the accuracy with which the predicted velocity variation (Abt, 1965) describes the observed variation. The radial velocities from spectra taken at the D.A.O. and measured visually by the author do not substantiate the variation predicted from Abt's (1965) orbital elements.

In an attempt to determine if a very short period variation in the radial velocity of μ Boo is present, many spectra were taken on one night. It was found that the radial velocity of the star during the two hours was constant, and it is, therefore, concluded that there is no short period variation in the radial velocity of μ Boo. Furthermore, the value of this constant radial velocity is different from that predicted for that night from Abt's elements.

Several estimates of internal measuring errors have been given and it has been shown that the dispersion in plate velocities is no larger than expected from errors of measurement, i.e. if there is an intrinsic variation in the velocity of the star, it is below the level of detection.

The metallic lines in the spectrum of μ Boo are broad and weak, because of the axial rotation of the star, and hence, the measurement of the radial velocity is difficult. It has been found, in two different cases, that it is possible to measure the radial velocities more accurately with the oscilloscope machine than with the visual machines. In one case, three lines on several spectrograms were

measured visually and with the B.G.&Z. It was found that, for each of the three lines, the standard error of a single measurement, (σ_i), was smaller for the oscilloscope machine measurements than for the measurements made on the visual machines. In the second case, the radial velocity of the same lines on several plates were measured visually by two different people (the author and Scarfe). The errors of measurement were compared with the values obtained from measurements made with the oscilloscope machine, also measured by two different observers (the author and Fletcher). In this case, it was found that the standard error of the mean for measurements with the B.G.&Z. was about half that for visual measurements.

Photographic prints of two spectrograms of the same dispersion but with different emulsions (high contrast IIIO and lower contrast IIaO) were found to show no vast difference between the line widths. It has also been found that the lines on the high contrast spectra cannot be measured more accurately than those on the lower contrast spectra.

From the data used in this work, it is concluded that there is no evidence for variability in the radial velocity of μ Boo. If the reasonable assumption that the radial velocity is constant is made, then the unweighted, unadjusted, mean velocity of μ Boo from 83 measurements (Tables III and XVI) is

$$\bar{V} = -13.0 \pm 0.3 \text{ (S.E.M.) km/sec}$$

This standard error of the mean is a formal error and it may be an underestimate of the uncertainty in the mean radial velocity. The

small standard error of the mean resulted from a small dispersion of the plate means, which themselves are not known very accurately (for the coudé measurements, the r.m.s.S.E.M. = 3.7 km/sec). A much larger uncertainty in $\bar{V}$ is implied by the individual line average velocities. For any particular line, i, the velocities, V_{ij}, determine a line velocity, $\bar{V}_i$ (Equation 5.7.1). Since the maximum number of lines measured was twelve, there are twelve such $\bar{V}_i$'s. The average of these twelve mean line velocities should and does equal the overall mean velocity, $\bar{V}$, of μ Boo. However, wavelength errors lead to a large scatter of the individual mean line velocities. For the coudé spectra, the standard error of the mean value of $\bar{V}_i$ was 2.4 km/sec. Therefore, the real uncertainty in the overall mean, $\bar{V}$, is about 2 km/sec and not 0.32 km/sec, as the formal calculation indicates. This uncertainty in the wavelengths probably applies to the velocities determined by previous observers, and as a result, the mean velocity determined in this work is consistent with those previously published.

APPENDIX A

DERIVATION OF THE EQUATION RELATING THE RADIAL VELOCITY OF A BINARY STAR TO THE ELEMENTS OF THE ORBIT

In this appendix the equation which relates the heliocentric radial velocity of a binary star to the elements of its orbit is derived. The diagram below (Figure 24, after Smart, 1962) will both aid in defining the elements of a spectroscopic binary orbit and in providing some general necessary relations. The derivation is found in any basic binary star text.

In a binary system, each star describes an elliptic orbit around the center of gravity of the system, G. Let the observer be located in the direction of the arrow. The line joining G to the observer intersects a sphere centered on G at T. The circle DEF is the great circle of which T is the pole; the plane DEF is the plane of the apparent orbit. Plane EHJ is the plane of the true orbit, inclined at an angle AEB = i to the plane DEF. The line of intersection of the two planes DEF and JEM is the line of nodes. Let the ascending node be at E. The stars are closest together at P (periastron) whose projection on circle EHJ is C. The longitude of periastron is the angle EGC = ω. Consider the star, at any time, at S, whose projection on the circle EHJ is A. If GS = r, and the true anomaly, v, is the angle CGA = angle PGS and if z is the distance from the star S to the plane DEF, then

$$z = GS \sin(AB) = r \sin(AB) \qquad (A.1.1)$$

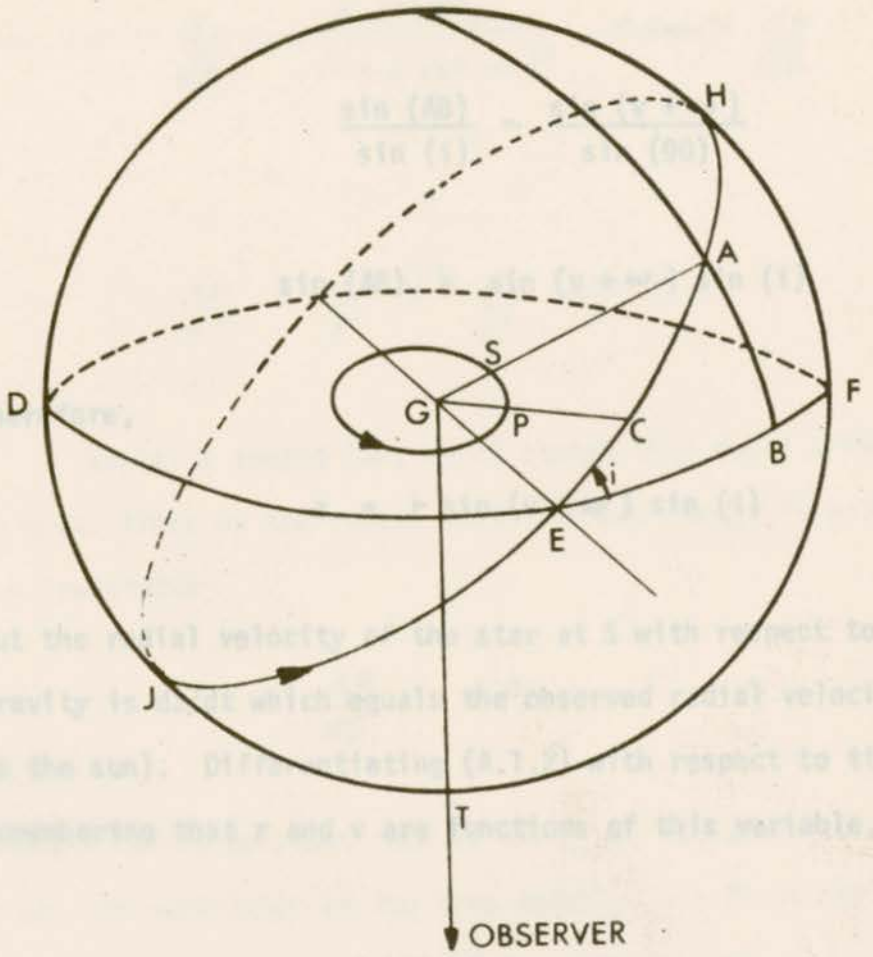

Figure 24. The orbit of a binary star.

Consider the spherical triange ΔEAB. In it, $AE = AC + EC = v + \omega$, $\angle AEB = i$, $\angle ABE = 90°$. Using the sine formula of spherical trigonometry,

$$\frac{\sin (AB)}{\sin (i)} = \frac{\sin (v + \omega)}{\sin (90)}$$

$$\sin (AB) = \sin (v + \omega) \sin (i)$$

Therefore,

$$z = r \sin (v + \omega) \sin (i) \qquad \text{(A.1.2)}$$

But the radial velocity of the star at S with respect to the center of gravity is dz/dt which equals the observed radial velocity (corrected to the sun). Differentiating (A.1.2) with respect to time, and remembering that r and v are functions of this variable, we have

$$\frac{dz}{dt} = \sin i \sin(v+\omega) \frac{dr}{dt} + r \sin i \cos(v+\omega) \frac{dv}{dt} \qquad \text{(A.1.3)}$$

We thus require expressions for dr/dt and dv/dt. For an elliptic orbit, we have

$$r = \frac{a(1-e^2)}{1+e\cos v} = \frac{p}{1+e\cos v} \qquad \text{(A.1.4)}$$

Hence,

$$\frac{dr}{dt} = \frac{a(1-e^2)}{(1+e\cos v)^2}\, e \sin v \, \frac{dv}{dt} \qquad \text{(A.1.5)}$$

or

$$\frac{dr}{dt} = \frac{e}{p}\, r^2 \, \frac{dv}{dt} \sin v \qquad \text{(A.1.6)}$$

Kepler's second law, which states that equal areas are swept out in equal times by the radius vector is now used. In mathematical form, the law states

$$r^2 \frac{d\theta}{dt} = 2A$$

where A is the constant rate at which the radius vector sweeps out the area. By definition of the true anomaly, v = 0° at periastron. However, the zero position of θ is arbitrary and

$$\frac{d\theta}{dt} = \frac{dv}{dt}$$

Therefore,

$$\frac{dr}{dt} = \frac{e}{p} \sin v \cdot (2A) \qquad \text{(A.1.7)}$$

The area of an ellipse with semimajor axis a, semiminor axis b, and eccentricity e, is πab, and since $b = a\sqrt{1-e^2}$, the area is $\pi a^2\sqrt{1-e^2}$. This area is swept out in period P. Therefore,

$$A = \frac{\pi a^2 \sqrt{1-e^2}}{P}$$

$$\frac{dr}{dt} = \frac{2\pi a^2 \sqrt{1-e^2}}{p P} e \sin\nu \qquad \text{(A.1.8)}$$

$$\frac{dr}{dt} = \frac{2\pi}{P} \frac{ae \sin\nu}{\sqrt{1-e^2}} \qquad \text{(A.1.9)}$$

$$\frac{dr}{dt} = \frac{\mu a e \sin\nu}{\sqrt{1-e^2}} \quad \text{and} \quad \mu \equiv \frac{2\pi}{P} \qquad \text{(A.1.10)}$$

To determine dv/dt, multiply (A.1.5) by r, and solve for r dv/dt.

$$r \frac{dv}{dt} = r \frac{dr}{dt} \frac{(1+e\cos v)^2}{ae \sin v\,(1-e^2)}$$

$$r \frac{dv}{dt} = \frac{r\,\mu\, ae \sin v\ (1+e\cos v)^2}{\sqrt{1-e^2}\ ae \sin v\ (1-e^2)} \qquad \text{(A.1.11)}$$

$$r \frac{dv}{dt} = \frac{\mu a\ (1+e\cos v)}{(1-e^2)^{1/2}} \qquad \text{(A.1.12)}$$

Substitute (A.1.10) and (A.1.12) into (A.1.3) and, after some simplification,

$$\frac{dz}{dt} = \frac{\mu a \sin i}{\sqrt{1-e^2}} \left\{ e \sin(v+\omega) \sin v + \cos(v+\omega) + e\cos(v+\omega)\cos v \right\}$$

$$\frac{dz}{dt} = \frac{\mu a \sin i}{\sqrt{1-e^2}} \left\{ \cos(v+w) + e \cos w \right\} \qquad \text{(A.1.13)}$$

Now define

$$K = \frac{\mu a \sin i}{\sqrt{1-e^2}}$$

Then,

$$\frac{dz}{dt} = K \cos(v+w) + Ke \cos w$$

However, if the system has a velocity with respect to the sun, (called the systemic velocity, γ) then the radial velocity observed, with respect to the sun, is

$$V = \gamma + \frac{dz}{dt} = \gamma + Ke \cos w + K \cos(v+w) \qquad \text{(A.1.14)}$$

This is the desired equation which relates the radial velocity of a star in a binary orbit to the elements of that orbit.

APPENDIX B

KODAK IIaO AND IIIO EMULSIONS

The characteristic curve of an emulsion is a plot of the optical density versus the logarithm of the exposure. It is obtained by subjecting the photographic emulsion to a series of exposures, each greater than the previous by a constant factor. This is achieved with the rotating sector when the calibration is placed on the plate (see text, Section 3.3). The resultant densities are read with a densitometer. When the density of each silver deposit is plotted against the logarithm of the exposure which produced that density, a smooth curve may be drawn through the points. This curve is the "characteristic curve".

Figure 25 represents qualitative characteristic curves of IIaO and IIIO emulsions. The slope of the curve at any point indicates how rapidly changes in exposure effect changes in density. The straight line portion of the curves is the range wherein the gradient is constant, and the density increases as a direct function of the logarithm of the exposure. For astronomical purposes, it is preferable that the exposure be placed on this part of the characteristic curve. It is clear in Figure 25 that the "useful density" region of the IIaO emulsion corresponds to a larger range in exposure, (AB), than the same "useful density" region of the IIIO emulsion, whose range in exposure is A'B'. For this reason, a properly exposed IIIO spectrogram is much more difficult to obtain than a IIaO spectrogram.

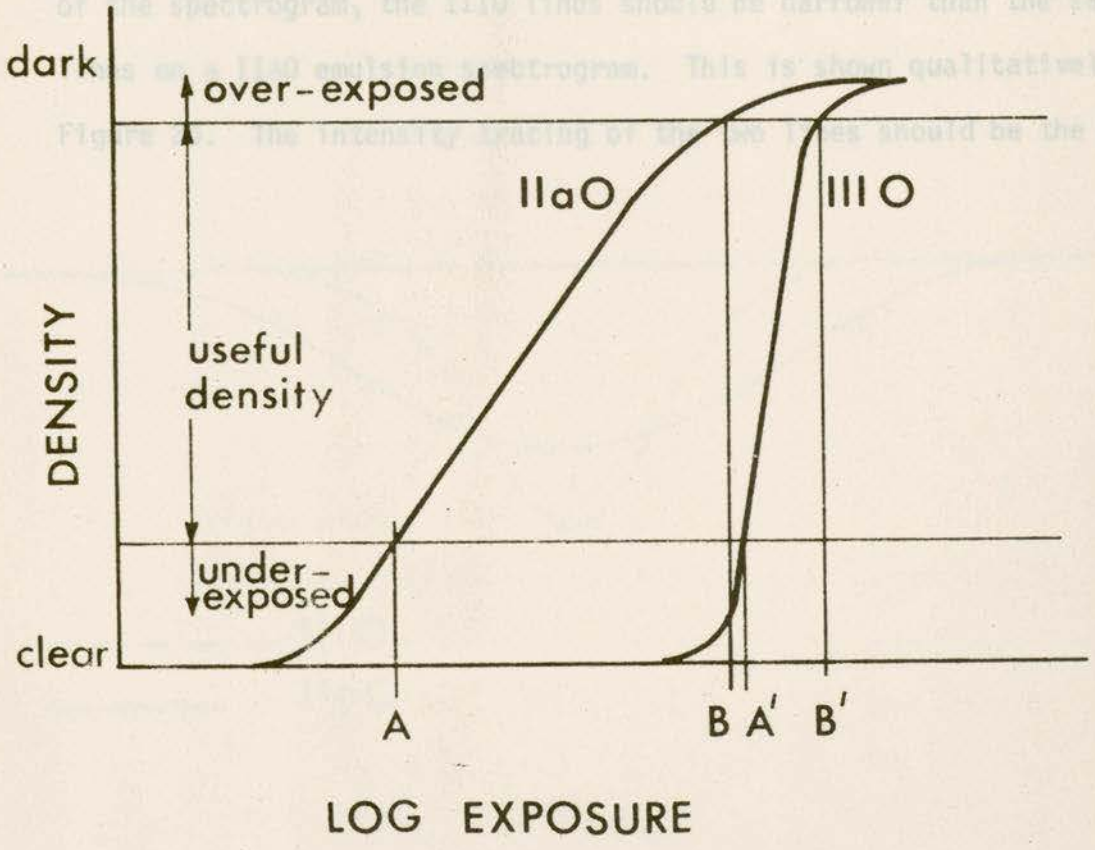

Figure 25. Qualitative characteristic curves of IIa0 and III0 emulsions.

Since the slope of the straight line portion of the IIIO characteristic curve is greater than that of a IIaO emulsion, a properly exposed IIIO plate has a greater range in density than a IIaO plate, for the same range in exposure. Therefore, in a density trace of the spectrogram, the IIIO lines should be narrower than the same lines on a IIaO emulsion spectrogram. This is shown qualitatively in Figure 26. The intensity tracing of the two lines should be the same.

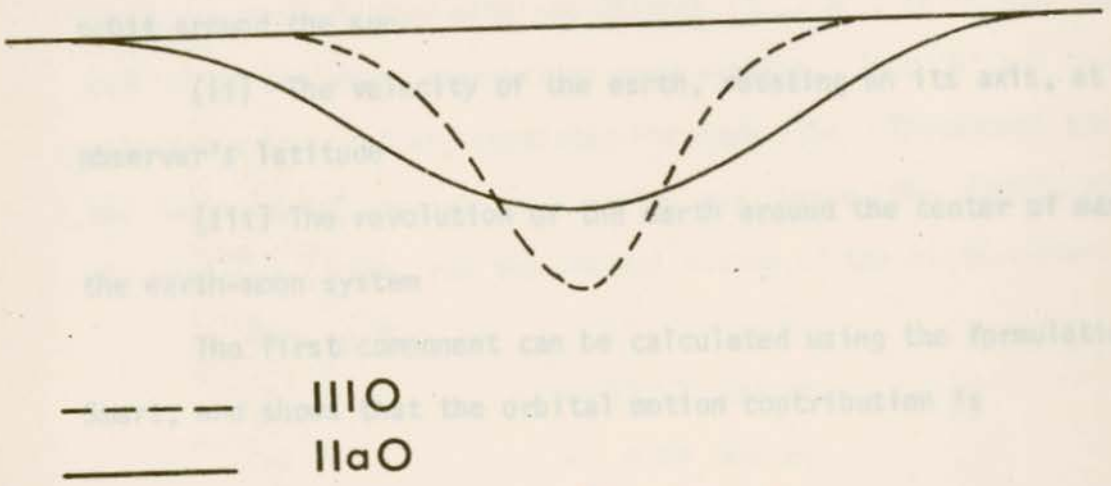

Figure 26. Qualitative effect of IIa0 and III0 emulsions on a line profile.

APPENDIX C

REDUCTION OF RADIAL VELOCITIES TO THE SUN

The radial velocity measured from the lines on a spectrogram is made up of the star's velocity with respect to the solar system, plus the velocity of the observer (i.e. the spectrograph) in the solar system. This latter velocity has three components: (Smart, 1962)

(i) The velocity of the earth revolving in its elliptical orbit around the sun

(ii) The velocity of the earth, rotating on its axis, at the observer's latitude

(iii) The revolution of the earth around the center of mass of the earth-moon system

The first component can be calculated using the formulation of Smart, who shows that the orbital motion contribution is

$$V_{\oplus} = b \sin(\lambda_{\odot} - \lambda_{*}) + c \qquad \text{(C.1.1)}$$

where

$$b = \frac{2\pi a}{P\sqrt{1-e^2}} \cos\beta_{*} \qquad \text{(C.1.2)}$$

and

$$c = be \sin(\omega - \lambda_{*}) \qquad \text{(C.1.3)}$$

and

a = semimajor axis of the earth's orbit

P = earth's orbital period

e = earth's orbital eccentricity

ω = longitude of the earth's perihelion

λ_*, β_* = the ecliptic coordinates of the star (longitude and latitude)

$\lambda_\odot$ = longitude of the sun

For any star with coordinates (λ_*, β_*) it is seen that 'b' and 'c' in the above expressions are constant. Thus 'b' and 'c' are calculated once and are tabulated for each star. Throughout the year, the longitude of the sun, $\lambda_\odot$, varies and, hence, the contribution to the radial velocity from the orbital motion of the earth varies.

For μ Boo,

b = 17.73 km/sec

c = 0.28 km/sec

(ii) The diurnal rotation of the earth contributes

$$R' = \frac{2\pi\rho}{\tau} \cos(\phi) \cos(\delta) \sin(H) \quad \frac{km}{sec} \qquad (C.1.4)$$

to the observed radial velocity, (Smart, pages 216, 217) where

ρ = radius of the earth in kilometers

τ = length of the sidereal day in mean seconds

ϕ = observer's latitude in degrees

δ = declination of the star in degrees

H = hour angle of the star

From this equation, it is seen that:

(a) the maximum value of R' occurs for $\cos(\delta) = 1$, $\sin(H) = 1$, or

$$R'_{max.} = 0.47 \cos(\phi) \text{ km/sec}$$

(b) the diurnal correction is 0 km/sec for H = 0, 12 hours, i.e. at upper and lower transits of the star.

(c) for any particular star (δ) and any particular observatory (ϕ), R' depends only on the hour angle of the star at the time of the observation.

(d) the correction is negative if the star is west of the prime meridian (H negative) and positive for the star east of the meridian (H positive).

(iii) According to Aitken (1964, page 145) the third component never exceeds the value of 0.014 km/sec and is always neglected.

Once these two corrections have been applied to the measured velocity, the resultant velocity is termed "with respect to the sun" and it is this velocity which is used in all radial velocity work.

APPENDIX D

ABBREVIATIONS FREQUENTLY USED

S.E.M. Standard error of the mean. For a plate measurement, it is given by Equation (5.3.3). As an estimate of the error in the overall mean, it is given by Equation (6.6.3) (weighted) or (8.2.3) (unweighted).

p.e.m. Probable error of the mean. Its value is given by p.e.m. = 0.6745 x S.E.M. for a Normally distributed variate.

D.A.O. Dominion Astrophysical Observatory at Victoria, B. C.

μ Boo Refers to the primary star, μ^1 Bootis, of the visual binary μ Bootis (see Section 1.4).

A/mm Dispersion of a spectrograph in Angstroms per millimeter.

B.G.&Z. Brower, Grant, and Zeiss oscilloscope measuring machine.

J.D. Julian Date.

r.m.s.S.E.M. Root mean square standard error of the mean, given by Equation (5.6.1).

REFERENCES

GENERAL

Adams, W. S., Struve, O., Albitzsky, V., Wilson, R. E., Neubauer, F. J., Petrie, R. M. Transactions of the International Astronomical Union. Report of the Sub-commission on Wavelengths 7, 318. Cambridge: The University Press, 1950.

Aitken, R. G. The Binary Stars. New York: Dover Publications, Inc., 1964.

Alder, H. L., and Roessler, E. B. Introduction to Probability and Statistics. San Franscisco: W. H. Freeman and Company, 1968.

Aller, L. H. Astrophysics The Atmospheres of the Sun and Stars. New York: The Ronald Press Company, 1963.

Berman, A. I. The Physical Principles of Astronautics. New York: John Wiley and Sons, Inc., 1961.

Cramer, H. The Elements of Probability Theory and Some of Its Applications. New York: John Wiley and Sons, Inc., 1955.

Dufay, J. Introduction to Astrophysics: The Stars. Translated by O. Gingerich. New York: Dover Publications, Inc., 1964.

Hynek, J. A. Astrophysics A Topical Symposium. New York: McGraw-Hill Book Company, Inc., 1951.

———— Kodak Plates and Films for Science and Industry. Kodak Publication No. P-9. Rochester: Eastman Kodak Company, 1967.

Lacey, O. L. Statistical Methods in Experimentation. Sixth Printing. New York: The MacMillan Company, 1953.

Mack, C. Essentials of Statistics for Scientists and Technologists. London: Heinemann Educational Books, Ltd., 1966.

Moore, C. E., Minnaert, M. G. J., and Houtgast, J. The Solar Spectrum 2935 A to 8770 A, Second Revision of Rowland's Preliminary Table of Solar Spectrum Wavelengths. National Bureau of Standards Monograph, No. 61. Washington, D.C.: U.S. Government Printing Office, 1966.

Moore, J. H. The Binary Stars by R. G. Aitken. Second edition. New York: McGraw Hill Book Company, Inc., 1935. Chapter V.

Petrie, R. M. Astronomical Techniques. Volume 2 of Stars and Stellar Systems. Edited by W. A. Hiltner. Chicago: The University of Chicago Press, 1962

Petrie, R. M., and Fletcher, J. M. Determination of Radial Velocities and Their Application, I.A.U. Symposium No. 30. London: Academic Press, 1967.

Smart, W. M. Spherical Astronomy. Fifth edition. Cambridge: The University Press, 1962.

Van de Kamp, P. Elements of Astromechanics. San Franscisco: W. H. Freeman and Company, 1964.

Wright, K. O. Astronomical Techniques. Volume 2 of Stars and Stellar Systems. Edited by W. A. Hiltner. Chicago: The University of Chicago Press, 1962.

PAPERS

Abt, H. A. 1965, Ap.J. Suppl., 11, 429.

1968, Pub. A.S.P., 80, 637.

Abt, H. A., and Smith, G. H. 1969, Pub. A.S.P., 81, 332.

Andrews, D. H. 1967, Contr. Dom. Ap. Obs., No. 103.

Baize, M. P. 1952, J. D. Obs., 35, 67.

Batten, A. H. 1967, Pub. Dom. Ap. Obs., 13, 119.

Batten, A. H., Moreby, C., Crampton, D., and Fletcher, J. M. 1970, Pub. Dom. Ap. Obs., 13, (in press).

Beals, C. S. 1936, M.N.R.A.S., 96, 730.

Binnendijk, L. 1967, Pub. Dom. Ap. Obs., 13, 27.

Campbell, W. W. 1928, Pub. Lick Obs., 16, 1.

Harper, W. E. 1937, Pub. Dom. Ap. Obs., 7, 1.

Herbig, G. H. and Spalding, J. F. 1955, Ap. J., 121, 118.

Huang, S-S. 1953, Ap.J., 118, 285.

Jordon, F. C. 1911, Pub. Allegheny Obs., 2, 121.

McDonald, J. K. 1948, J.R.A.S. Canada, 42, 220.

Moore, J. H. 1932, Pub. Lick Obs., 18, 1.

Moore, C. E. 1945, Contr. Princeton Obs. No. 20.

Petrie, R. M. 1946, J.R.A.S. Canada, 40, 325.

1947, ibid., 41, 311.

1948, ibid., 42, 213.

Richardson, E. H. 1968, J.R.A.S. Canada, 62, 313.

Schlesinger, F. 1915, Ap.J., 41, 162.

Schlesinger, F. and Udick, S. 1912, Pub. Allegheny Obs., 2, 155.

Slettebak, A. 1949, Ap.J., 110, 498.

1955, ibid., 121, 653.

Slettebak, A., and Howard, R. F. 1955, Ap.J., 121, 102.

Thackeray, A. D. 1967, I.A.U. Symposium No. 30, 226.

VITA

Surname: NIEHAUS Given Names: RUSSELL JOSEPH

Place of Birth: LADYSMITH, B. C. Date of Birth: MAY 28, 1945

Educational Institutions Attended, with Dates of Entering and Leaving:

UNIVERSITY OF VICTORIA, VICTORIA	1963 to 1966
UNIVERSITY OF VICTORIA, VICTORIA	1967 to 1970

Degrees, Diplomas, Etc., Awarded, with Dates and Names of Institutions:

B.Sc.	1966	University of Victoria, Victoria

Honors and Awards:

Rotary Scholarship, 1963/64

Don Ingham Memorial Scholarship, 1965/66

National Research Council of Canada Scholarships, 1968/70

Publications:

THE UNIVERSITY OF VICTORIA LIBRARY

MANUSCRIPT DISSERTATION (or THESIS)

AUTHORITY TO DISTRIBUTE

AUTHOR: This dissertation may be lent or microfilm copies made available:

(a) Without restriction

(b) With the restriction that, for a period of five years (until)the written approval of the following is required:

(1) The Chairman, School of Graduate Studies .....

(2) The Author .....

(3) both the Chairman, School of Graduate Studies, and the Author .....

BORROWERS: The borrower undertakes, by signing below, to give proper credit for any use made of the dissertation, and to obtain the consent of the author if it is proposed to make extensive quotations, or to reproduce the dissertation in whole or in part.

Signature of Borrower	Address	Date